Significance of Lateral Variations of Topography and Near-Surface Geology on Earthquake Locations and Structural Images

Jer-Ming Chiu
CERI/Dept. of Earth Sciences
University of Memphis

March 21, 2014

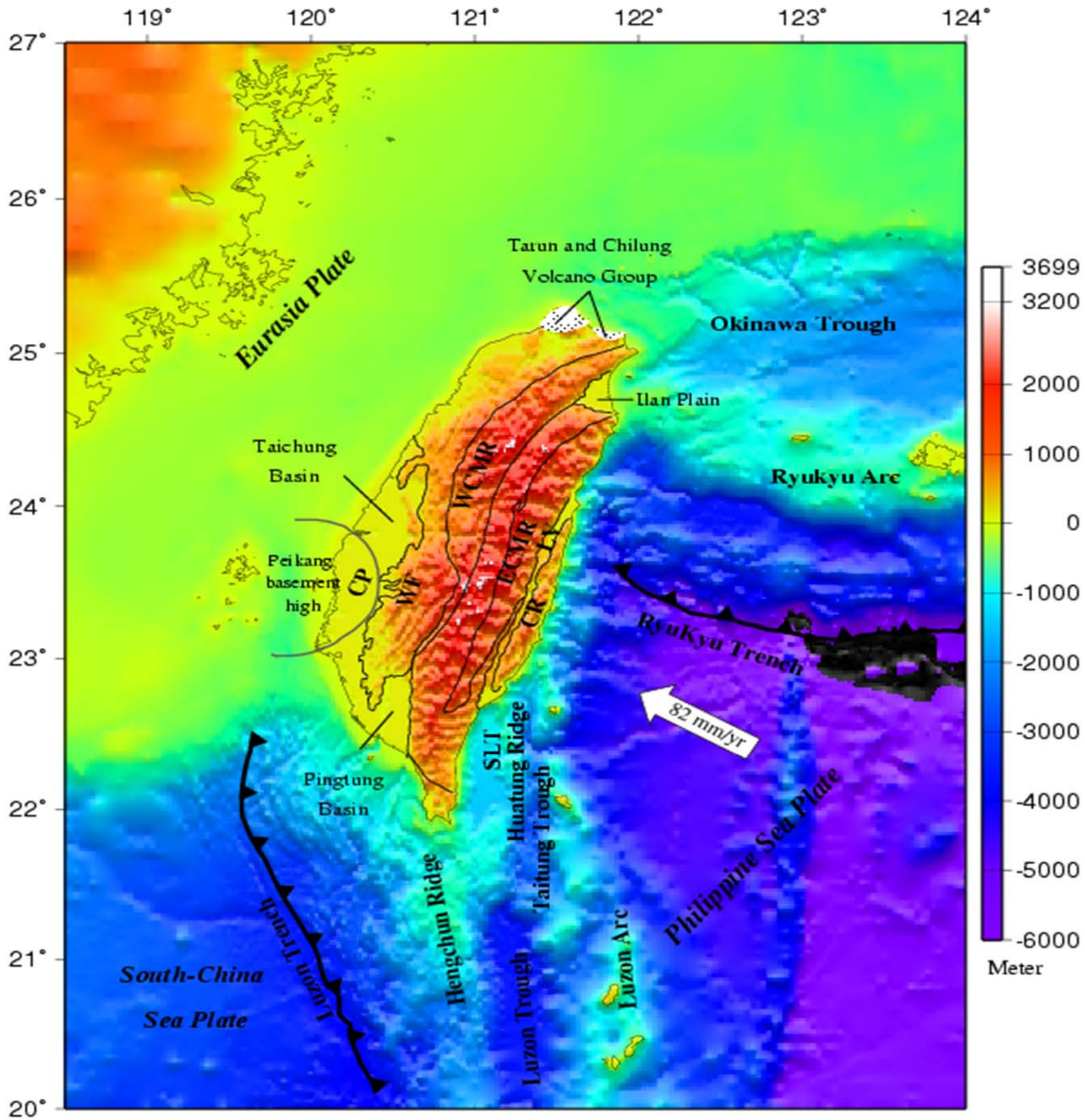
119°
120°
121°
122°
123°
124°
27°
26°
25°
24°
23°
22°
21°
20°
Eurasia Plate
Tatun and Chilung
Volcano Group
Okinawa Trough
Ilan Plain
Taichung
Basin
WCMR
ECMR
LV
CR
WF
CP
Peikang
basement
high
Ryukyu Arc
RyuKyu Trench
82 mm/yr
Pingtung
Basin
SLT
Huatung Ridge
Taitung Trough
Hengchun Ridge
Luzon Trough
Luzon Arc
Luzon Trench
Philippine Sea Plate
South-China
Sea Plate
3699
3200
2000
1000
0
-1000
-2000
-3000
-4000
-5000
-6000
Meter

Pn waves observed at two stations (TWG and SGS) at 146.5 km are not a surprise. The first surprise is that there is 4 seconds travel time difference between the two stations.

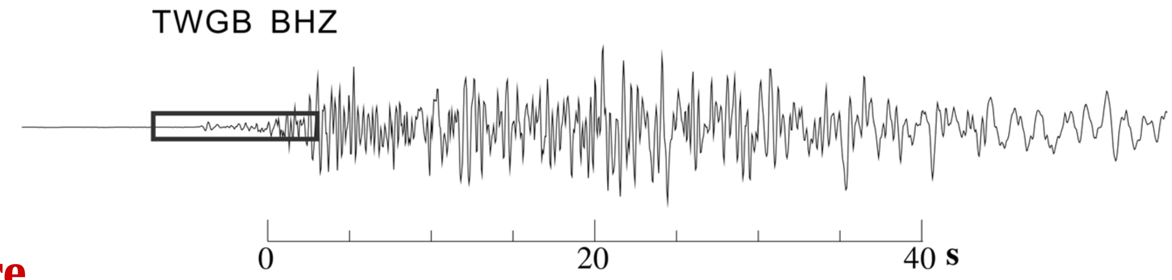

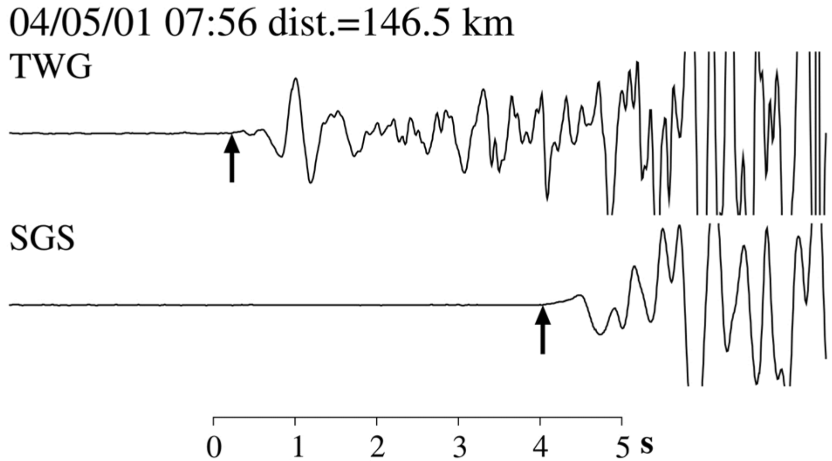

No obvious Pn type arrival at the TWQ station is not a surprise. The second surprise is that the small amplitude Pn type arrival is observed at TWF station but not at TWQ station, both at the same epicenter distance (83 km).

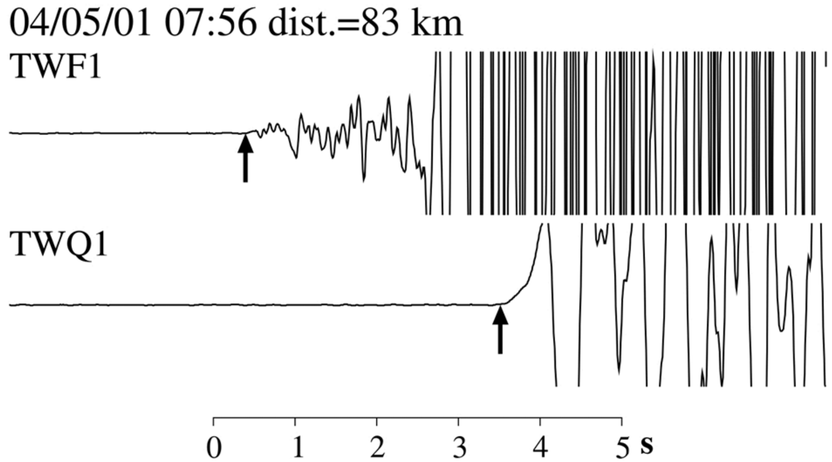

The third surprise is that there is ~3.3 sec travel time difference between the two station.

Example of 3-component broadband seismograms from an intermediate depth earthquake

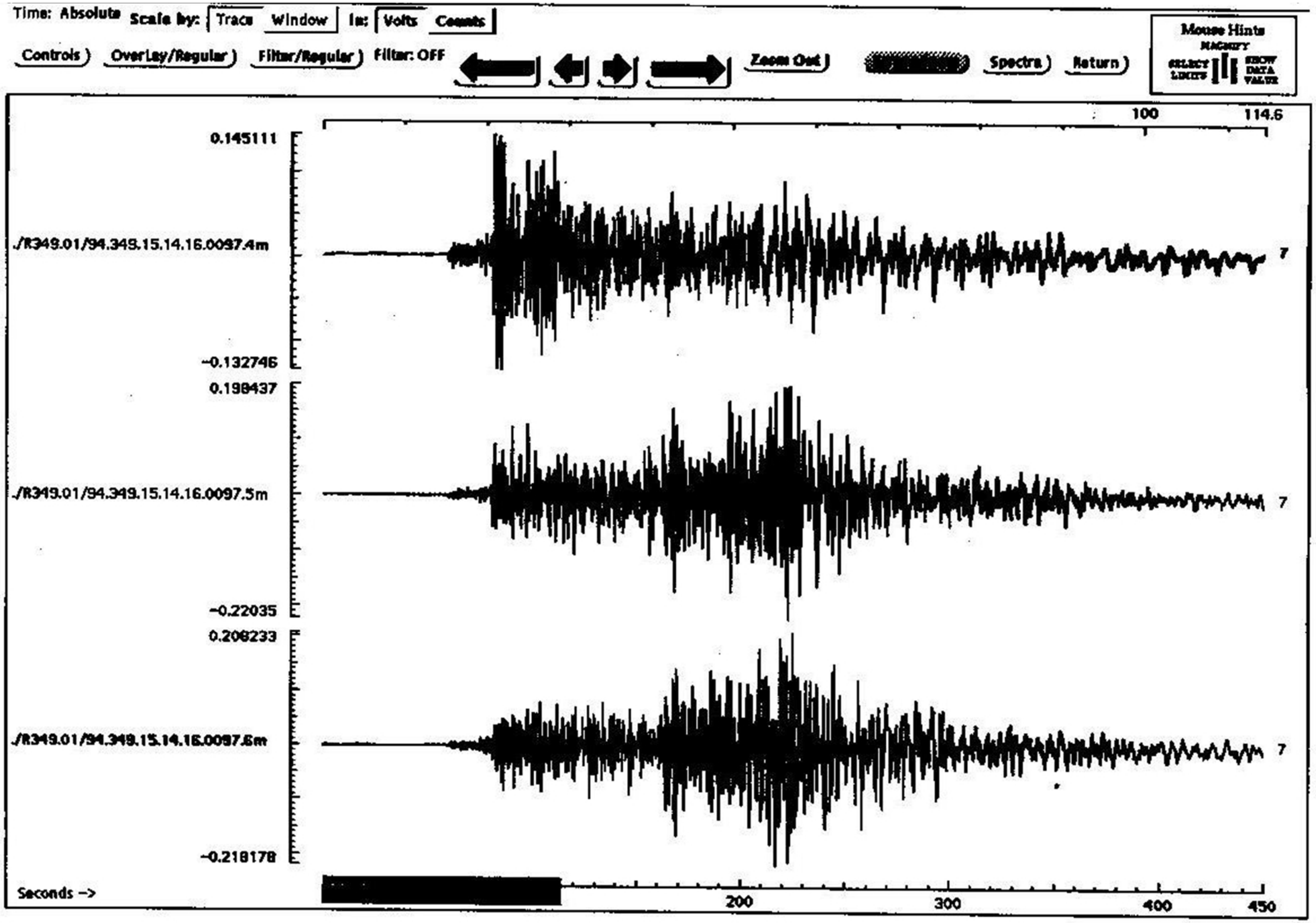

Earthquake Location

1. Fundamental theory for earthquake location
2. Parameters required for an earthquake location
3. Evaluate quality of earthquake location

Reliable Earthquake Location

will provide essential information leading to

- the identification of active faults,
- the exploration of physical properties of an active fault,
- our understanding of earthquake source process,
- the exploration of earth's interior structure,
- how seismic waves propagate along the ray paths,
- ……………………………………..

Question is

"Are earthquakes in a catalog reliably located?".

Seismicity in North Island, New Zealand
(Aug. 1993 - May 1995)

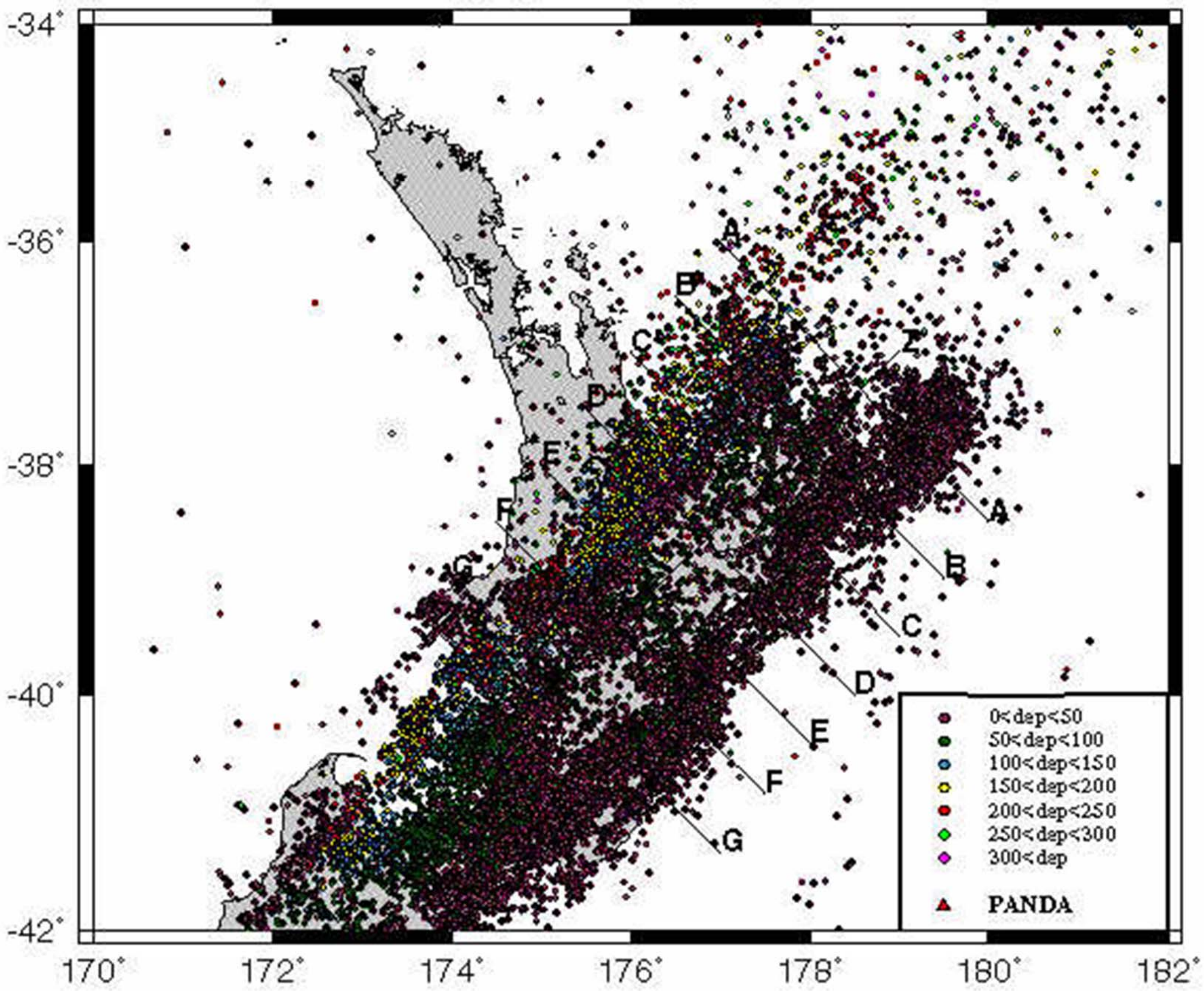

Examples of a few cross-sectional views of seismicity showing that thickness of seismogenic zone is generally 20~40 km.

Earthquakes are poorly located due to lack of reliable velocity structure.

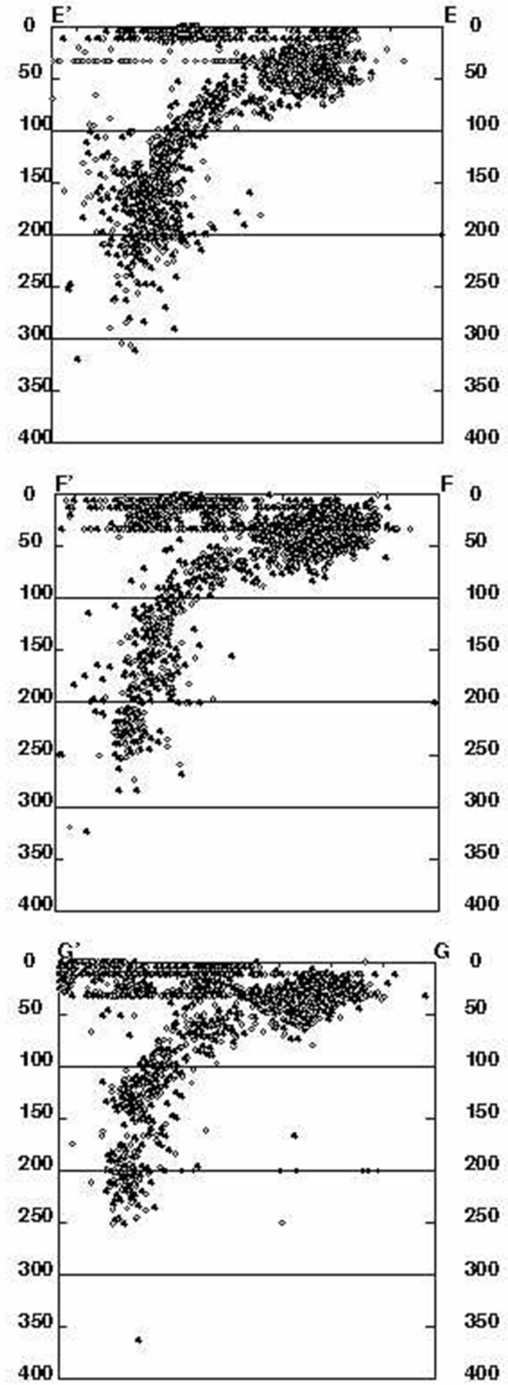

Earthquake locations above a flat subduction zone in South American are not affected by the complicated internal structure of a subduction zone.

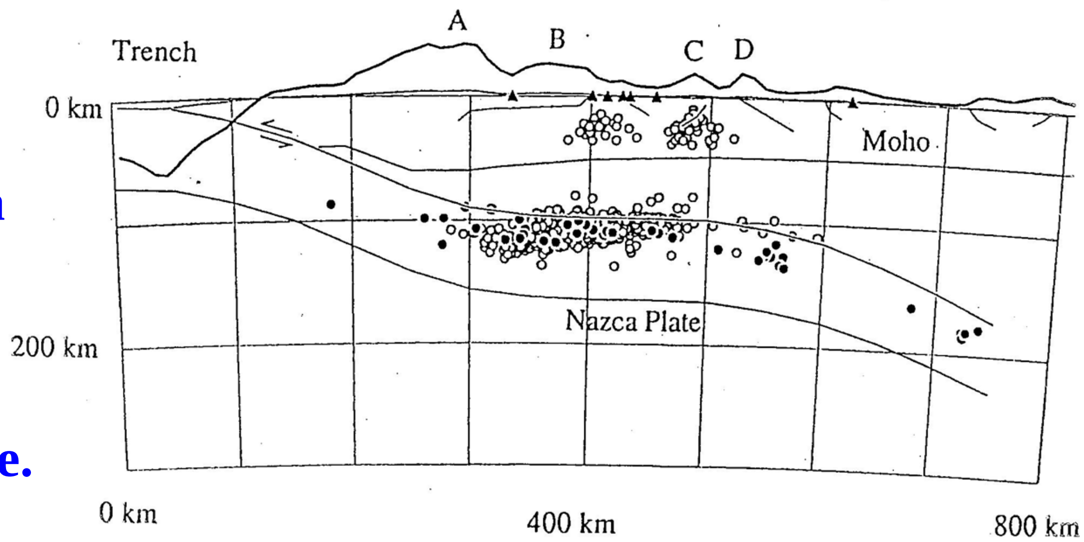

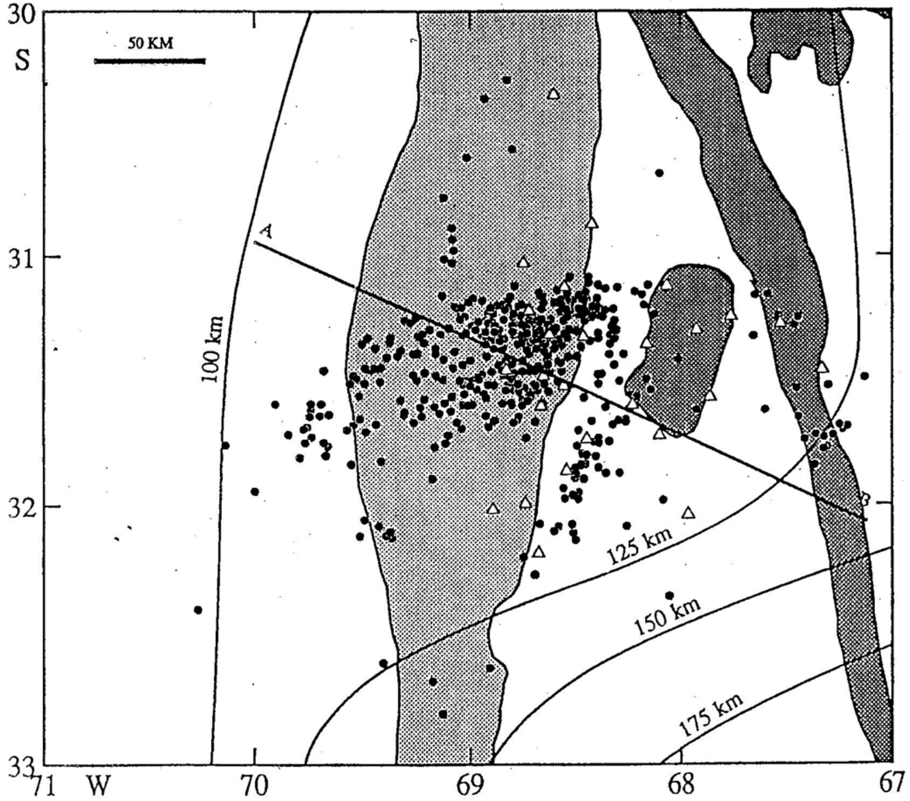

Traditionally, it is well accepted that thickness of seismogenic zone is 20~40 km in most subduction zones.

ISC data

PANDA data – original location

PANDA data – JHD relocation

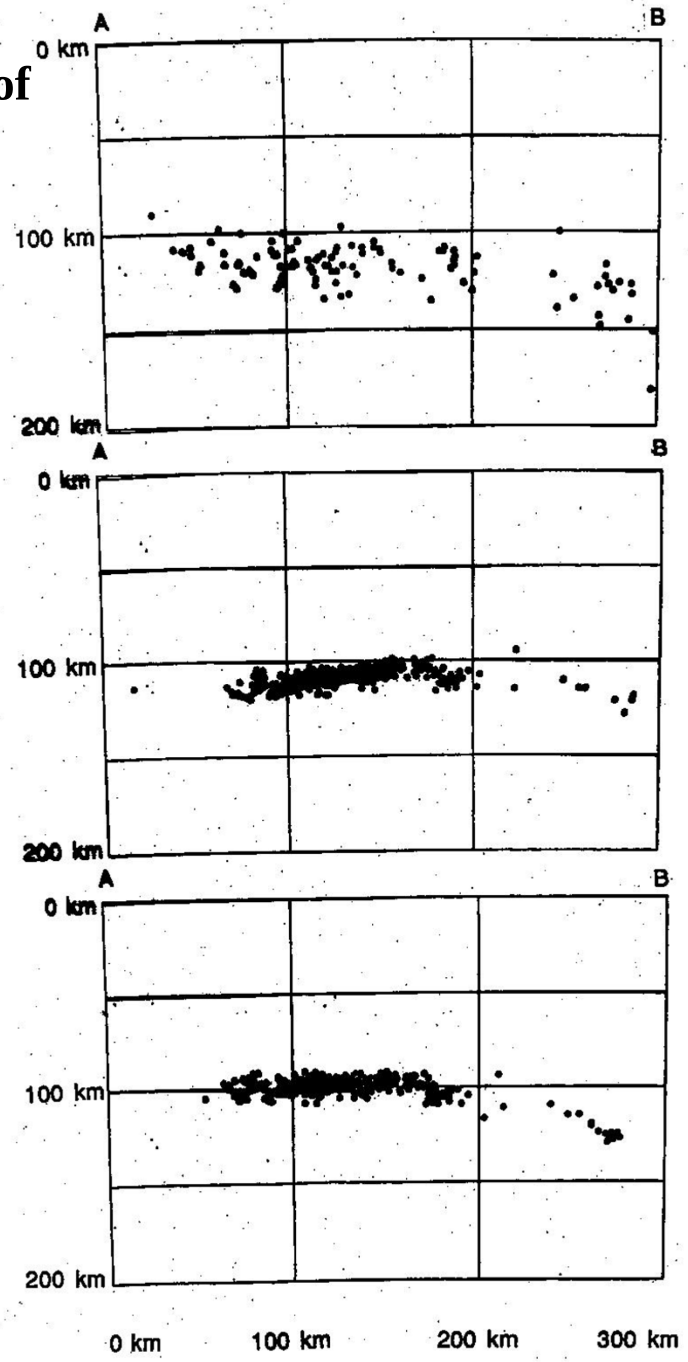

For the northern central segment

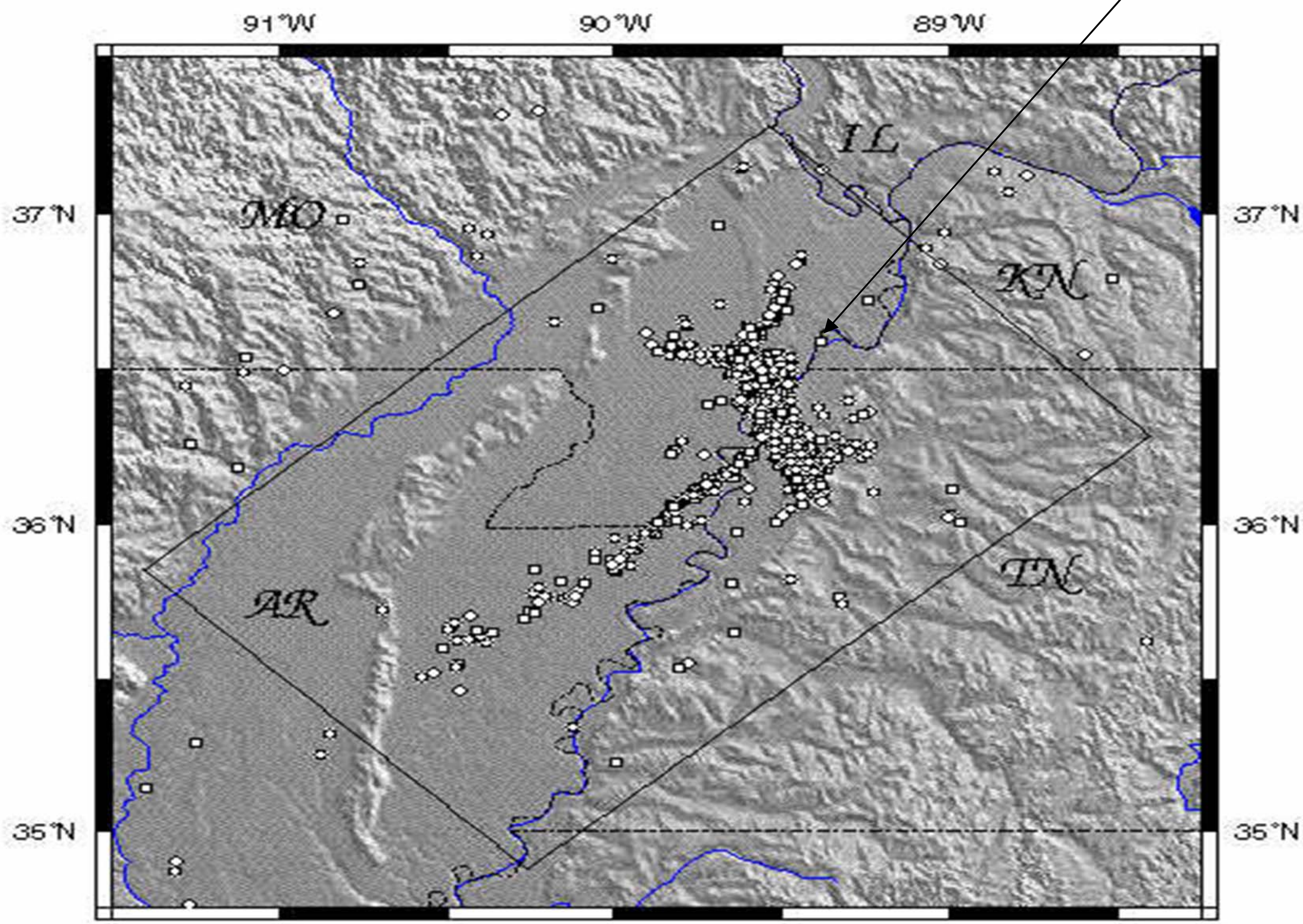

Figure 1. Map showing the original epicentral locatoins from PANDA and CERI regional seismic network. Study area is marked by the thick rectangle box.

A few cross-sectional views of seismicity for the central segment of the NMSZ using regional seismic network catalog

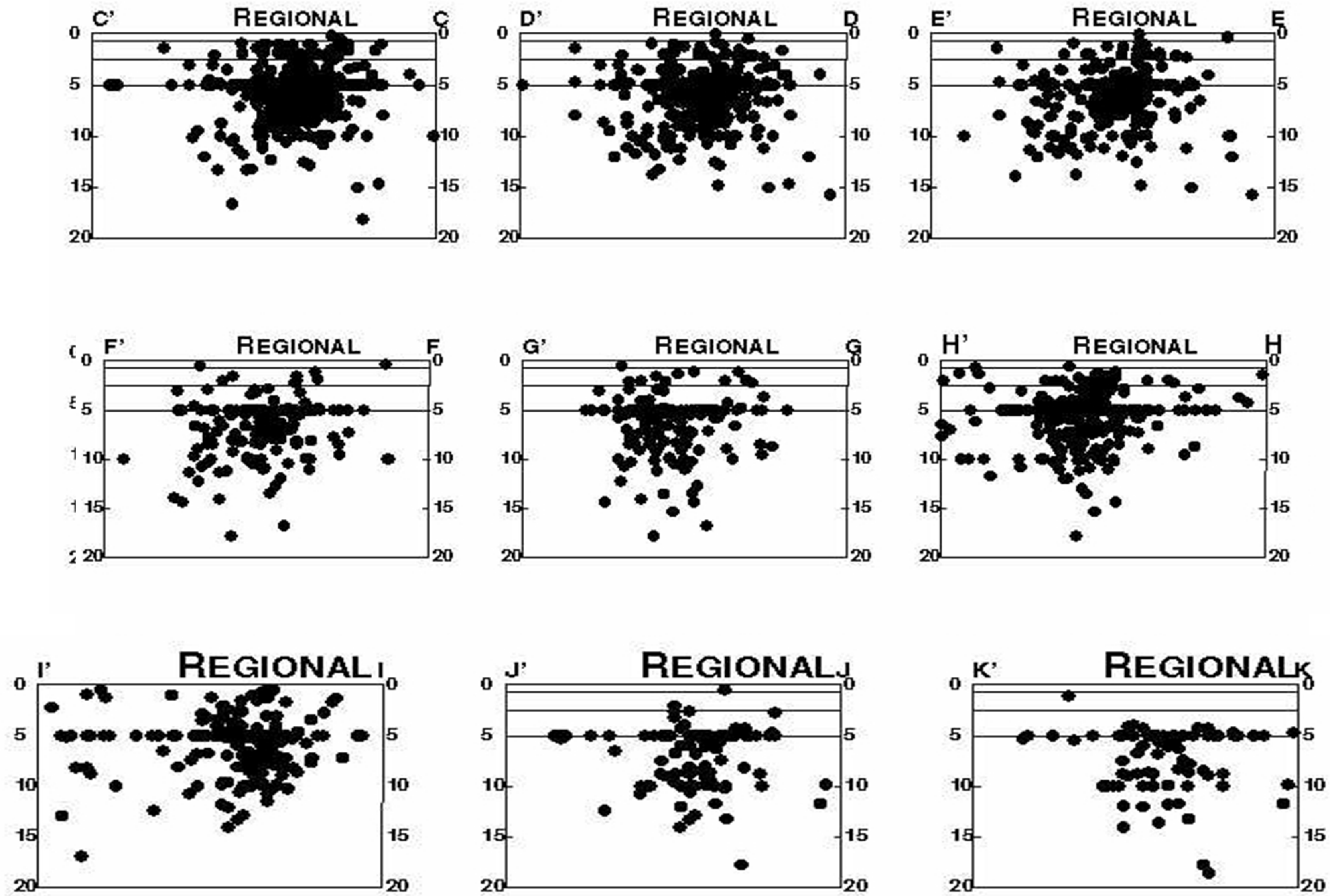

How can earthquake be reliably located?

It requires

1. **A seismic network of at least three seismic stations** – basically a preliminary earthquake location can be obtained graphically from the P-wave arrival times observed on at least three stations.

2. **A velocity model for both P- and S-waves –** either 1-D or 3-D.

3. **A reliable earthquake location algorithm –** suitable for today's computer technology and local and regional needs.

Review of currently available earthquake location techniques

Traditional earthquake location techniques using "**homogenous layered velocity model**"

<u>HYPO71</u> – Lee and Lahr (1975), the first computer oriented earthquake location program. It is still the most popular earthquake location program up-to-date. Specific features of HYPO71 include

(a) Use 1-dimensional homogeneous layered P-wave velocity model. S-wave velocity model is determined by a given Vp/Vs ratio. P- and S-wave velocity increase as a function of depth.

(b) Data clarity is weighted by using 0~4 scale (0=100%, 1=75%, …..,4=0%) to minimize the effect of poor or bad quality data on earthquake location.

(c) Distance weighting is also applied

HYPOINVERSE : Klein (2001) The program is designed for earthquake location in Hawaii. Program is similar to HYPO71 except that low velocity layer is allowed in the velocity model.

HYPOELLIPSE : Lahr (1999). Similar to HYPO71 with significant modifications

(a) Allow low velocity layer in the velocity model, allow input of multiple velocity models, flexible input of velocity models…

(b) Provide error ellipses for vertical and horizontal errors

(c) Allow stations to be located at elevation lower than the depths of hypocenters

There are a few other location programs developed for routine seismic network location by individuals which are, however, similar to the HYPO71, HYPOINVERSE, and HYPOELLIPSE.

The fundamental concept of earthquake location in these programs is the “**Geiger’s Method”**

Geiger's Method

Let

- $(\mathbf{x_i}, \mathbf{y_i}, \mathbf{z_i})$: the coordinates of the i^{th} station
- $\tau_\mathbf{i}$: the observed arrival time.
- $\mathbf{t_i}$: the computed arrival time based on a trial solution (i.e. an assumed origin time (t) and hypocenter (x,y,z) along a ray path).

If the time residual

$$R_i = \tau_i - t_i \tag{1}$$

is small, Taylor expansion of (1) wil give:

$$R_i = dt + \frac{\partial t_i}{\partial x} dx + \frac{\partial t_i}{\partial y} dy + \frac{\partial t_i}{\partial z} dz + e_i \tag{2}$$

Since the travel time and derivatives can be computed from a given crustal model, we may obtain the adjustment vector dt, dx, dy, dz) by least square, i.e. demanding that the error e_i be such that:

$$\sum {e_i}^2 = a \quad minimum \tag{3}$$

where $\sum$ denotes summation over all stations, i.e. i=1 to i=n.

This is accomplished by solving the following normal equation which are derived from applying condition (3) to equation (2):

$$\begin{aligned} ndt + \sum a_i dx + \sum b_i dy + \sum c_i dz &= \sum R_i \\ \sum a_i dt + \sum {a_i}^2 dx + \sum a_i b_i dy + \sum a_i c_i dz &= \sum a_i R_i \\ \sum b_i dt + \sum a_i b_i dx + \sum {b_i}^2 dy + \sum b_i c_i dz &= \sum b_i R_i \\ \sum c_i dt + \sum a_i c_i dx + \sum b_i c_i dy + \sum {c_i}^2 dz &= \sum c_i R_i \end{aligned} \tag{4}$$

Where

$$a_i = \frac{\partial t_i}{\partial x}; b_i = \frac{\partial t_i}{\partial y}; c_i = \frac{\partial t_i}{\partial z} \tag{5}$$

Solve equation (4) to determine a set of (dt, dx, dy, dz) to satisfy equation (3).

The improved origin time and hypocenter then becomes:

$$t + dt, and(x + dx, y + dy, z + dz) \tag{6}$$

Now (6)may be taken as the next trial solution, and the same procedure is repeated until some cutoff criteria are met.

Other modern earthquake location techniques dealing with inhomogeneous velocity model include :

(a) **Joint Hypocenter Determination (JHD)** – Pujol (1988). Relative arrival time information from a clustered earthquakes are used to locate earthquakes. The JHD output include (1) relative earthquake location and (2) station corrections. Station corrections can be used to explore the lateral velocity variations. The method is independent of the real earth model.

(b) **Double Difference Method (DD)** : Waldauser and Ellsworth (2000). Use cross-correlation of waveforms between adjacent earthquakes to determine high-resolution arrival time differences between different events recorded at the same station and from one earthquake recorded at different stations. Relative arrival time differences between adjacent earthquakes recorded at a set of stations are used to determine relative earthquake locations.

Other modern earthquake location techniques (continue) :

(c) 3-D velocity inversion and earthquake relocation : A few programs have been developed to use selected high quality arrival time data to invert 3-dimensional velocity structure and at the same time to relocate the selected earthquakes.

Problems and limitations:

JHD – no real earth structure is involved. Earthquakes must be clustered. The location is relative.

DD – The location is relative that can be systematically biased if significant lateral velocity variations exist.

3-D Tomographic Inversion – Only best quality earthquakes are selected, used, and relocated. Majority of smaller earthquakes are not relocated during inversion.

Solution for a reliable earthquake location

(a) Determination of a reliable 3-D Vp and Vs velocity model – a big challenge for seismologists

(b) Development of a single-earthquake location algorithm using the resultant 3-D Vp and Vs velocity model -- a dream

(c) A reliable arrival time picks for both P- and S-waves – additional analysis tools are needed to verify the arrival time picks, especially for the S-wave. Tools such as cross-correlation, stacking (summing), bandpass filter, and polarization filter can be applied.

Resolution of a Seismic Network

For a seismic network, its spatial resolution on velocity structure and earthquake location depends on

(a) Network station configuration – a compromise between spatial resolution and spatial coverage

(b) Distribution between background seismicity and station location

Addition of selected CWB strong motion sites

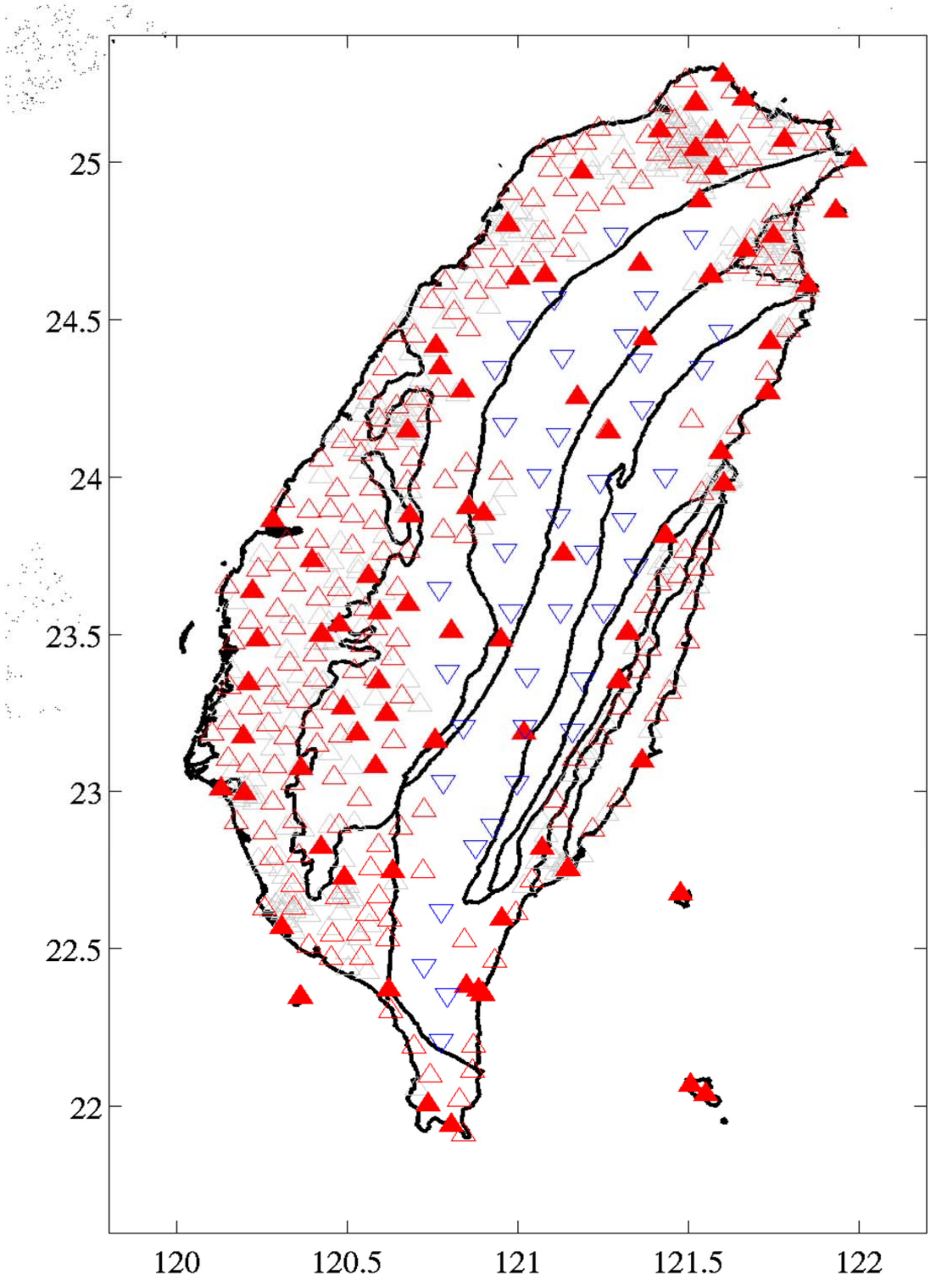

Background seismicity remains the same. Additional seismic stations will affect the resolution of a seismic network significantly.

Design checkerboard initial models for both P- and S-waves. Generate synthetic travel times from selected background earthquakes to all surface stations across the initial models.

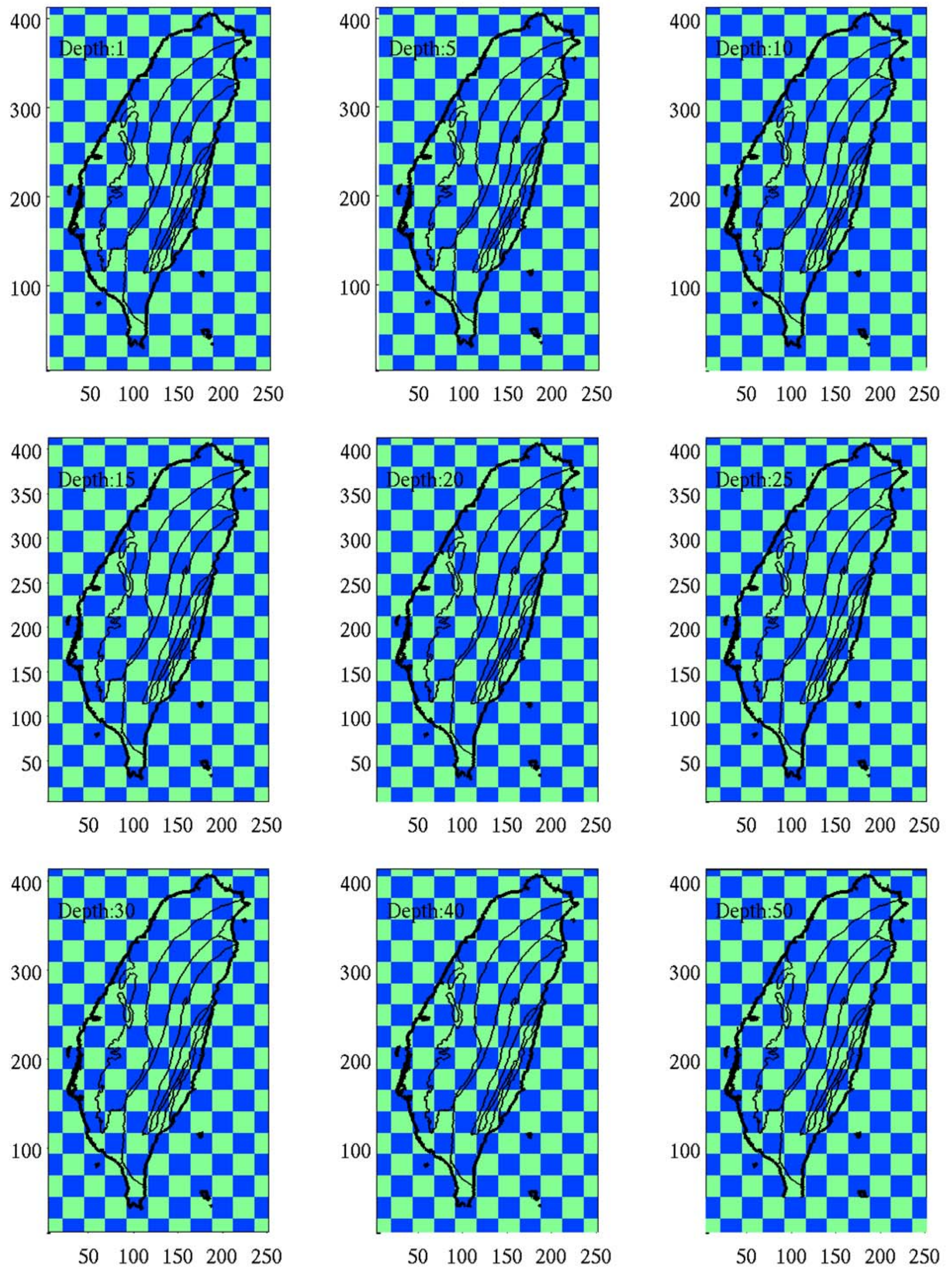

Using homogeneous layered models as the initial model for both P- and S-waves

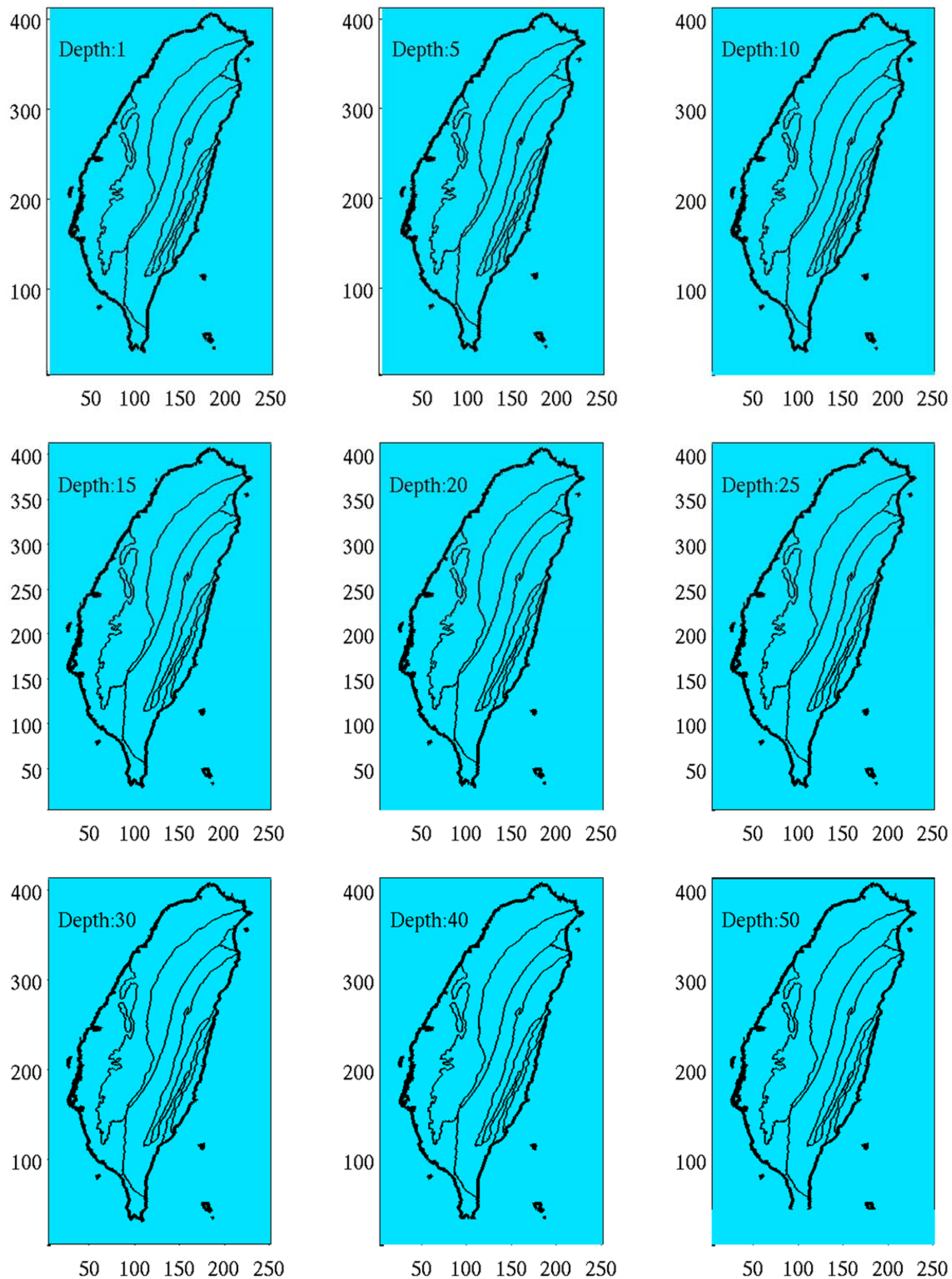

Addition stations in a seismic network will provide very significant improvement of resolution for subsurface structures at various depths.

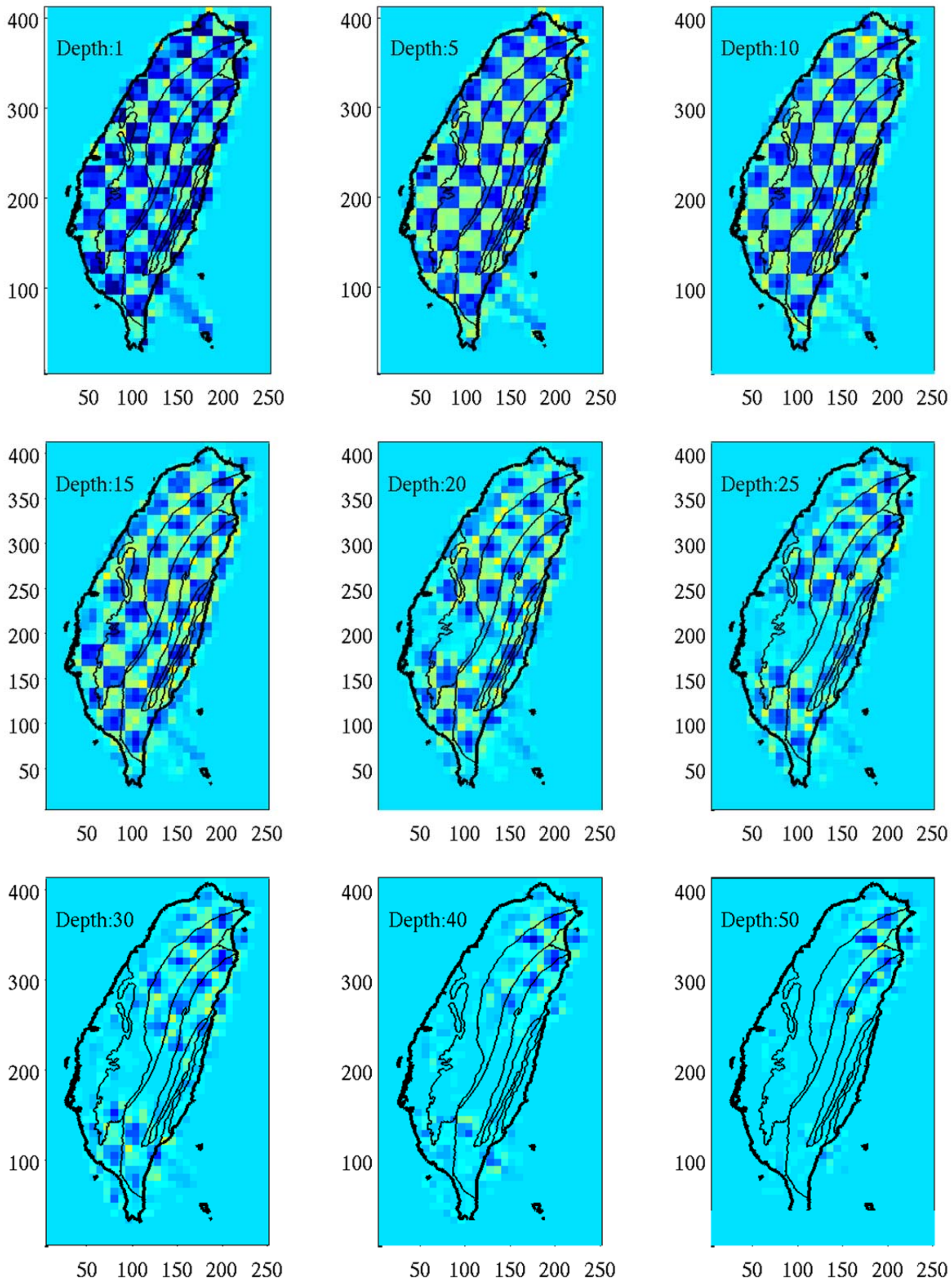

Test of structural resolution of a seismic network with additional OBS stations offshore.

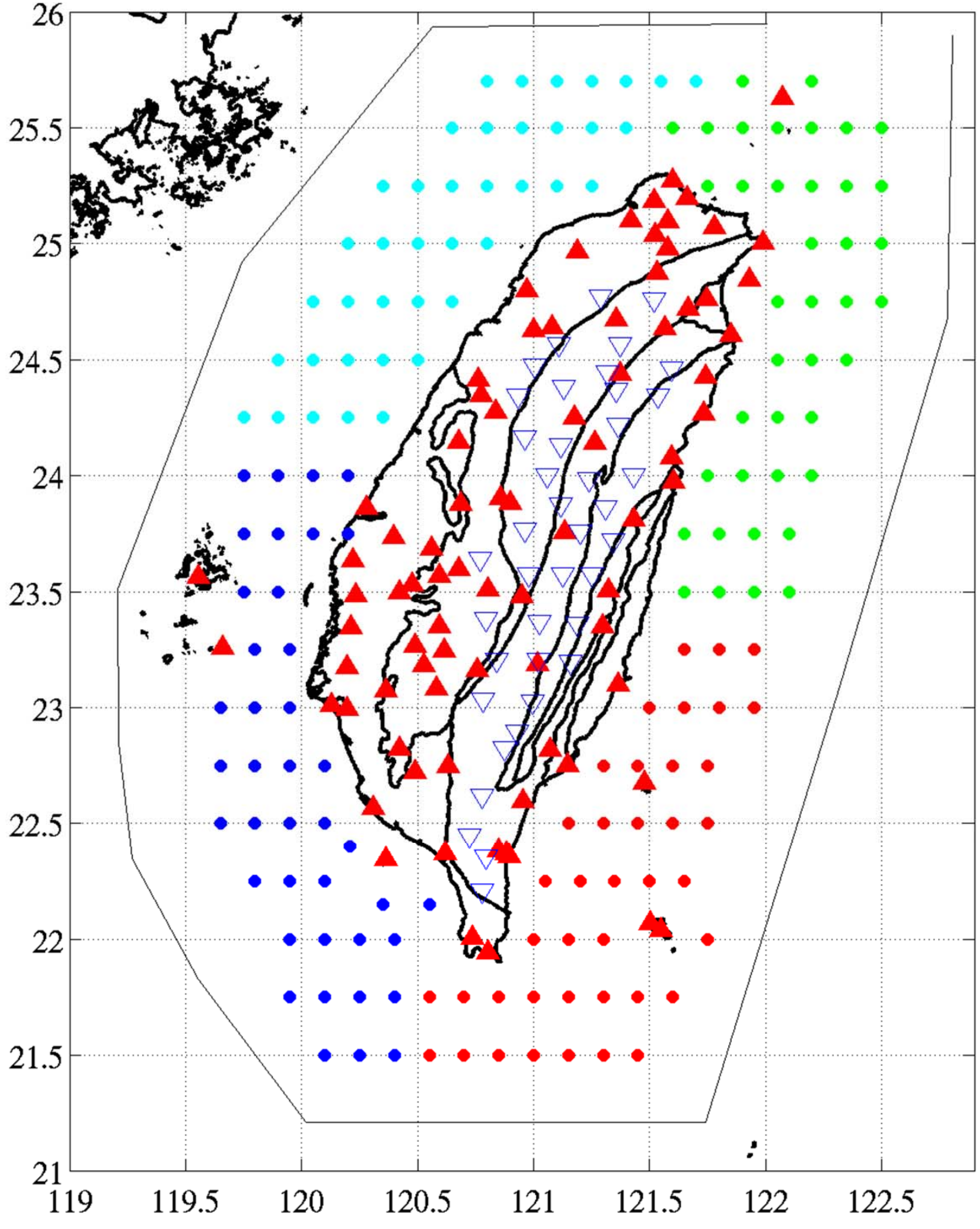

Structural resolution as a function of depths for a seismic network with OBSs. Note the lack of resolution at shallow and deeper depths.

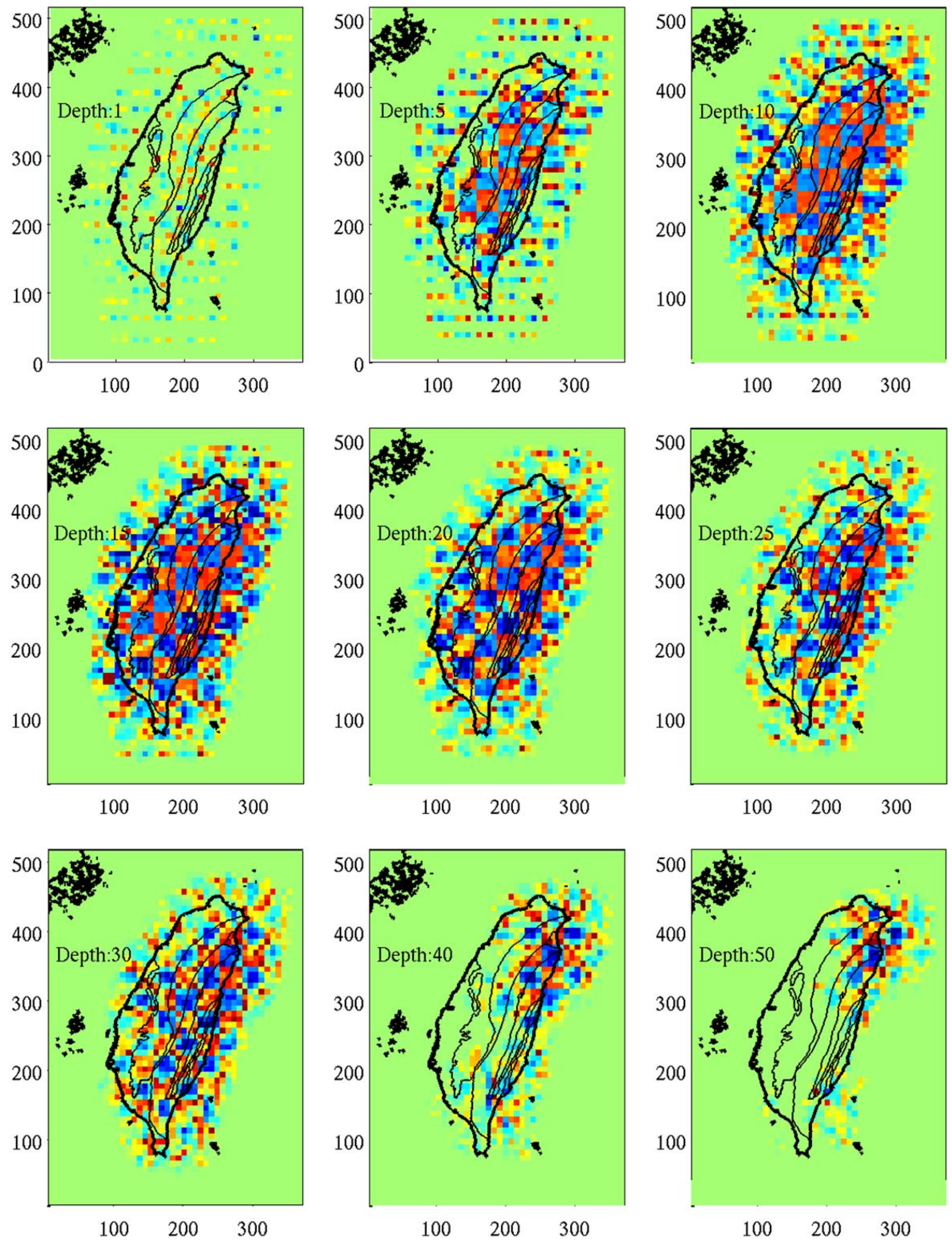

A few east-west cross-sectional views of P-wave velocity perturbations from 3-D inversion of P-wave only (left) and P+PmP waves (right) (from Xia et al., 2007)

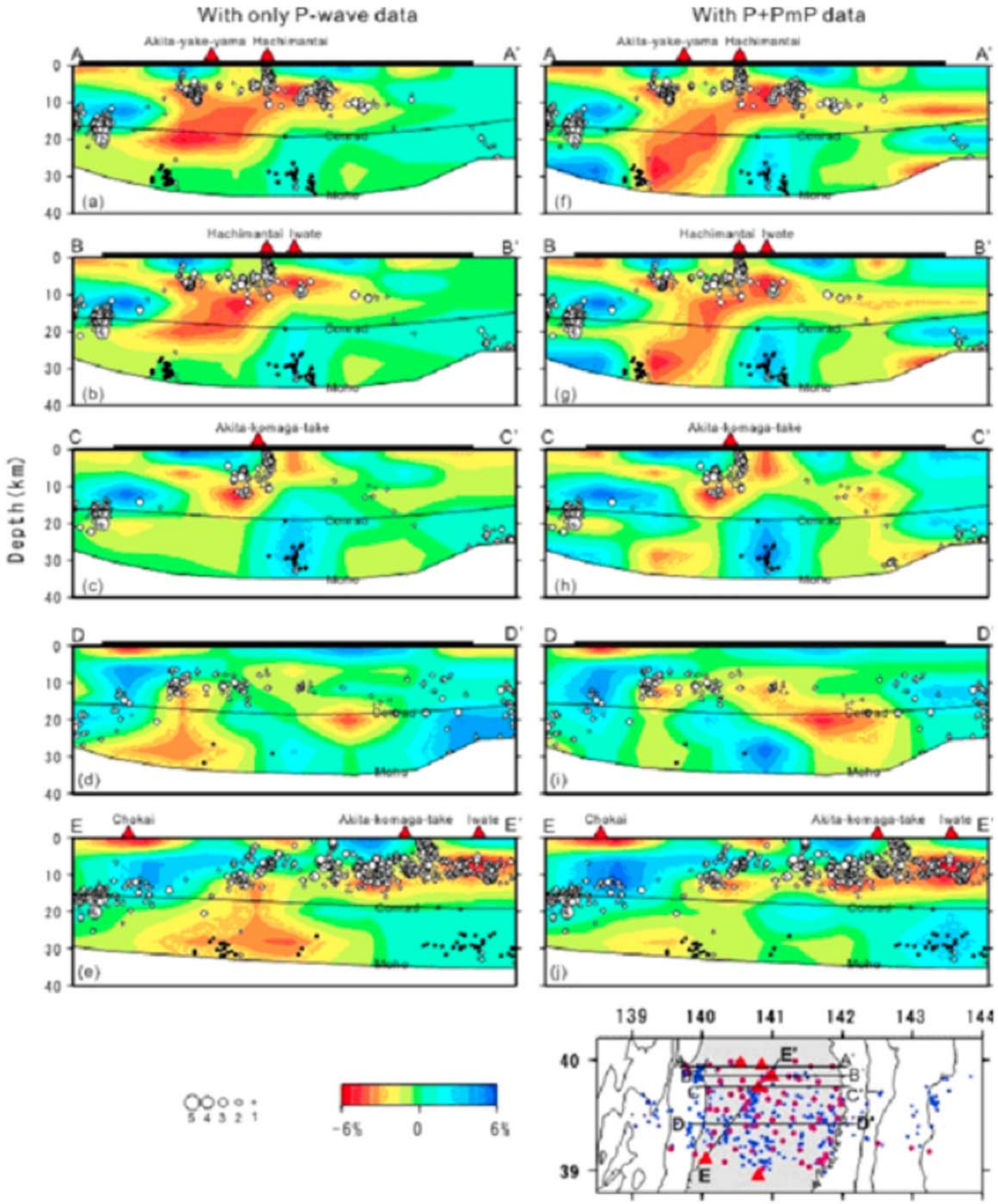

Volcano Earthquakes

Research in Volcanoes

Hazard mitigation ---

prediction of volcanic eruption

hazard assessment

Geothermal exploration ---

geothermal power plant

spa and medical treatment

mineral resources

Others ---

study of materials from deep earth interior

tourism

Volcanoes – around the world

Most deadly volcanic eruption

1815	Atanpola Volcano, Indonesia	92,000
1883	Aklakto Volcano, Indonesia	36,000
1902	Beirei Volcano, Martinix Island	30,000
1985	Columbia	25,000
1792	Yuenshen Volcano, Japan	15,000
1586	Indonesia	10,000
1783	Lucky Volcano, Iceland	9,000
1919	Java, Indonesia	5,110
1902	St. Mary Volcano, Guatemala	4,500
79	Weswei Volcano, Italy	3,360

The most powerful volcano eruptions

Time	Location	Casualties	Note
5/8/1902	Martinix Island	40,000+	

(Peirei Volcano has been dormant for a few decades, after the eruption, entire town of St. Pier had only two survivors, one of them was a prisoner who survived because of the ventilation inside the jail was very poor that he was freed from inhale the volcanic ash.)

May 7, 1902:
Volcanic eruption buries Caribbean city

On this day in 1902, Martinique's Mount Pele begins the deadliest volcanic eruption of the 20th century. The following day, the city of Saint Pierre, which some called the Paris of the Caribbean, was virtually wiped off the map.

Mount Pele, the name meaning bald in French, was a 4,500-foot mountain on the north side of the Caribbean island of Martinique. On April 2, 1902, new steam vents were spotted on the peak, which overlooked the port city of Saint Pierre. Three weeks later, tremors were felt on the island and Mount Pele belched up a cloud of ash.

Caught up in the midst of an important election, residents of Saint Pierre failed to heed the mountain's warnings and evacuate. The nearby residents mistakenly believed that the only danger from the volcano was lava flow and that if lava started to flow, they would have plenty of time to flee to safety. In fact, some people came from outside the city to view the action, even after ash from the eruption began to block roads.

On May 7, activity on the volcano increased dramatically and the blasts grew significantly stronger. Overnight, there were several strong tremors and a cloud of gas with a temperature of more than 3,000 degrees Fahrenheit spilled out of the mountain. Finally, a tremendous blast in the early morning hours sent an avalanche of boiling ash down the side of the mountain.

The city of Saint Pierre was buried within minutes and virtually everyone died instantly. There were only two reported survivors--one was a prisoner held in an underground cell. Legend has it that he went on to be a circus attraction. In addition, 15 ships in the harbor were capsized by the eruption. One ship managed to stay afloat with half the crew surviving, although most suffered serious burns.

Vulcanologists are still unsure about exactly what causes volcanic eruptions and how they can be predicted.

The most powerful volcano eruptions

11/1985	Columbia	25,000

Town Amero was covered by mudflow twice from previous volcanic eruptions, one in 1595 and the other in 1845. They didn't learn the lesson from history that the town was totally destroyed again in 1985 by mudflow.

5/19/1919	Indonesia	5,100
10/24/1902	St. Mary Volcano, Guatemala	4500
1/24/1951	New Guinea	2,942
3/29/1982	El Kichuan, Mexico	1,879
8/21/1986	Lake Kameroneo	1700+

(Poison gases relieved from the volcano eruption kill many people)

5/7~8/1902	Lasuferi Volcano, St. Winson Island	1565
12/18/1931	Molapi Volcano, Java Island	1369
1/30/1911	Tar Volcano, Philippine	1335


©colorview publications, ltd.

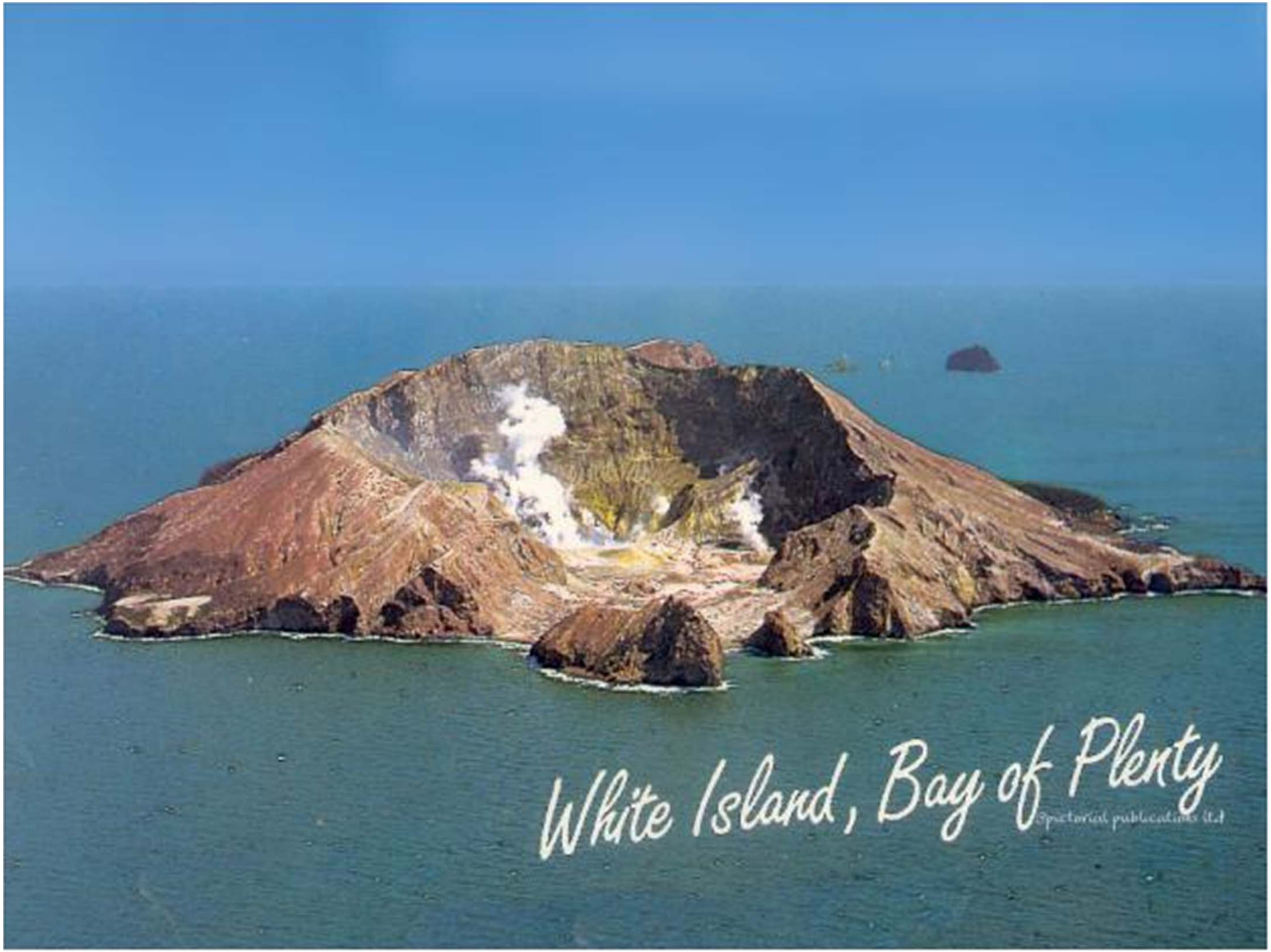
White Island, Bay of Plenty
©pictorial publications ltd

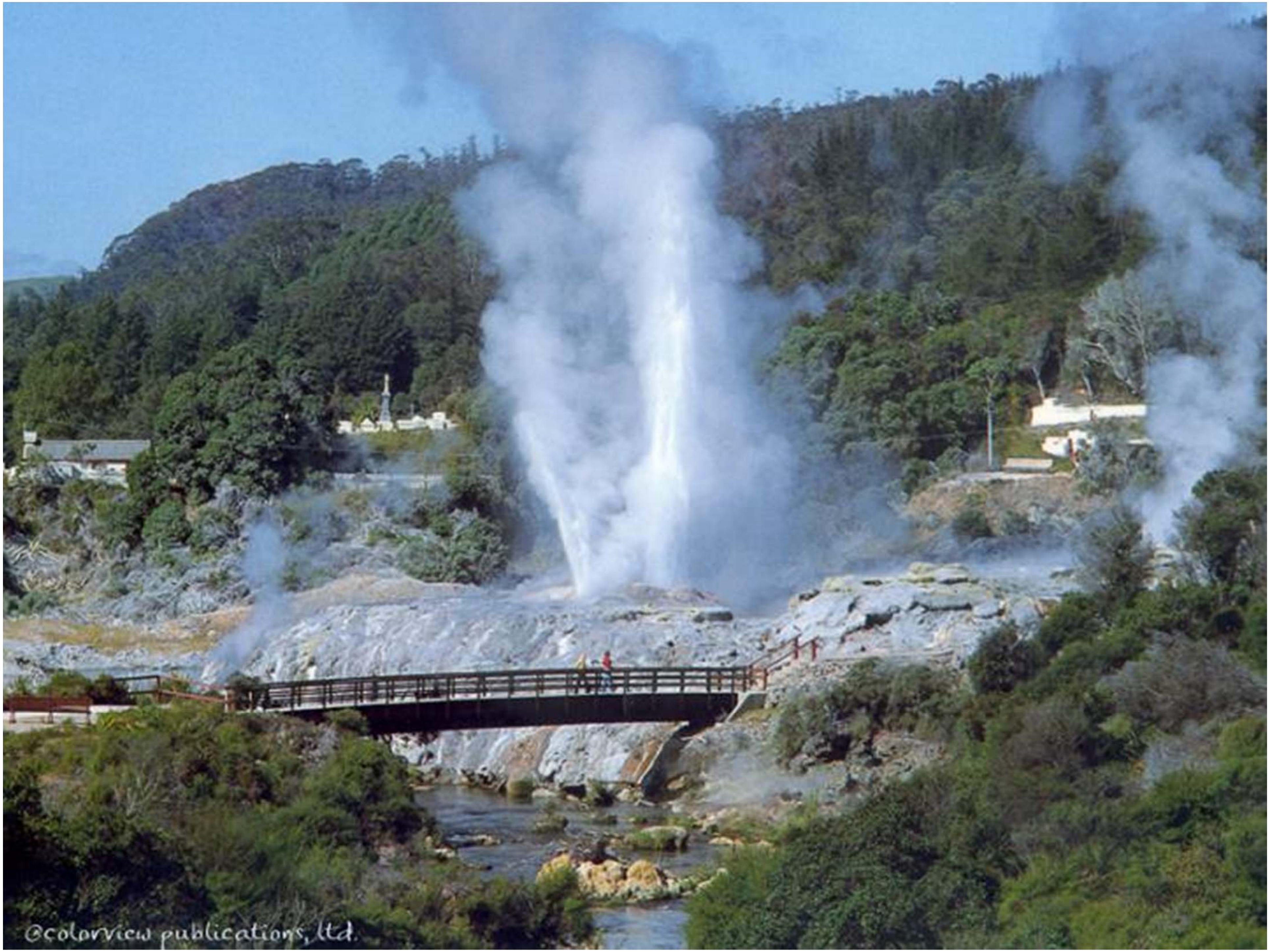
@colorview publications, ltd.

<u>Example: Hawaii Islands</u>

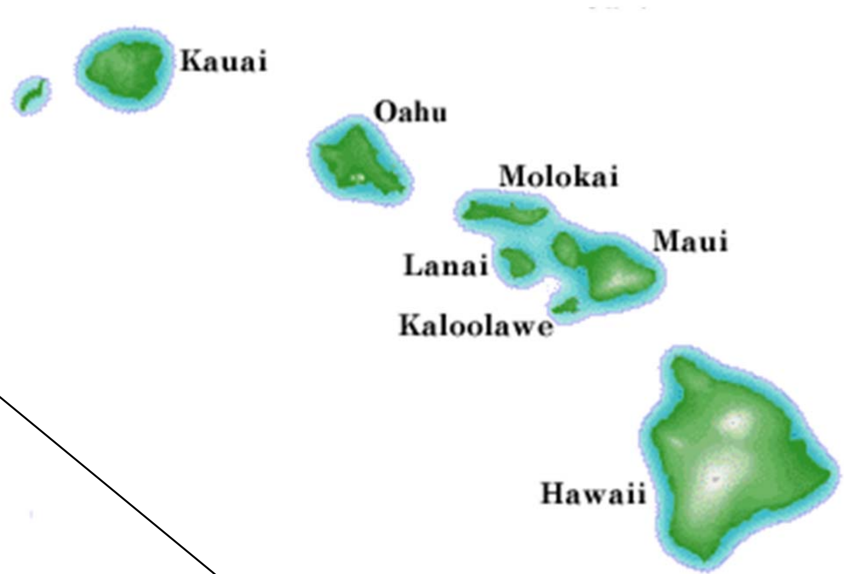

Older age

PuuOo Eruption

What do they have in Hawaii Islands?

Volcanoes – active volcanoes are everywhere in Hawaii Island

Earthquakes – tectonic earthquakes, volcano earthquakes thermal earthquakes, landslide events

No energy resource – all electricity has to depend 100% on burning imported gasoline.

Recent Volcano Eruption History in Hawaii

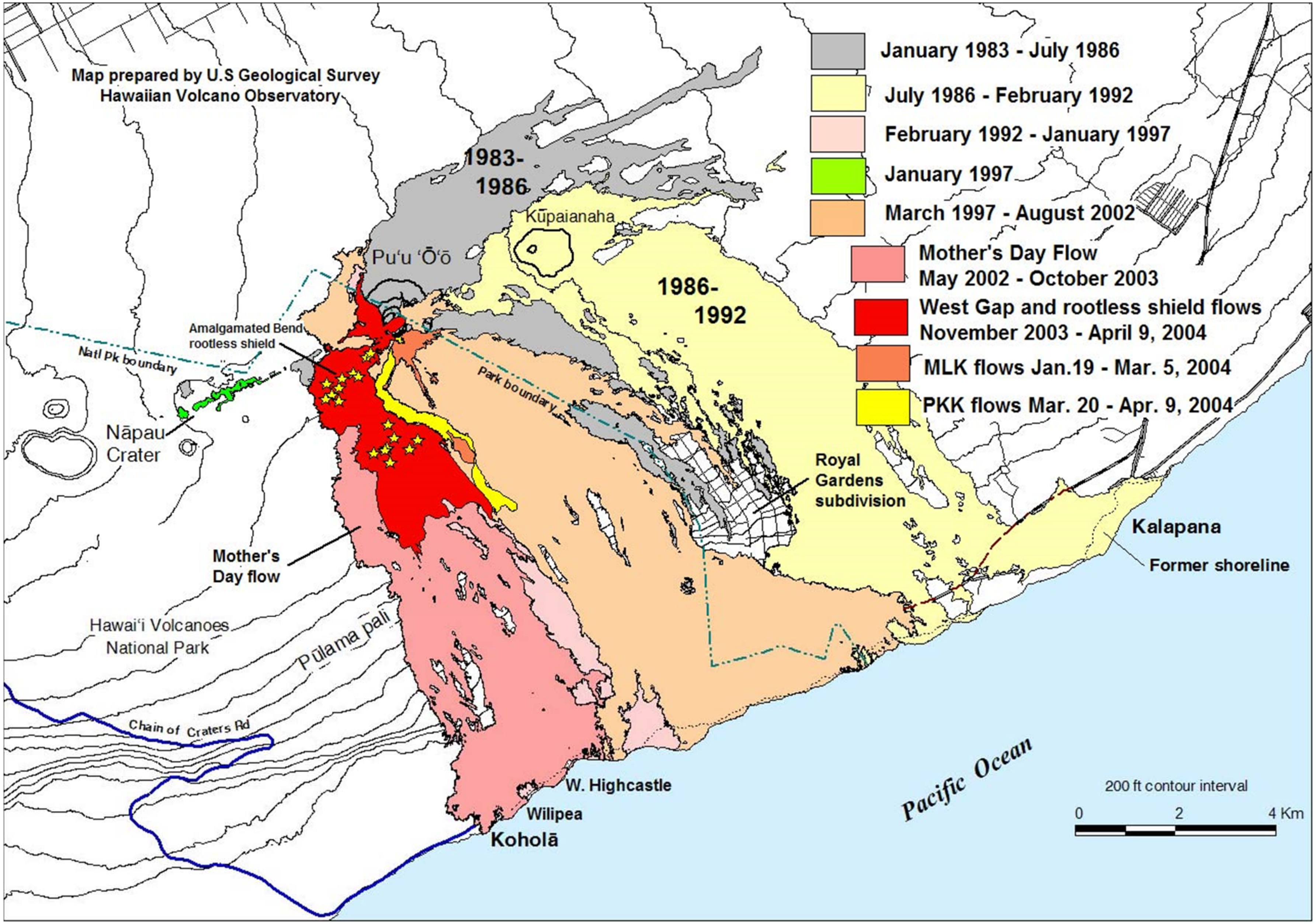

April 23, 1990 A store in Kalapana region

June 13, 1990


"Oldest Water Well In Puna"
WALTER'S
KALAPANA STORE
AND
DRIVE INN
HOT MEALS
COLD BEER
7up
WALTER & MAIZIE YAMAGUCHI

June 19, 1990

Recent Pu’uOo Volcano Eruption History in Hawaii

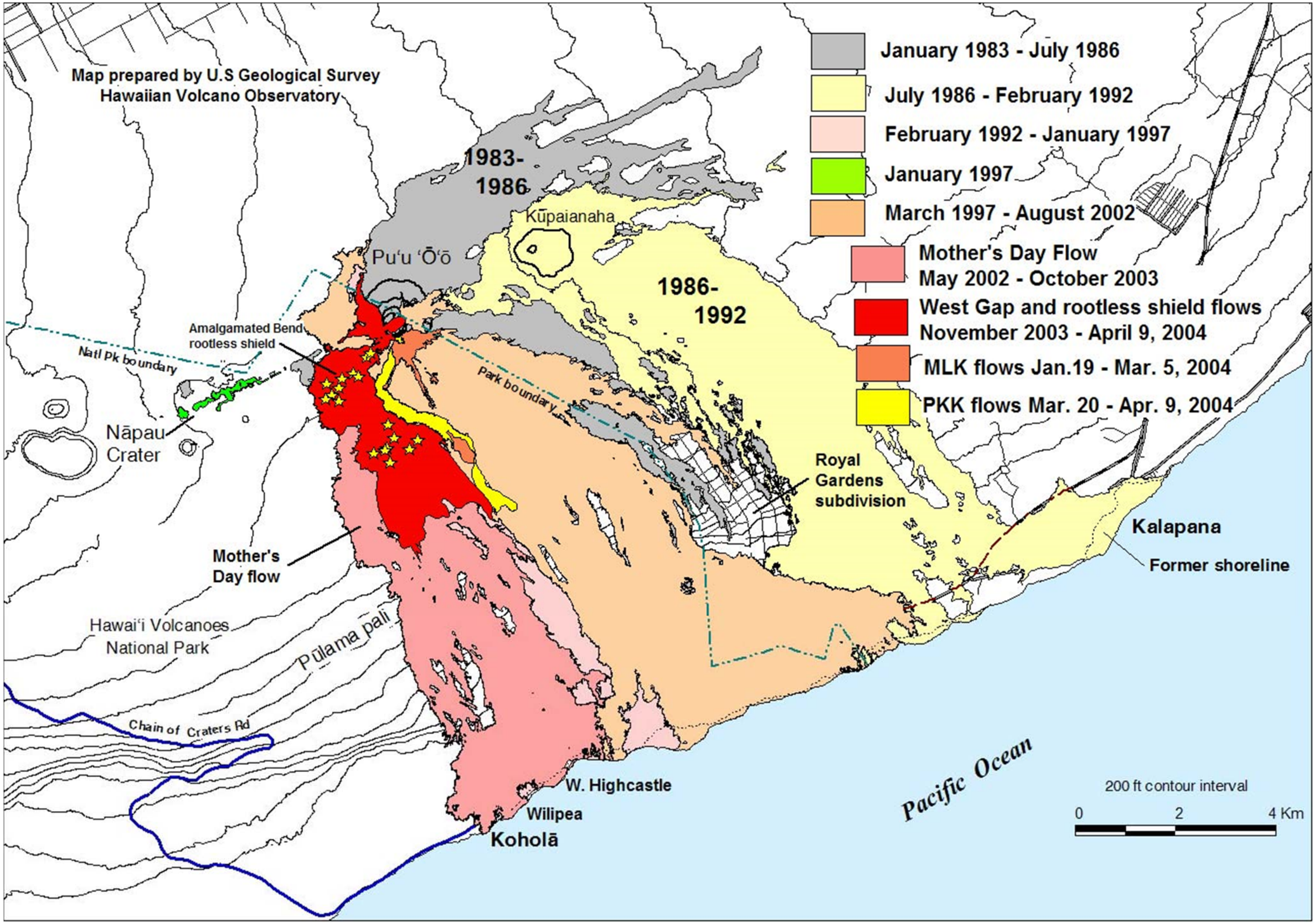

<u>Volcano eruption is predictable but it depends on continuous monitoring of temporal and spatial variations of</u>

1.earthquake activities and reliable earthquake locations(e.g. 1991 Pinatubo volcano prediction was based on the migration of microearthquake locations)
2.geochemical composition, temperature, and pressure changes of hot springs, water in crater lakes, and geysers
3.geodetic variations

However, reliable earthquake location in a volcano region is still a big <u>challenge</u> and a <u>dream</u> for seismologists. (Volcanic region and sedimentary basin are the two most in-homogeneous regions on earth)

Basic understanding of earthquake distributions in a volcanic region ----

1. **Earthquakes will not occur within a region of magma reservoir**
2. **Microearthquakes may be distributed either surrounding a partially melting magma reservoir or a magma conduit**
3. **There will be travel time delay for P-wave but no S-wave is expected across a magma reservoir**
4. **For an earthquake nearby a magma reservoir, there will be direct P- and S-waves as well as reflect P- and S-waves from the surface of magma, recorded at stations above**
5. **S-wave may experience more significant time-delay than that of P-wave traveling trough a partially melted magma reservoir.**

Typical problems encountered in trying to determine reliable earthquake locations in Volcanic region------

1.Poorly known seismic velocity structures -- very significant lateral and vertical variations of shallow structures
2.Large elevation differences of topographic reliefs between seismic stations that depth of earthquakes may be higher than some stations of lower elevations
3.Highly scattered seismic waves and high background noises that large arrival time uncertainties for seismic waves, especially the S-wave, are expected.
4.Lack of efficient computational algorithms for reliable earthquake locations.

How do we know there are magma reservoirs beneath a volcano?

$$V_p = \sqrt{\frac{\lambda + 2\mu}{\rho}}$$

$$V_s = \sqrt{\frac{\mu}{\rho}}$$

Where μ is rigidity, 0 for liquid, and ~1 for solid materials. 0~1 for partial melting materials

Therefore, we would expect a low Vp but high Vp/Vs ratio for a region of magma reservoir

Examples from Socorro magma body

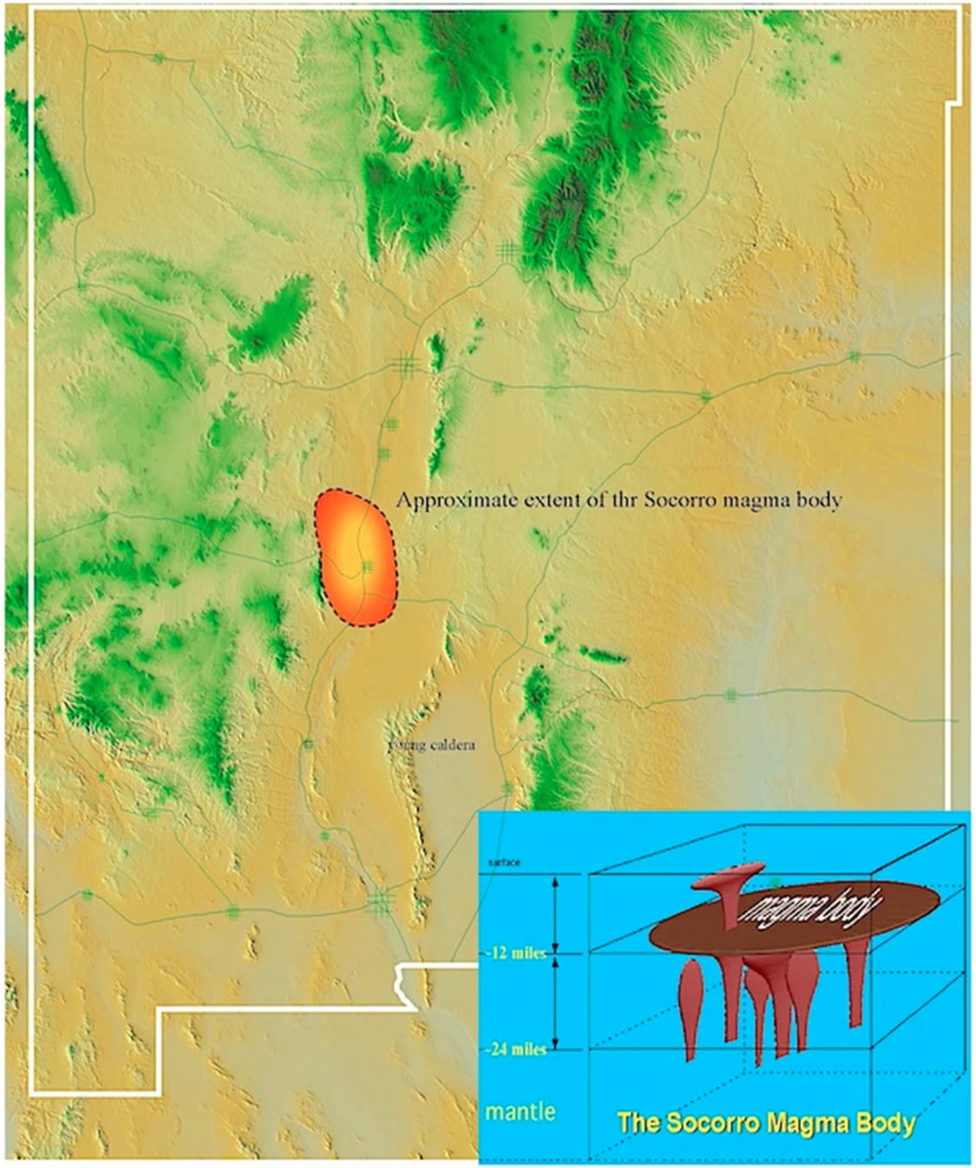

Microearthquakes occurred above and outside of the magma body

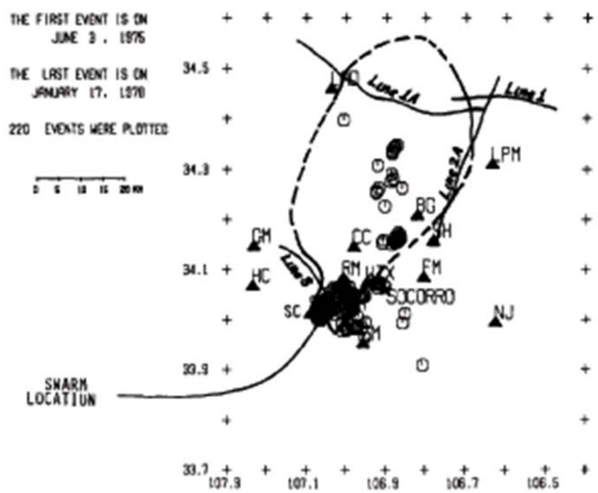

FIG. 1. Seismicity of the Socorro area for the period 3 June 1975 to 11 January 1978. Triangles mark the location of the seismograph stations operated during that time period. The outline of the mid-crustal magma body and positions of the COCORP profiles are indicated.

Direct P- and S-waves as well as reflected P- and S-waves from the surface of the magma body were observed

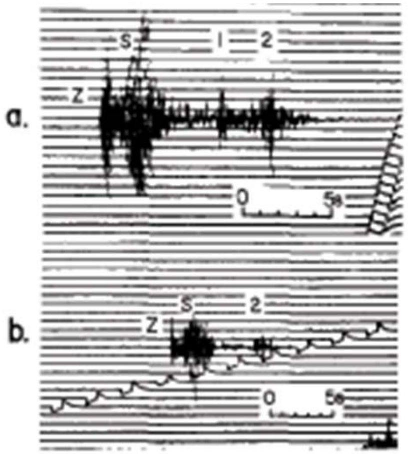

FIG. 9. Seismograms of microearthquakes with a depth of focus near zero (a) and an epicentral distance near zero (b).

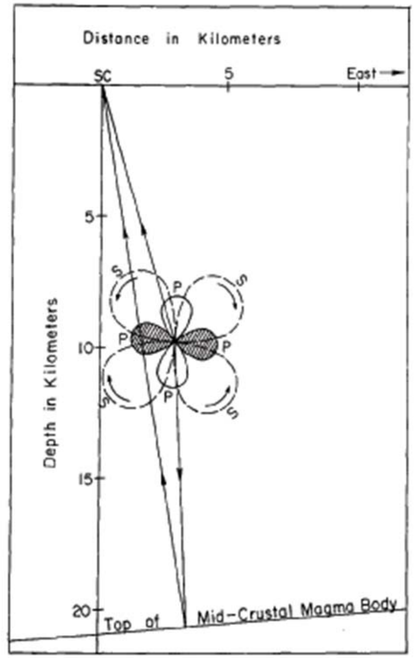

FIG. 2. Positions of microearthquake hypocenters relative to the recording station (SC) and the reflecting interface. The radiation lobes are illustrative of position but not magnitude. The ray paths for the direct and reflected phases are indicated. The focal mechanism appears to be well-constrained. A very limited amount of rotation of the nodal planes is permissible; however, it is not enough to change the relative polarity of the direct and reflected phases.

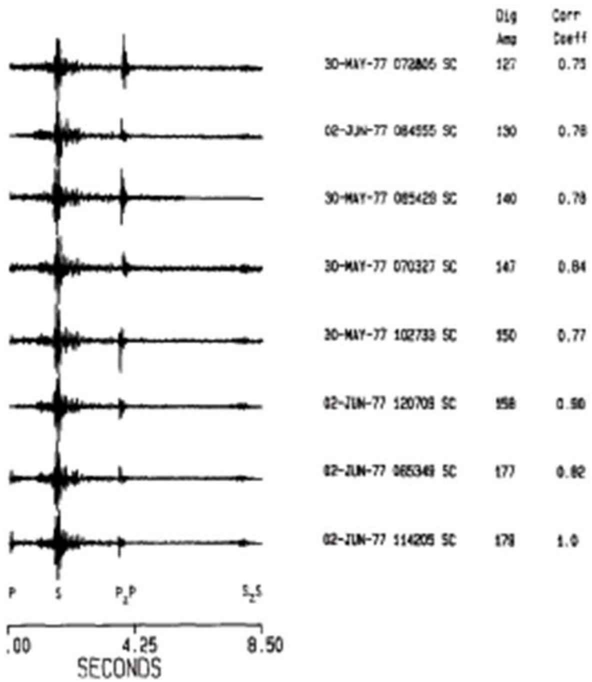

FIG. 3. Seismograms showing direct P and S phases and reflected P_2P and S_2S phases. Magnitudes of the events are all less than zero. Amplitudes have been normalized for plotting. Maximum digital amplitudes and cross-correlation coefficients relative to the last earthquake are listed for each event. For some events, either the beginning or ending of the earthquake was not recorded and appears as a straight line. The sampling interval is 0.01 sec. Recordings are for ground velocity.

Significant travel time delay and filtering as well as attenuation of high frequency seismic waves, especially S-waves are expected across a magma reservoir

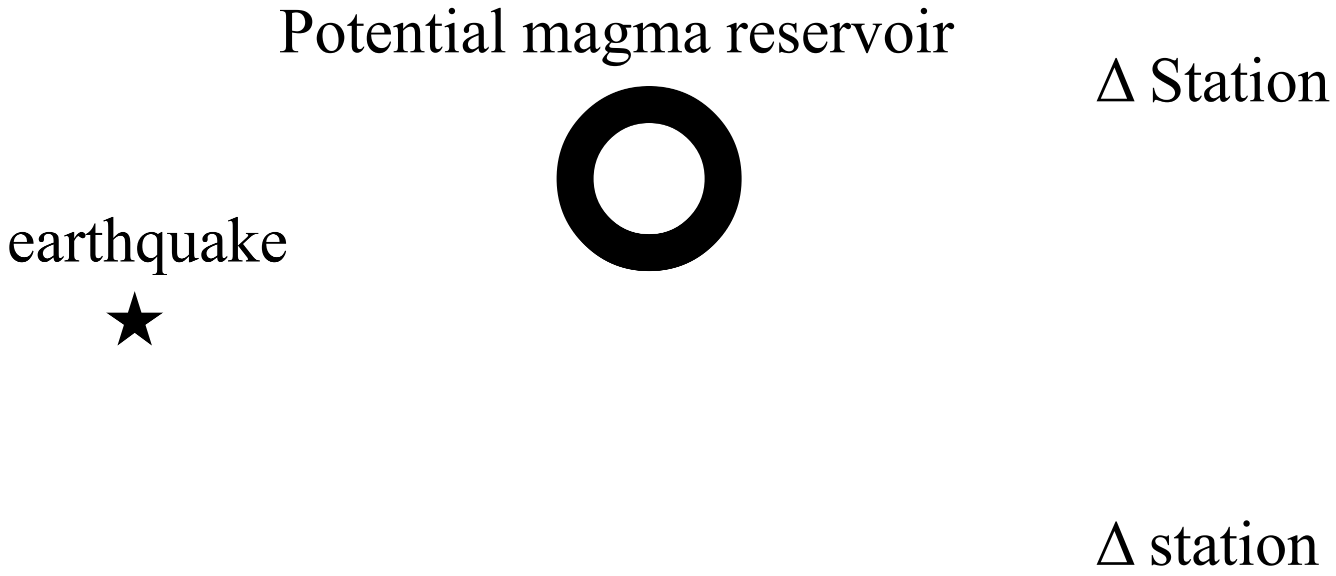

Examples from northern Honshu, Japan

A few east-west cross-sectional views of P-wave velocity perturbations from 3-D inversion of P-wave only (left) and P+PmP waves (right) (from Xia et al., 2007)

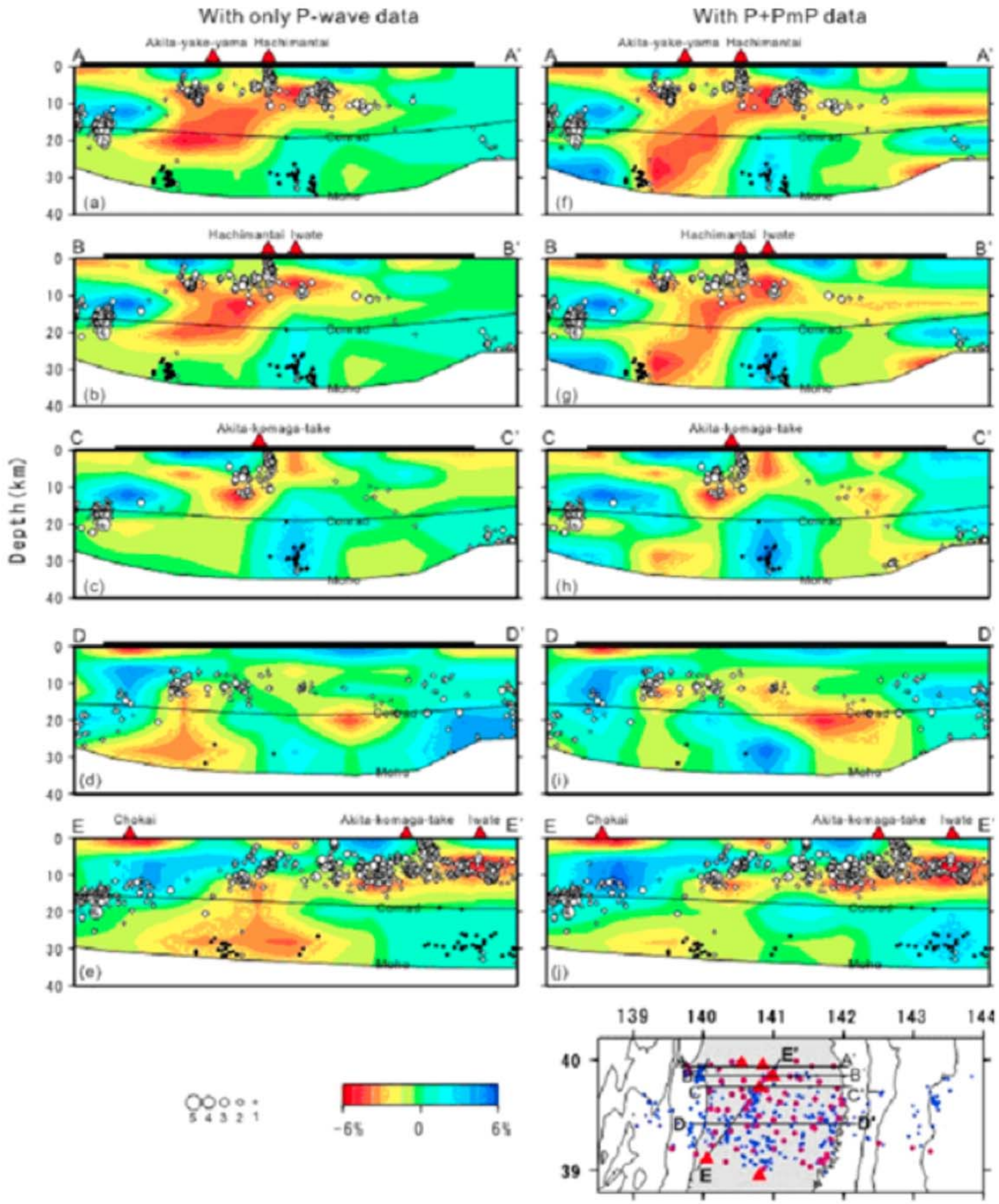

Examples from Tatung Volcanoes, Taiwan

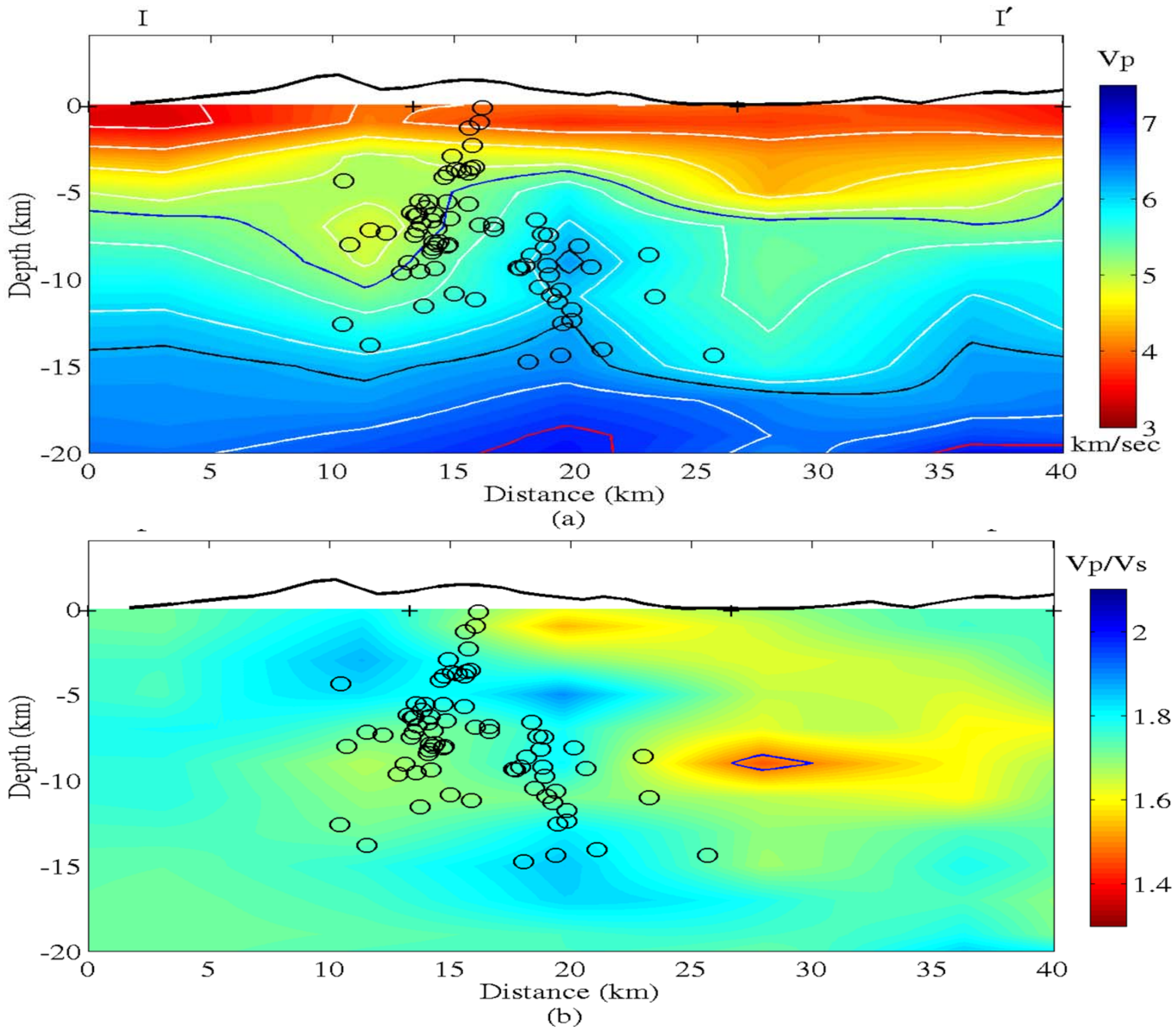

Cross-section of Vp (top) and Vp/Vs ratio across the Tatung-Chilung volcanic group where volcanism ceased in Pliocene. The low Vp but high Vp/Vs ratio beneath the volcano may suggest a potential of partially melted magmatic reservoir at shallow depth.

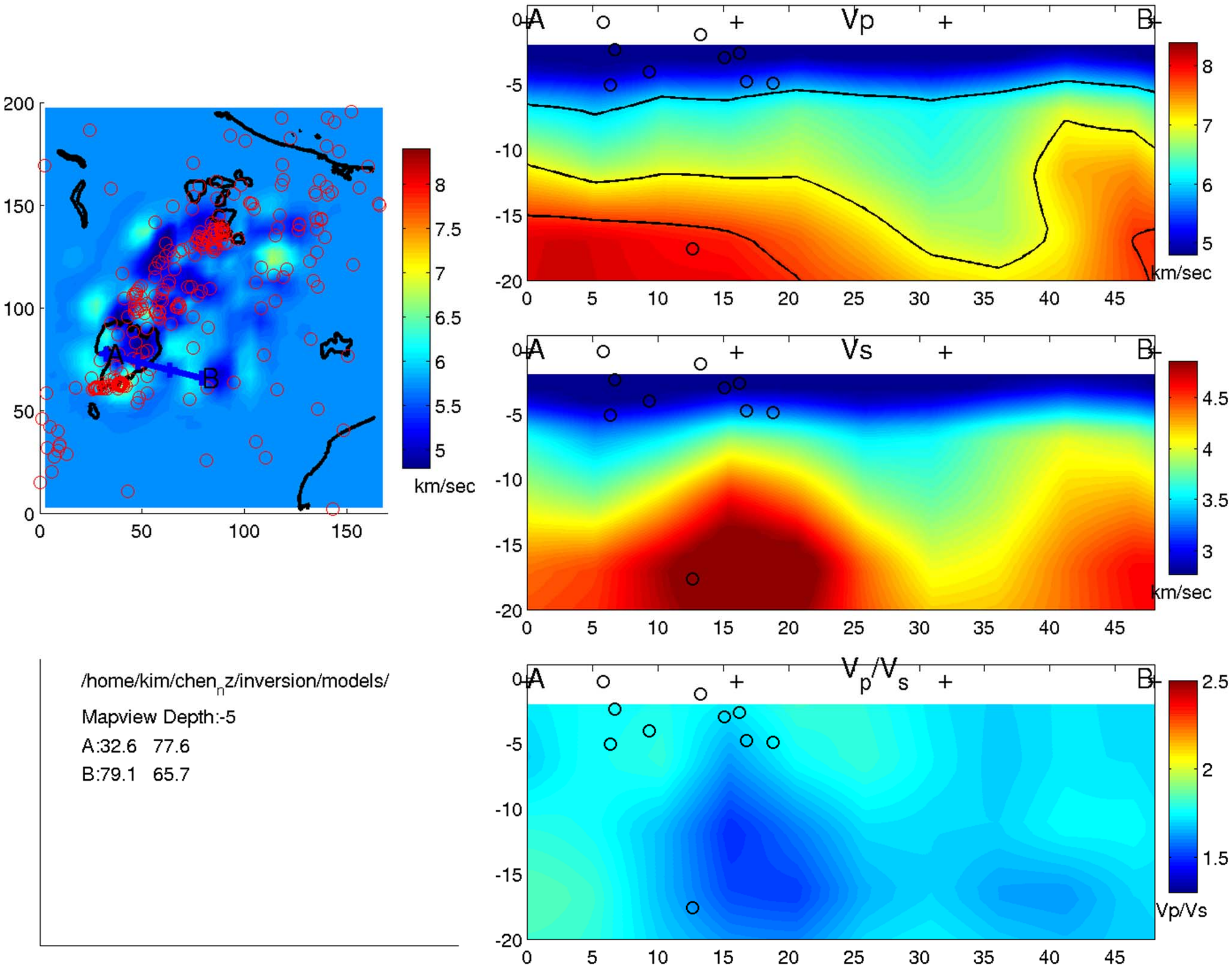

A
B
Vp
Vs
V_p/V_s
km/sec
Vp/Vs
/home/kim/chen_nz/inversion/models/
Mapview Depth:-5
A:32.6 77.6
B:79.1 65.7

How to quantify lateral structure variations apparent on surface geology?

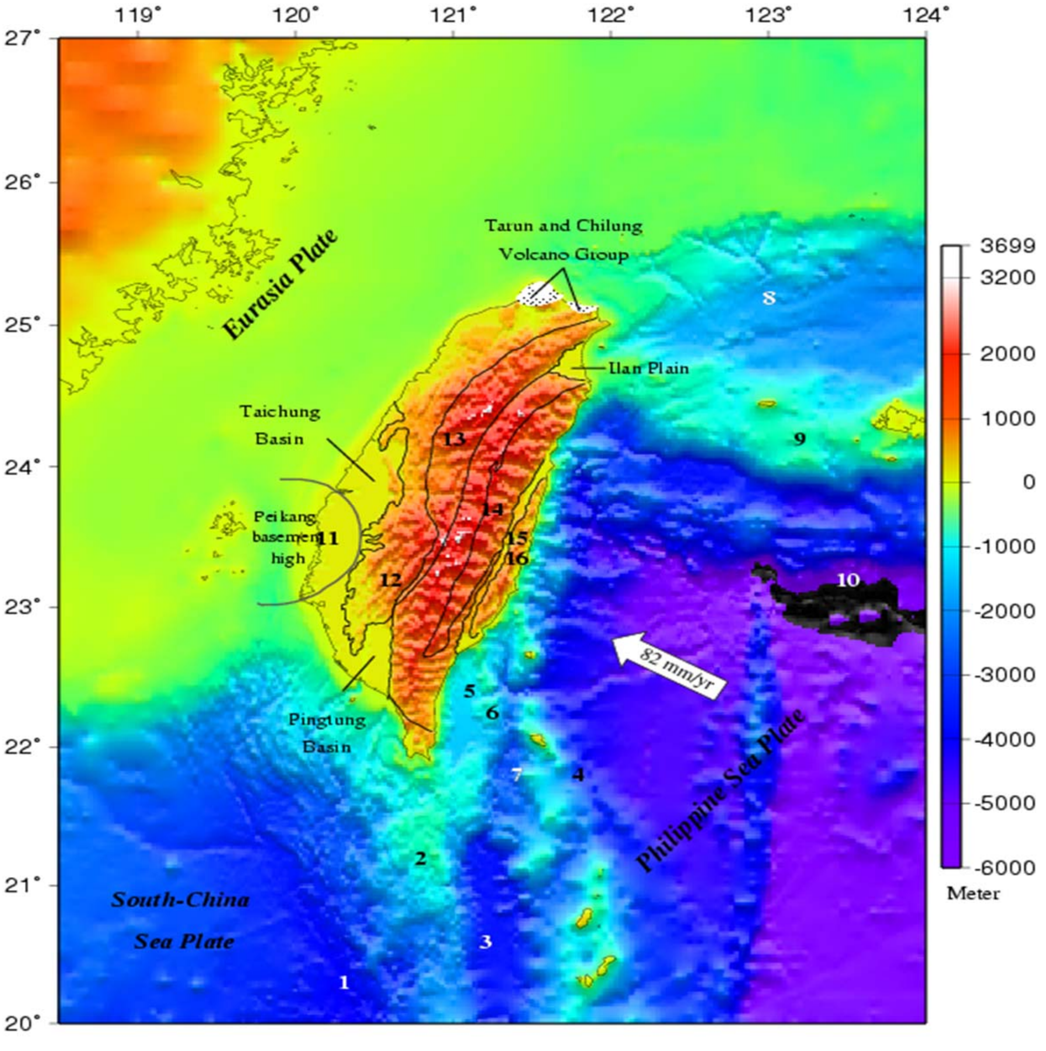

Why lateral variations of topography and near-surface geology are important?

Existing Island-wide 3-D Velocity Models

- **Rau and Wu (1995) –A 3-D Vp model for the entire Taiwan region was determined using Cliff Thurber’s inversion program, earthquakes were relocated to infer the “Lithospheric Deformation Model (Wu, 1997)”**
- **Ma and Zhao (1996) – A 3-D Vp model was also determined using D.P. Zhao’s inversion program**

Existing Island-wide 3-D Velocity Models

- **Kim, et al., (2005)**
- **Wu, et al., (2007)**
- **Kou-Chen, et al., (2011)**

P-wave travel time residuals from anti-pole earthquakes reported by B.S. Huang (1998)

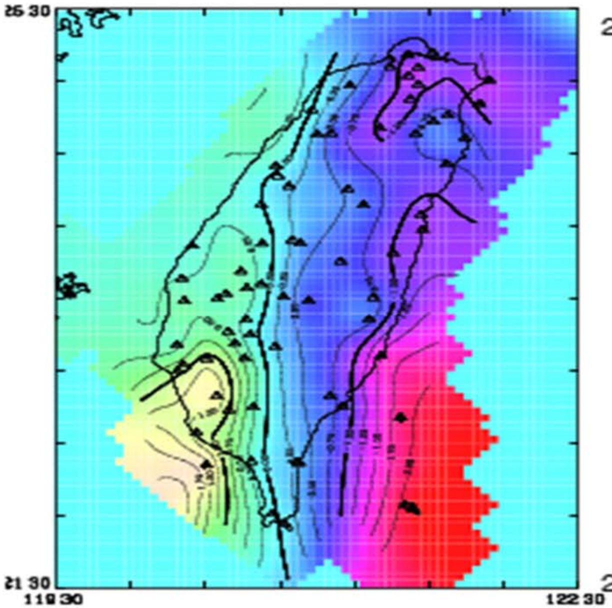

P-wave travel time residuals generated from 3D model of Rau and Wu (1995)

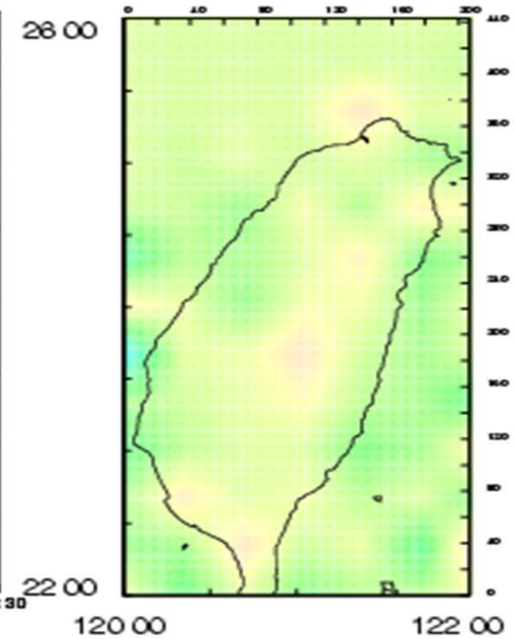

P-wave travel time residuals generated from 3D model of Ma and Zhao (1996)

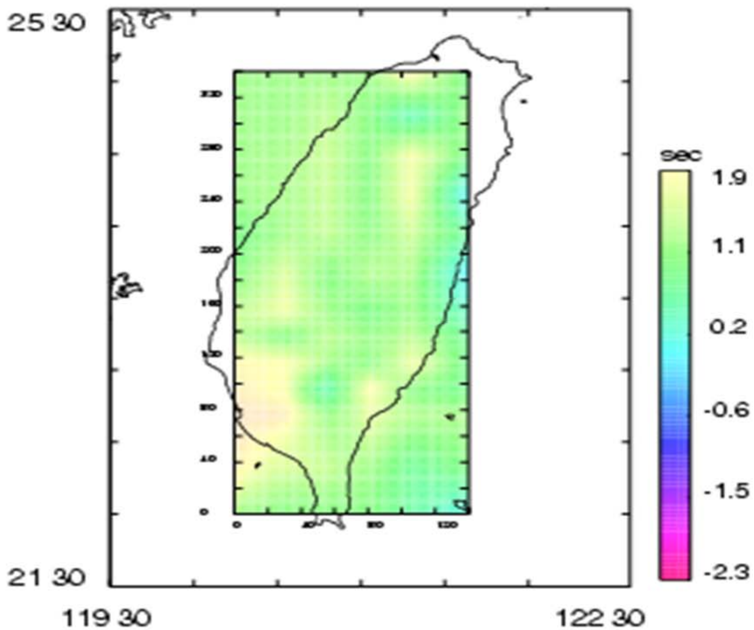

P-wave travel time residuals from crustal earthquakes recorded by PANDA array (Chen 1997)

P-wave travel time residuals from anti-pole earthquakes reported by B.S. Huang (1998)

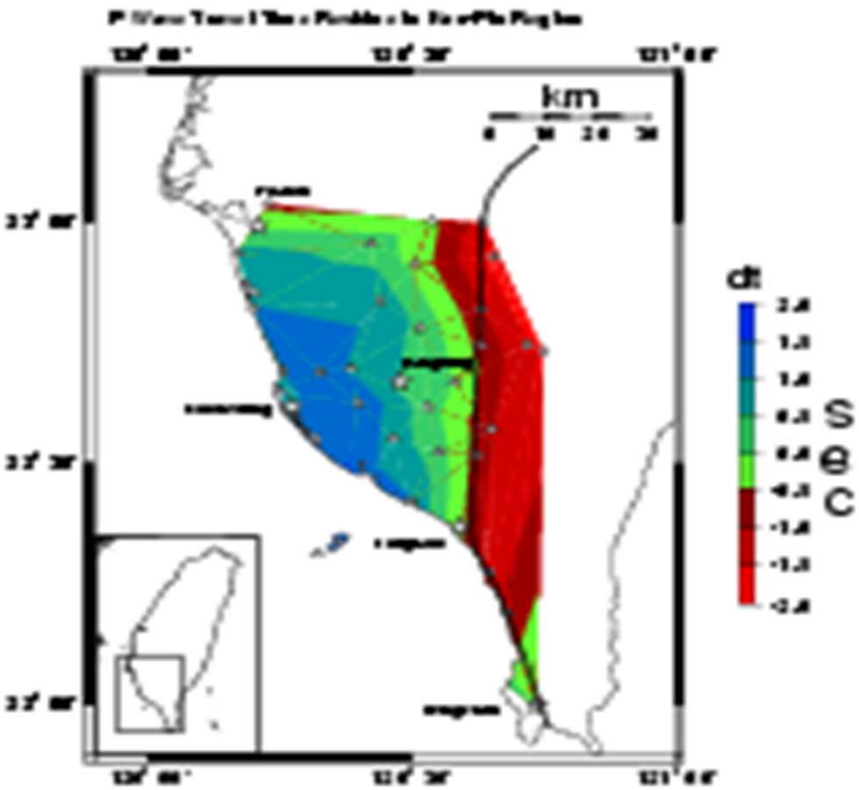

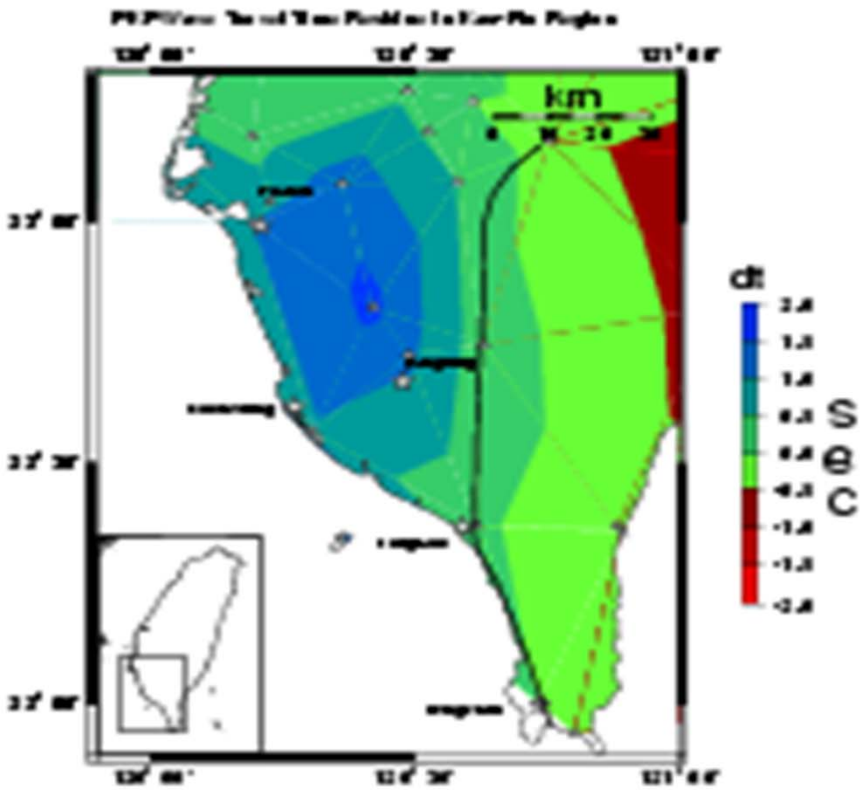

P-wave travel time residuals from anti-pole earthquakes reported by B.S. Huang (1998)

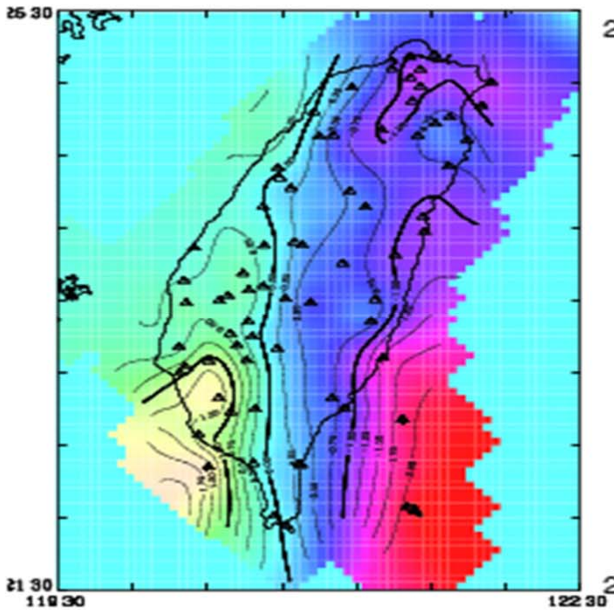

P-wave travel time residuals generated from 3D model of Rau and Wu (1995)

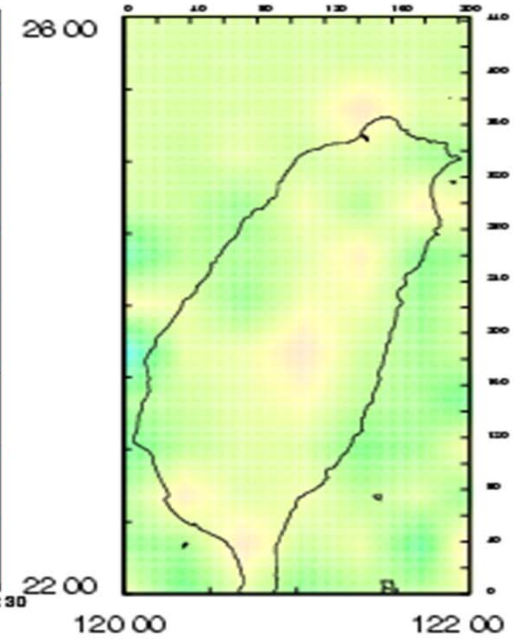

P-wave travel time residuals generated from 3D model of Ma and Zhao (1996)

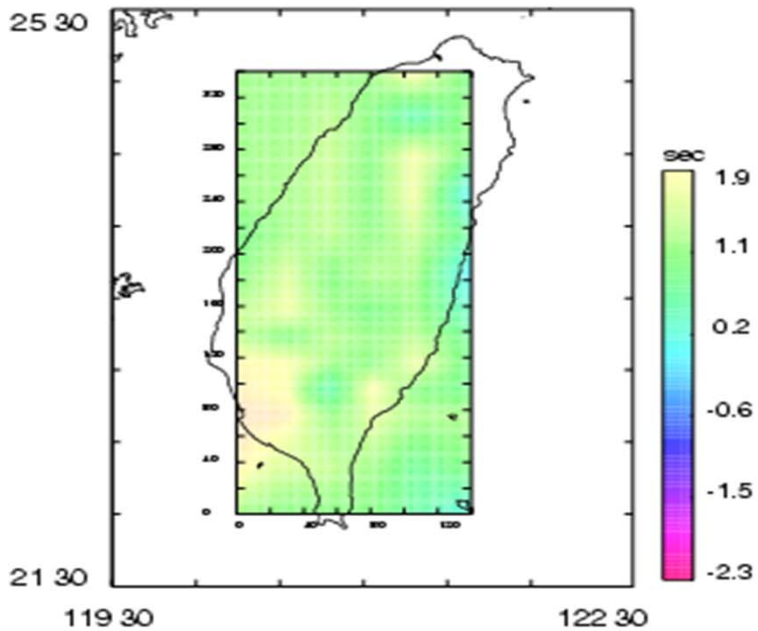

Conclusion – the observed P-wave travel time residuals from the anti-pole earthquakes must be generated mainly from upper crust. Questions are why the existing two 3-D crust and upper mantle models fail to explain the observed travel time residuals apparent from the surface geology?

Therefore our challenges are:

Why traditional 3-D tomographic imaging techniques doesn’t work in Taiwan region?

How can we improve it in order to obtain a comprehensive 3-D structural images beneath Taiwan region?

Our Approaches

1. **Evaluate the spatial structural resolution of the current seismic station configuration and earthquake distribution – *what's to expect*?**

2. **Quantify lateral structural variations, especially for shallow crust -- *how will they affect on earthquake location? and structure resolution?***

3. **Determine reliable 3-D Vp and Vs models ---*how to validate the resultant models?***

4. **Develop a new algorithm to locate all earthquakes using the resultant 3-D models ---*can earthquakes be reliably located?***

5. **Interpret and model the results base on the resultant 3-D velocity images and the best relocated seismicity --- *what can we learn when all the ambiguities are minimized?***

5 groups of clustered earthquakes are randomly selected for the JHD analysis to quantify the significance of lateral structural variations in Taiwan region. Station corrections created from the JHD analysis represent the discrepancies of the real earth structure in the region from a “homogeneous layered model”.

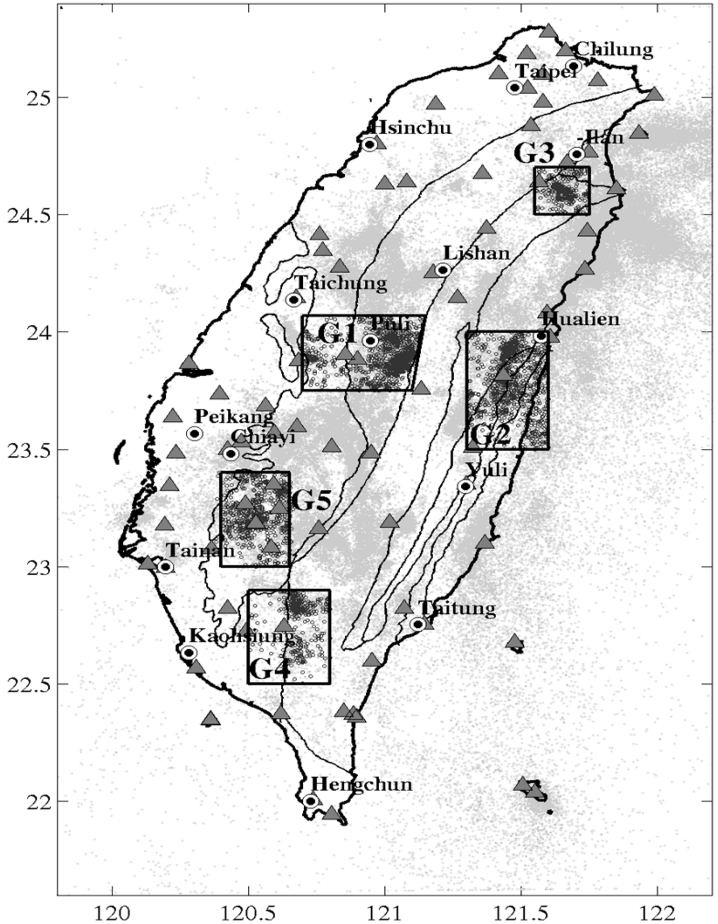

P-station corrections

S-station corrections

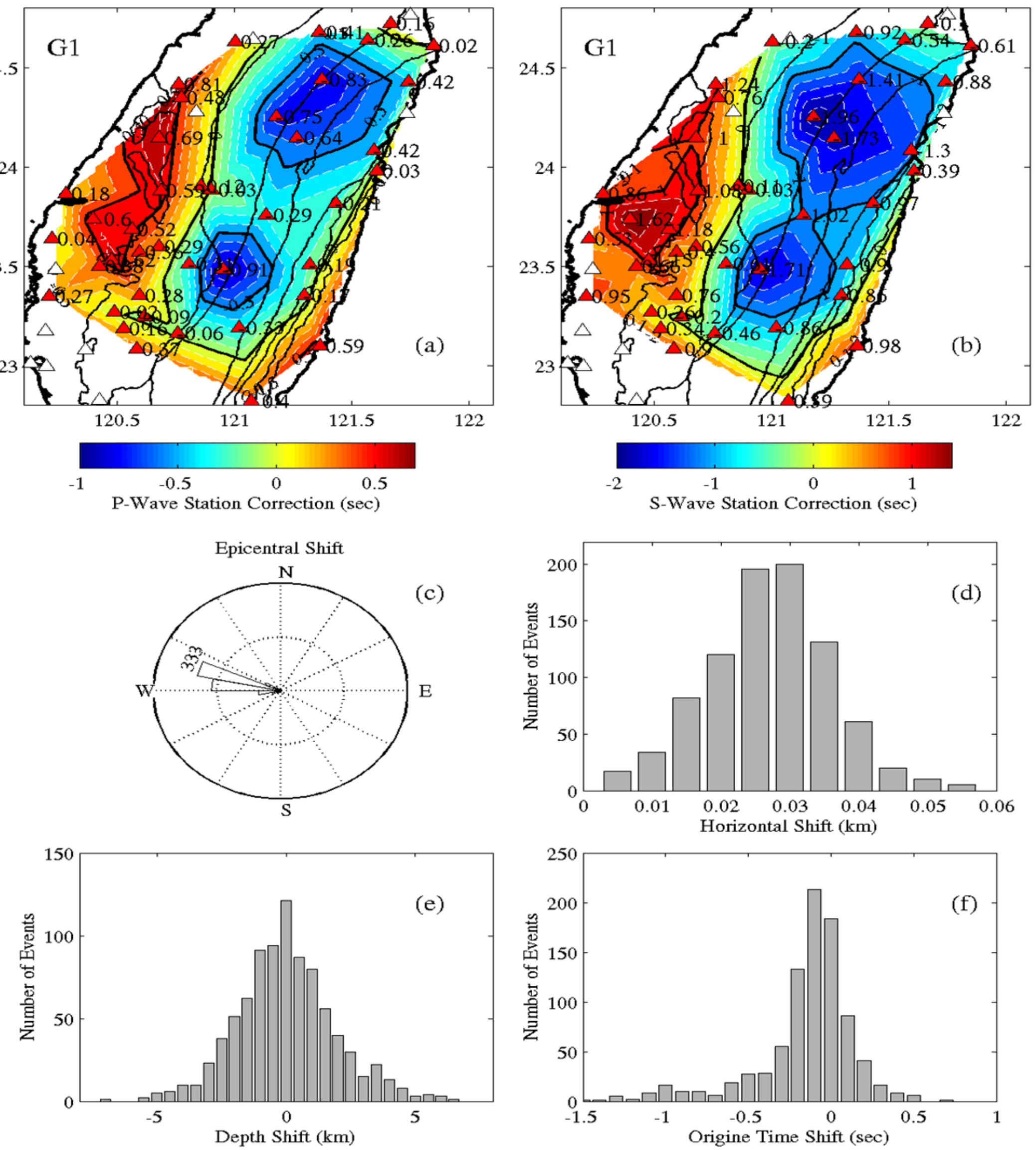

P-station corrections S-station corrections

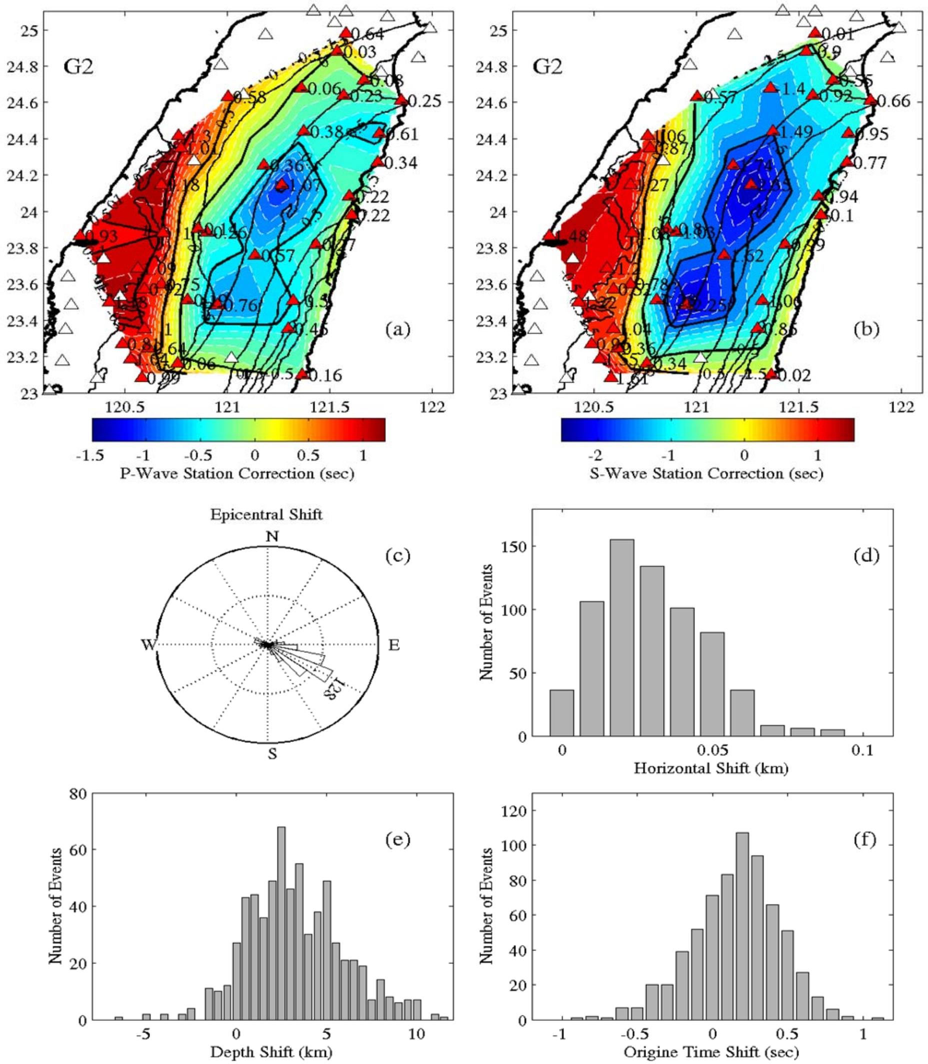

P-station corrections   S-station corrections

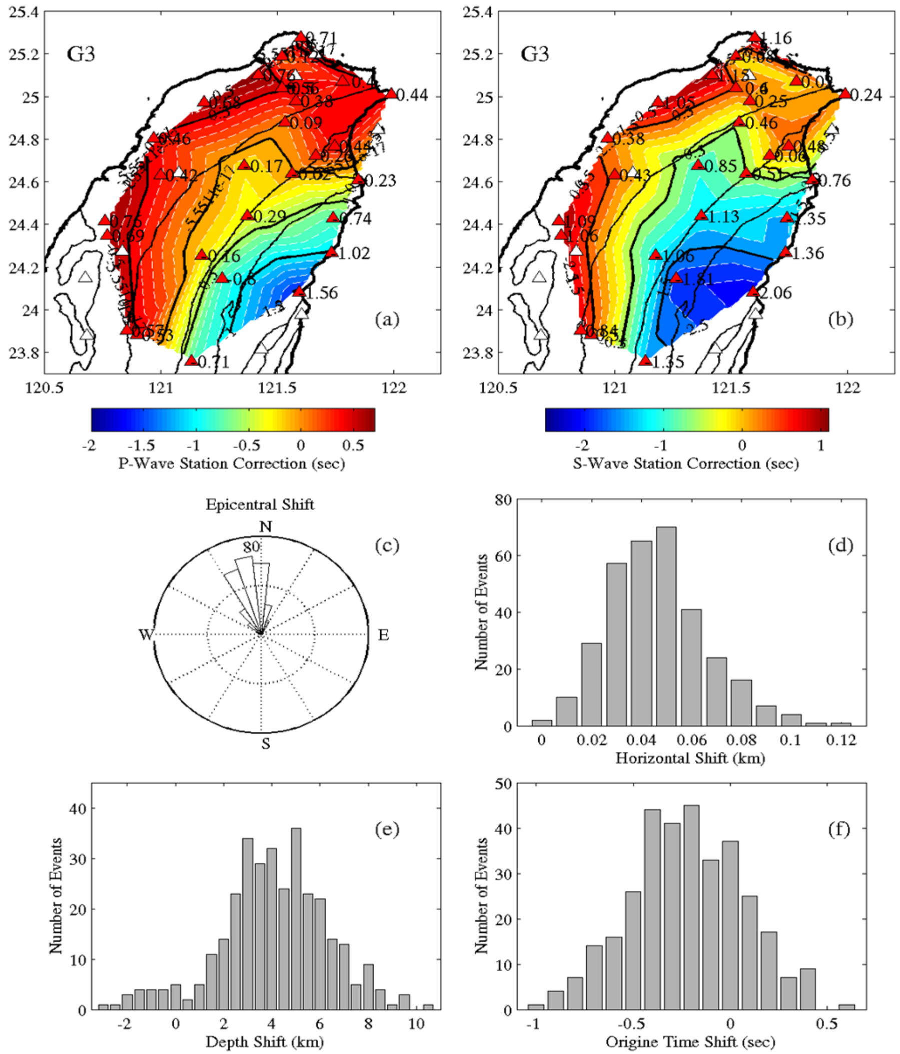

P-station corrections

S-station corrections

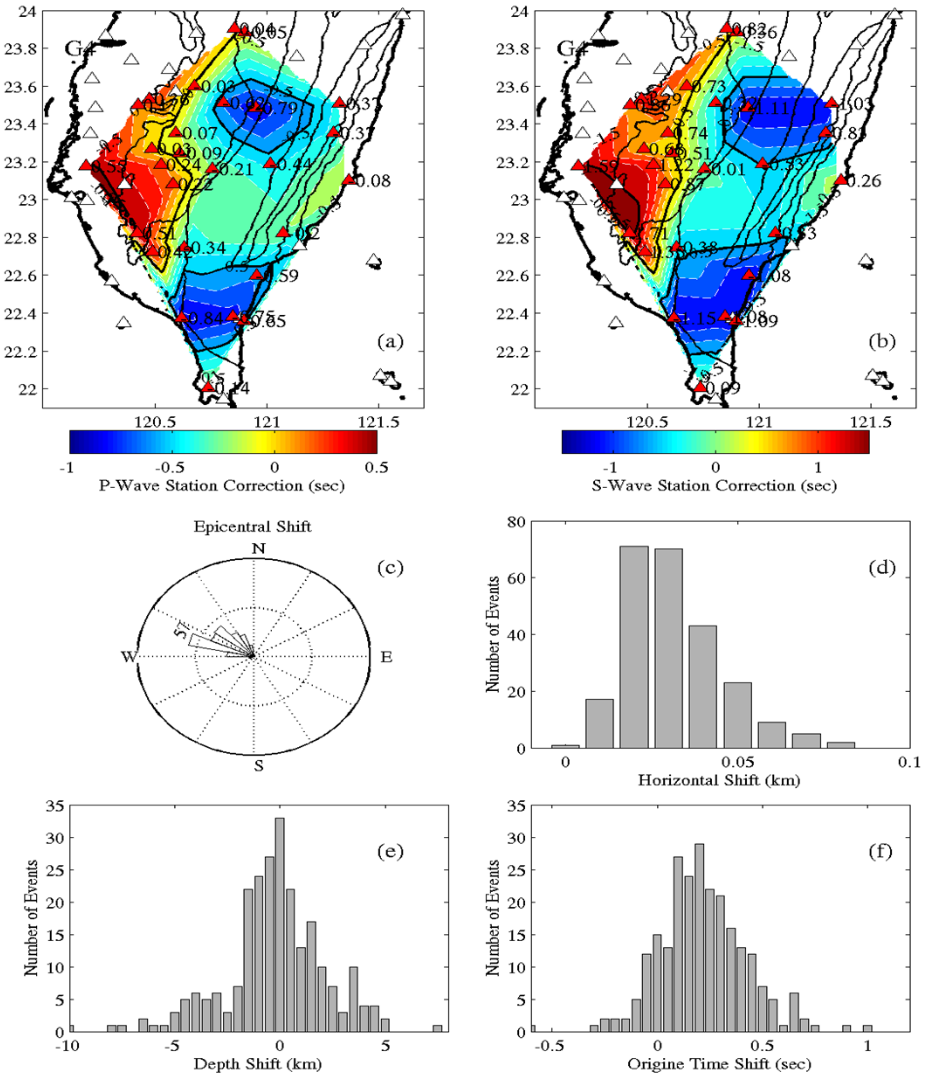

P-station corrections   S-station corrections

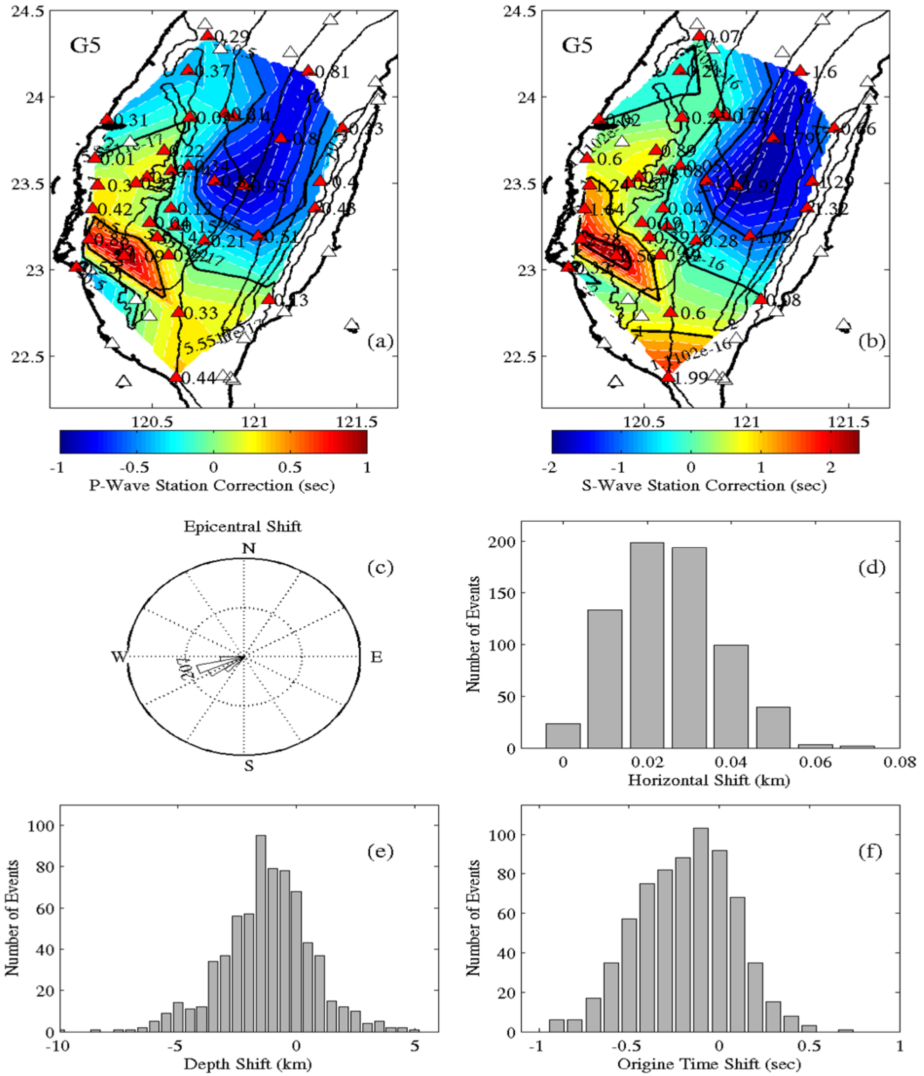

Our Approaches

1. **Evaluate the spatial structural resolution of the current seismic station configuration and earthquake distribution – *what's to expect*?**

2. **Quantify lateral structural variations, especially for shallow crust -- *how will they affect on earthquake location? and structure resolution?***

3. **Determine reliable 3-D Vp and Vs models ---*how to validate the resultant models?***

4. **Develop a new algorithm to locate all earthquakes using the resultant 3-D models ---*can earthquakes be reliably located?***

5. **Interpret and model the results base on the resultant 3-D velocity images and the best relocated seismicity --- *what can we learn when all the ambiguities are minimized?***

Processes to Determine <u>Reliable 3-D Vp and Vs Models</u> and to <u>Relocate all Earthquakes</u>

(1) P- and S-wave travel time residuals are implemented into an initial velocity model for a 3-D tomographic inversion – especially for the upper crust

(2) Select the best quality of earthquakes from a regional seismic network for a 3-D tomographic inversion (usually about 5~10% of data are selected)

(3) Relocate all earthquakes in the catalog using the resultant 3-D Vp and Vs velocity models.

Earthquake data recorded in Taiwan region from 1991 to 2002 are selected and analyzed

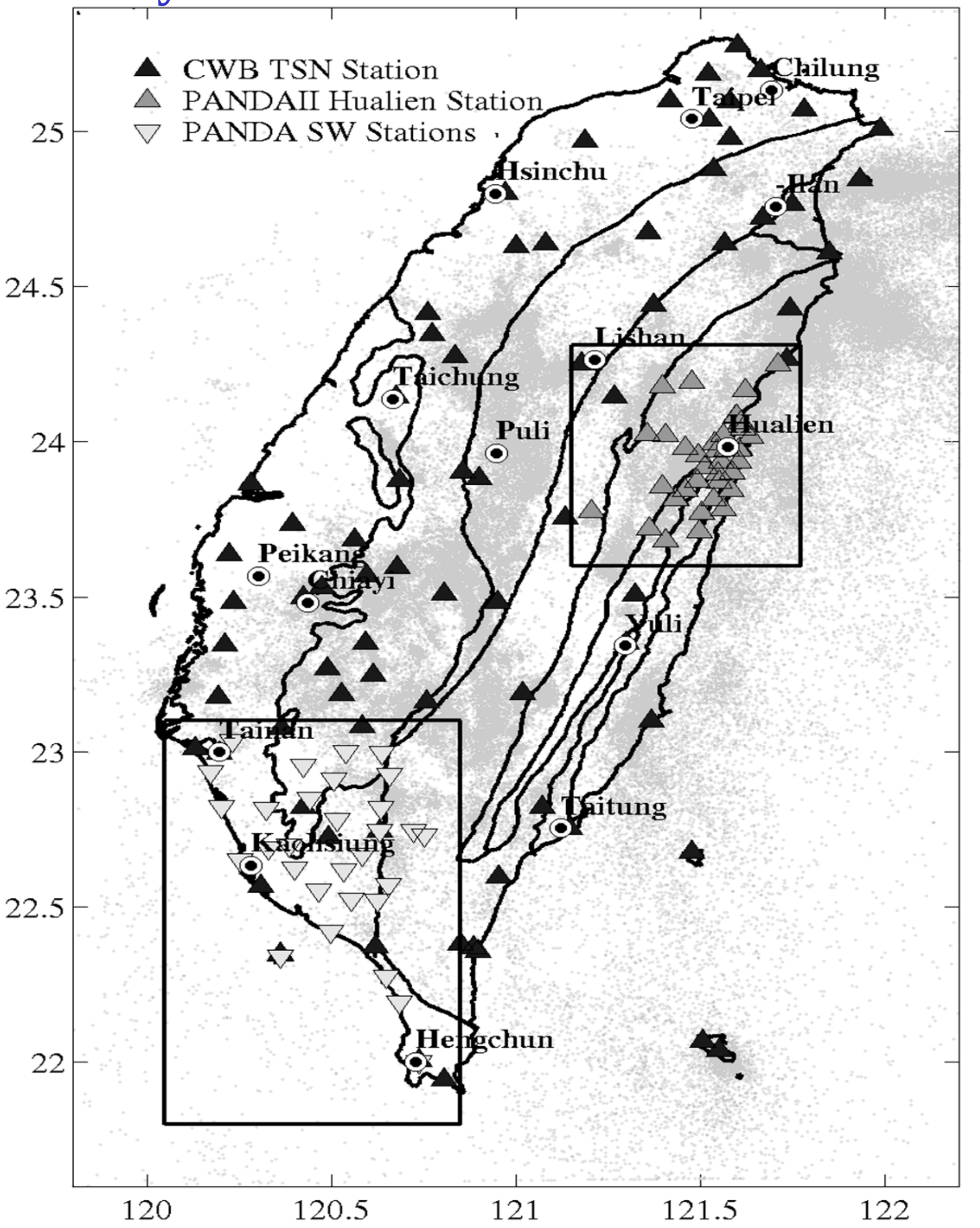

Thin-sliced Vp anomalies at various depths from 3-D inversion

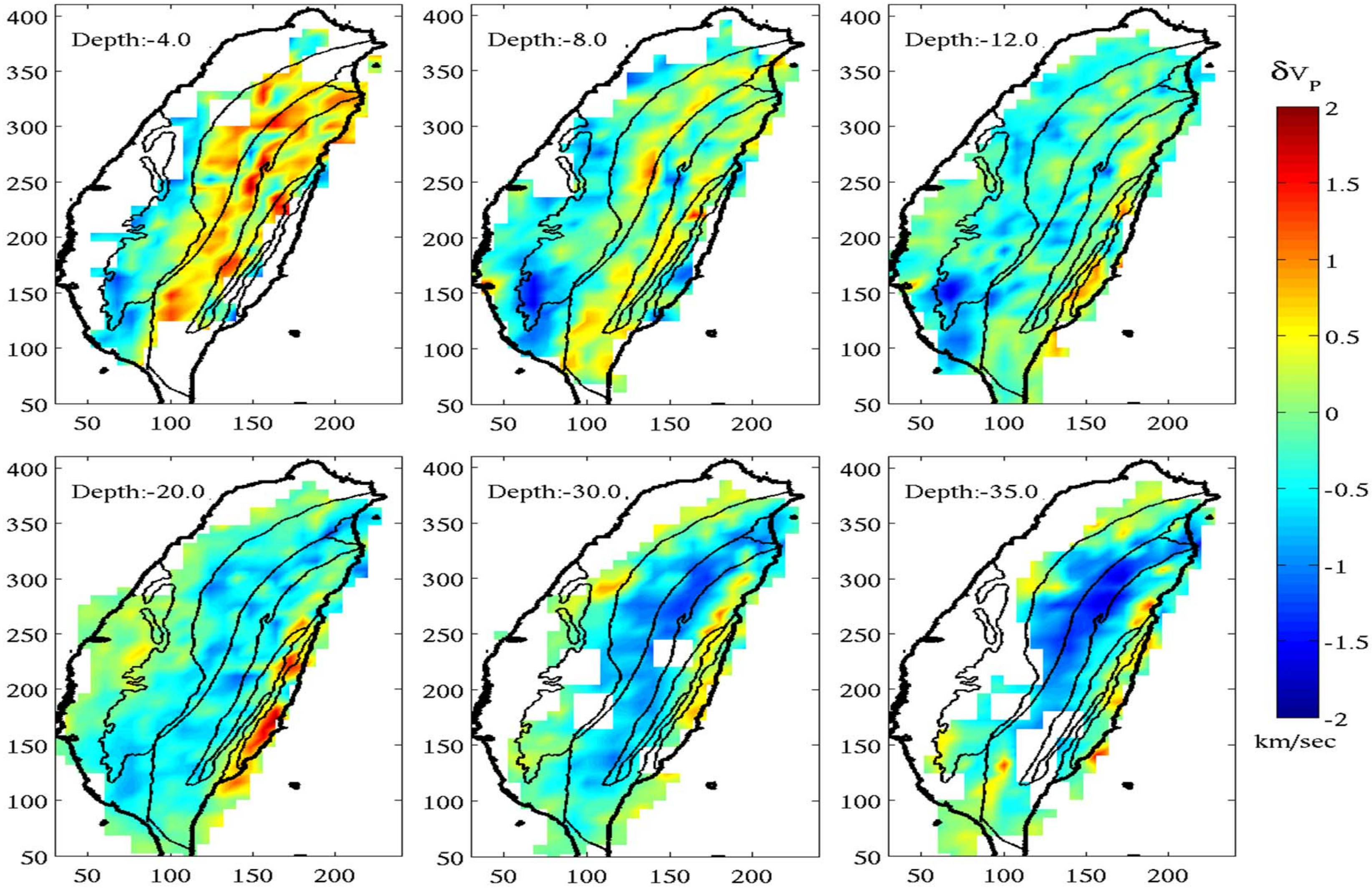

The high-velocity mountain region becomes low velocity at mid-to-lower crust

Thin-sliced Vs model at various depths

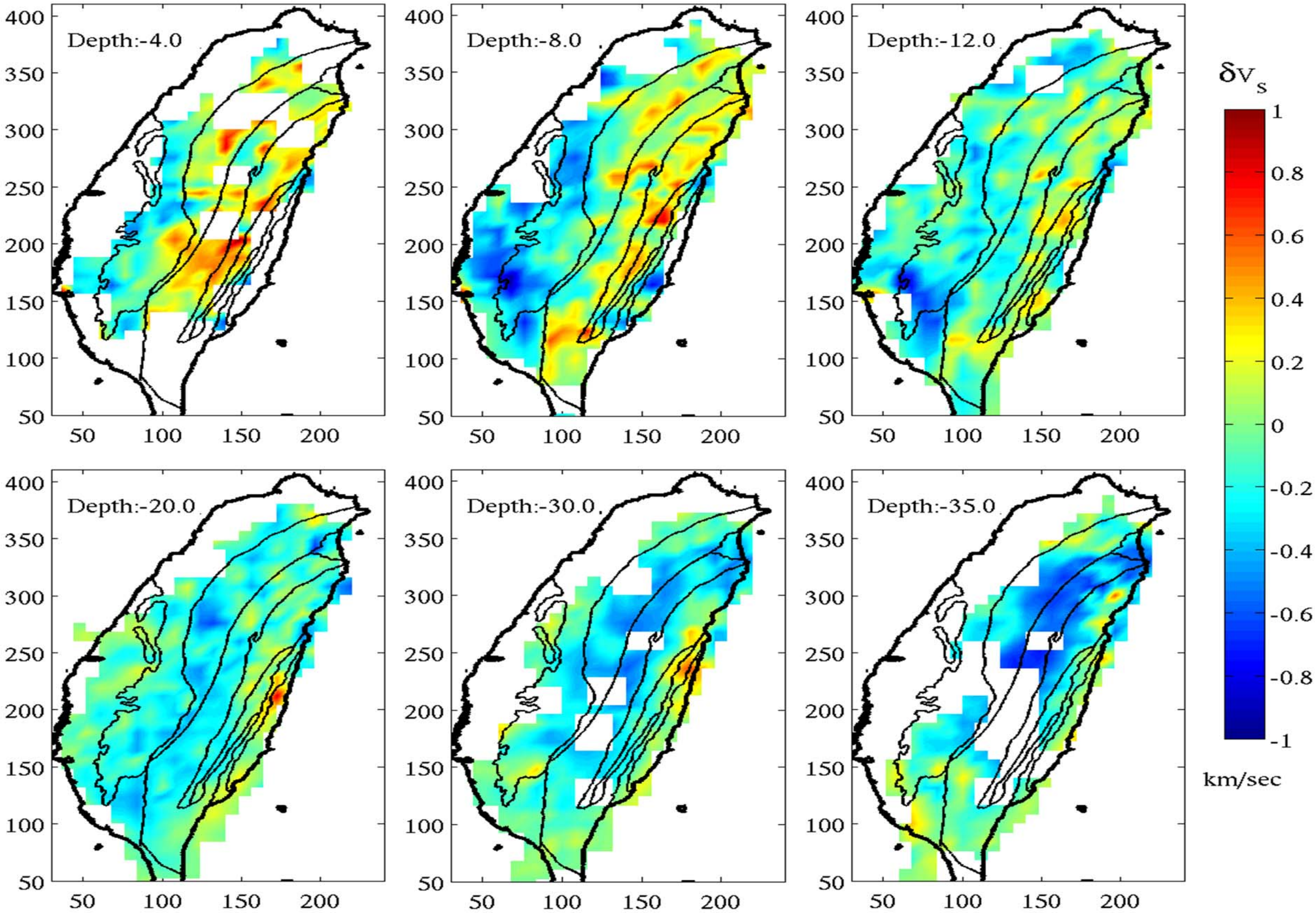

The high-velocity mountain region becomes low velocity at mid-to-lower crust

How do you know that the resultant 3-D structural images are different or better than any previous or other studies?

Three independent tests can be applied to verify the resultant 3-D Vp and Vs models

They are

- **Synthetic test to verify 3D inversion results using the JHD method**
- **Verify suture zone structure from a modeling of anomalous propagation of Pn waves**
- **Comparison of the observed gravity data with that converted from the resultant velocity models**

1. Synthetic test to verify 3D inversion results using the JHD method

1. Calculate P- and S-wave travel times using the resultant 3-D Vp and Vs model
2. Determine P- and S-wave station corrections using JHD method
3. compared the synthetic P- and S-wave station corrections with those obtained from the observed data.

The amplitudes and patterns of the observed and synthetic P- and S-wave station corrections should be similar if the resultant 3-D Vp and Vs model is close to the real earth

5 groups of clustered earthquakes are selected for the JHD analysis to quantify the significance of lateral structural variations in Taiwan region.

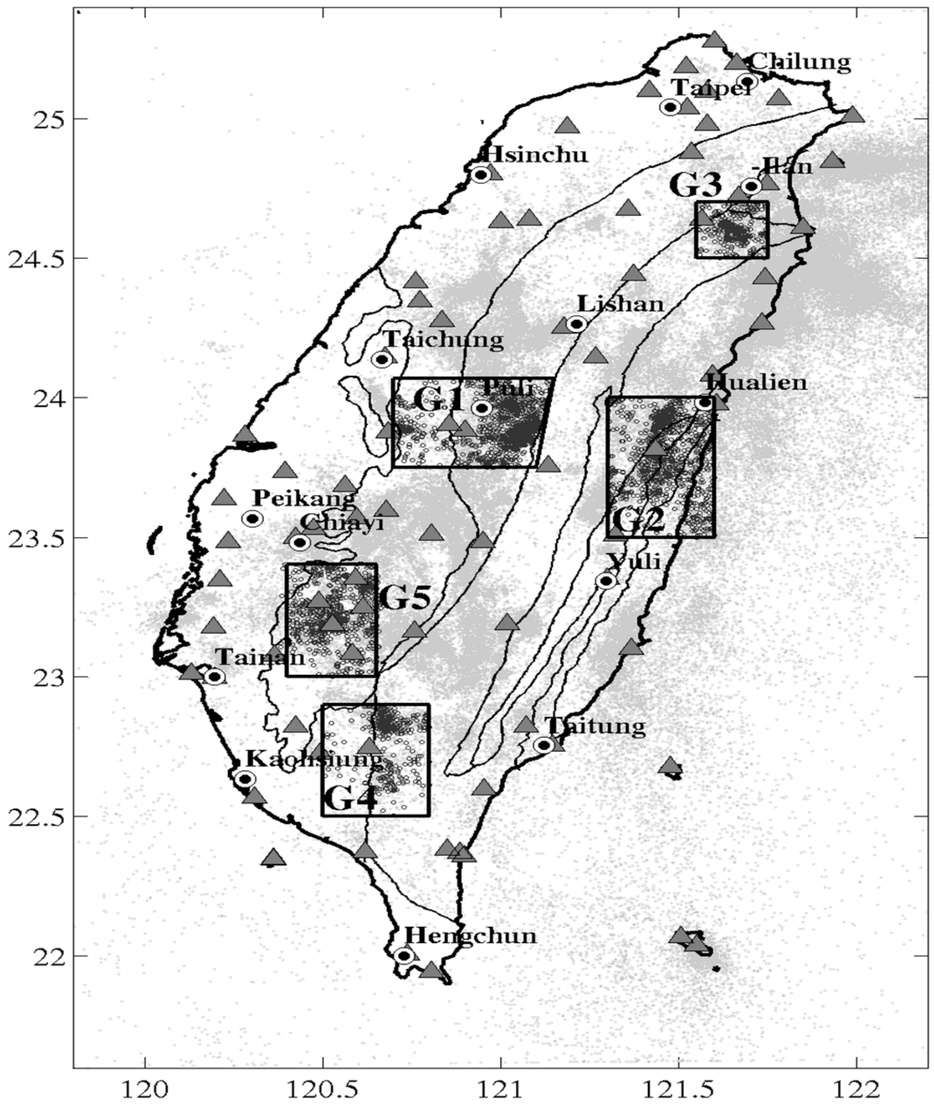

Pattern of JHD station corrections for G1 events

Obs.

Syn

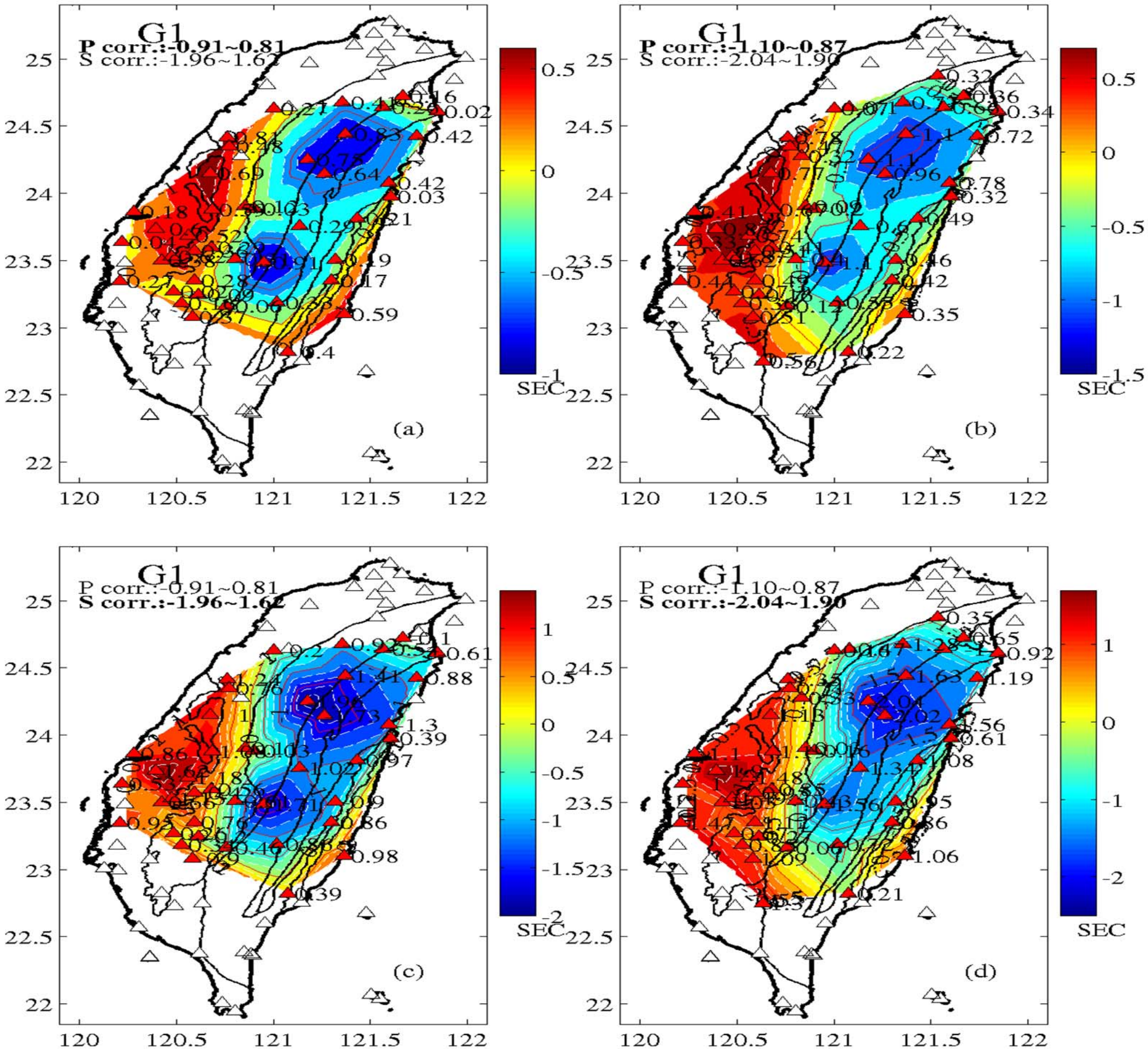

For Group 2 in Eastern Taiwan

Obs

Syn

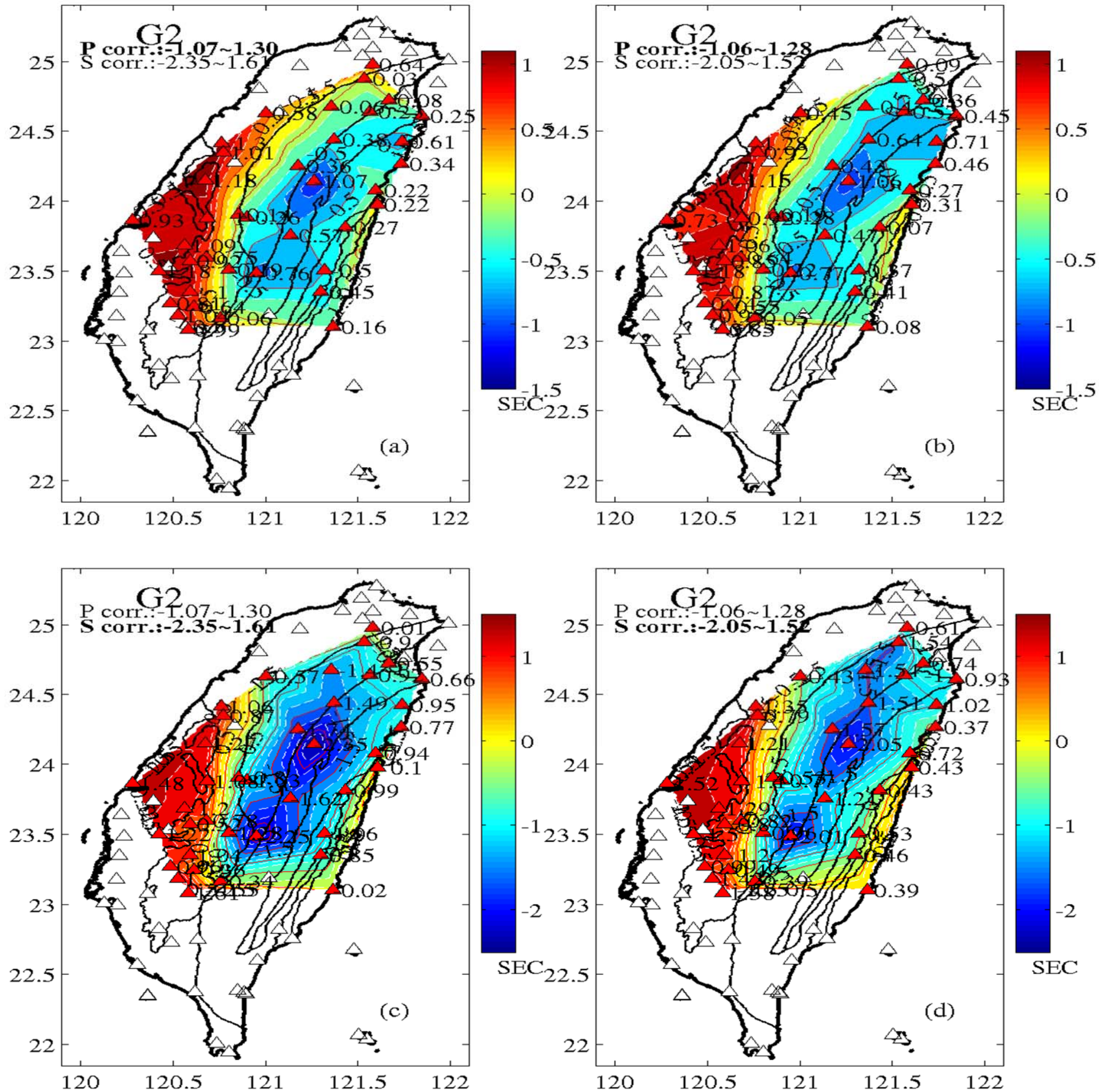

For Group 3 in northern Taiwan

Obs

Syn

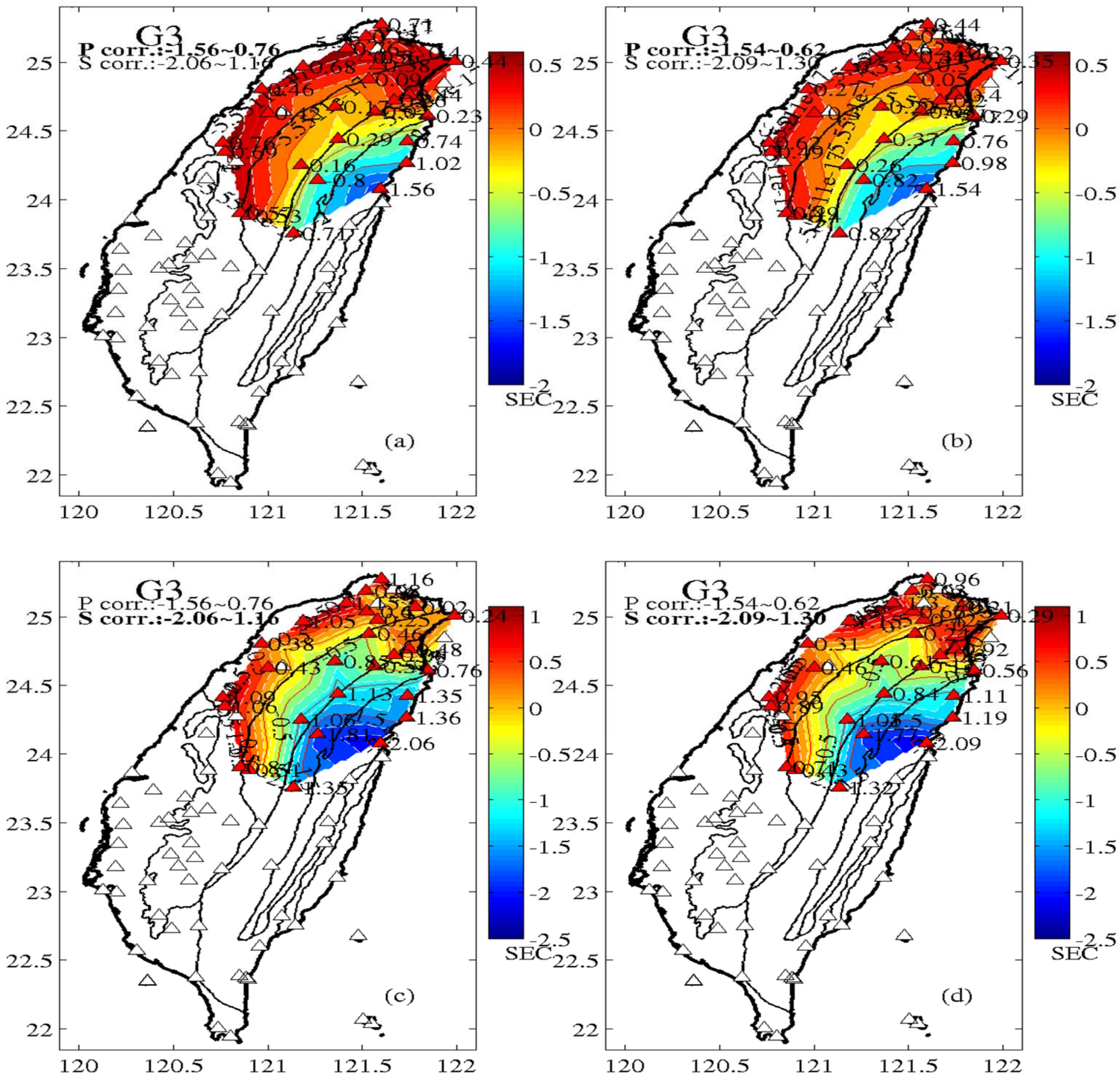

For Group 4 in southern Taiwan

Obs

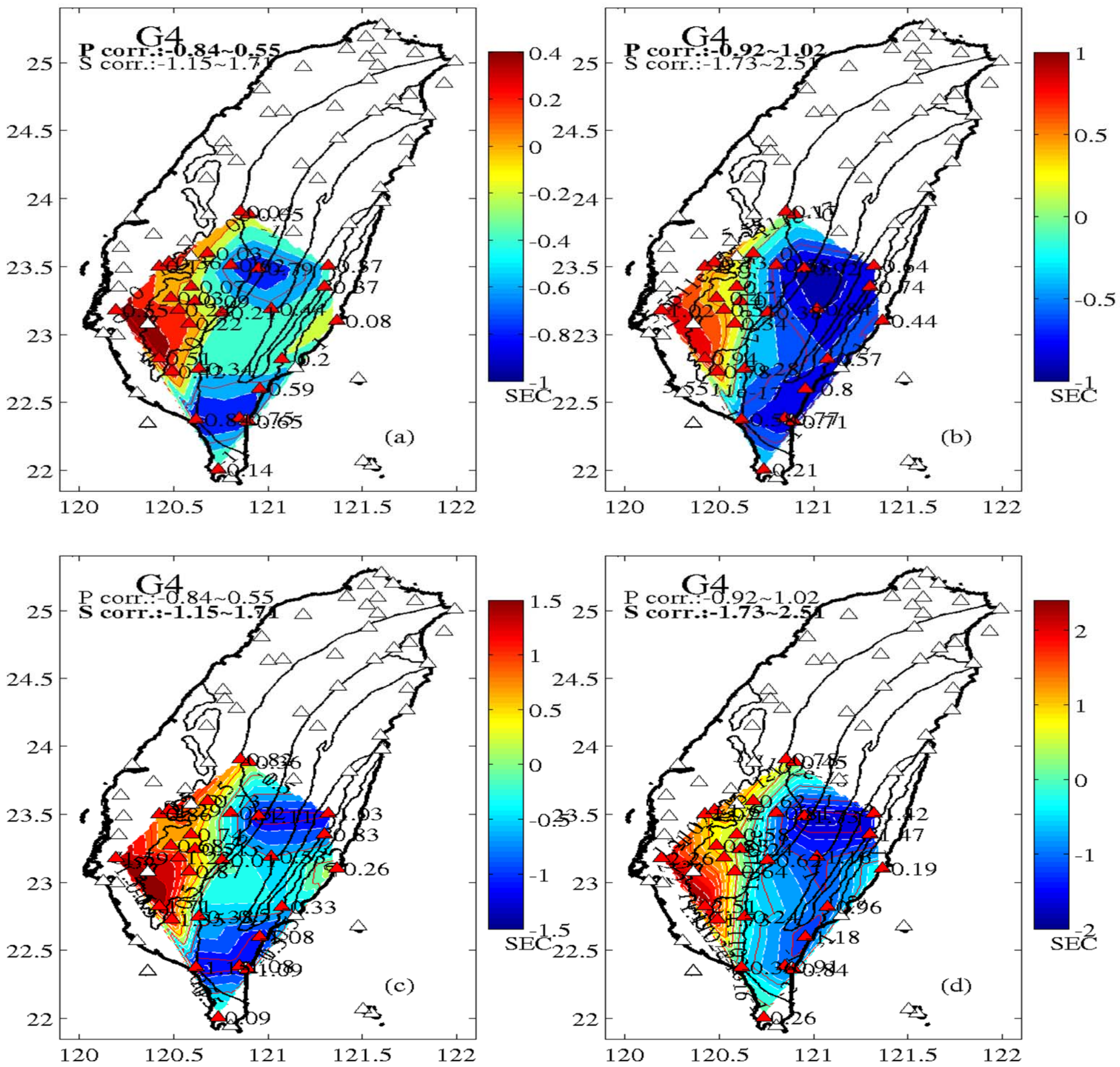

Syn

For Group 5 in southwestern Taiwan

Obs

Syn

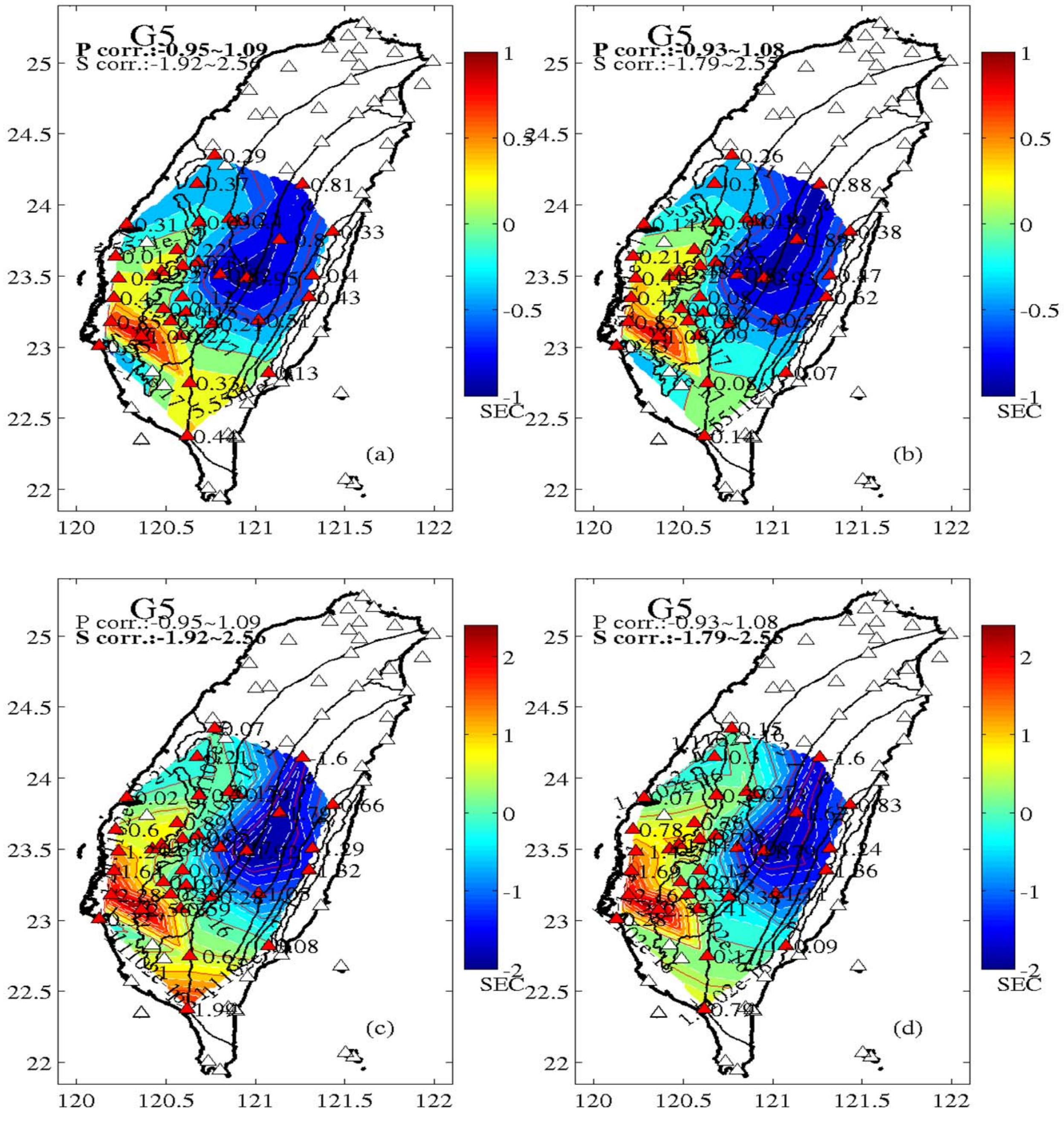

Only selected best earthquake data (2% from CWB catalog) have been used in 3-D tomographic inversion and relocated during the process.

There are other 98% of earthquakes not selected and thus not relocated using the resultant 3-D Vp and Vs models.

Our Approaches

1. **Evaluate the spatial structural resolution of the current seismic station configuration and earthquake distribution – *what's to expect*?**
2. **Quantify lateral structural variations, especially for shallow crust -- *how will they affect on earthquake location? and structure resolution?***
3. **Determine reliable 3-D Vp and Vs models ---*how to validate the resultant models?***
4. **Develop a new algorithm to locate all earthquakes using the resultant 3-D models ---*can earthquakes be reliably located?***
5. **Interpret and model the results base on the resultant 3-D velocity images and the best relocated seismicity --- *what can we learn when all the ambiguities are minimized?***

Procedures for a reliable earthquake location using 3D models

Determine a 3-D Vp and Vs model from 3-D tomographic inversion

↓

Design a 3-D grid model and calculate travel time from each grid point to all seismic stations using3D ray tracing across the 3D velocity model

↓

Save travel time information in disk files

↓

Travel time from any trial hypocenter to any station can be easily calculated from a linear interpolation from the adjacent eight grid pts

↓

Repeated iteration to minimize the differences between the observed and calculated travel time to determine an optimized single earthquake location

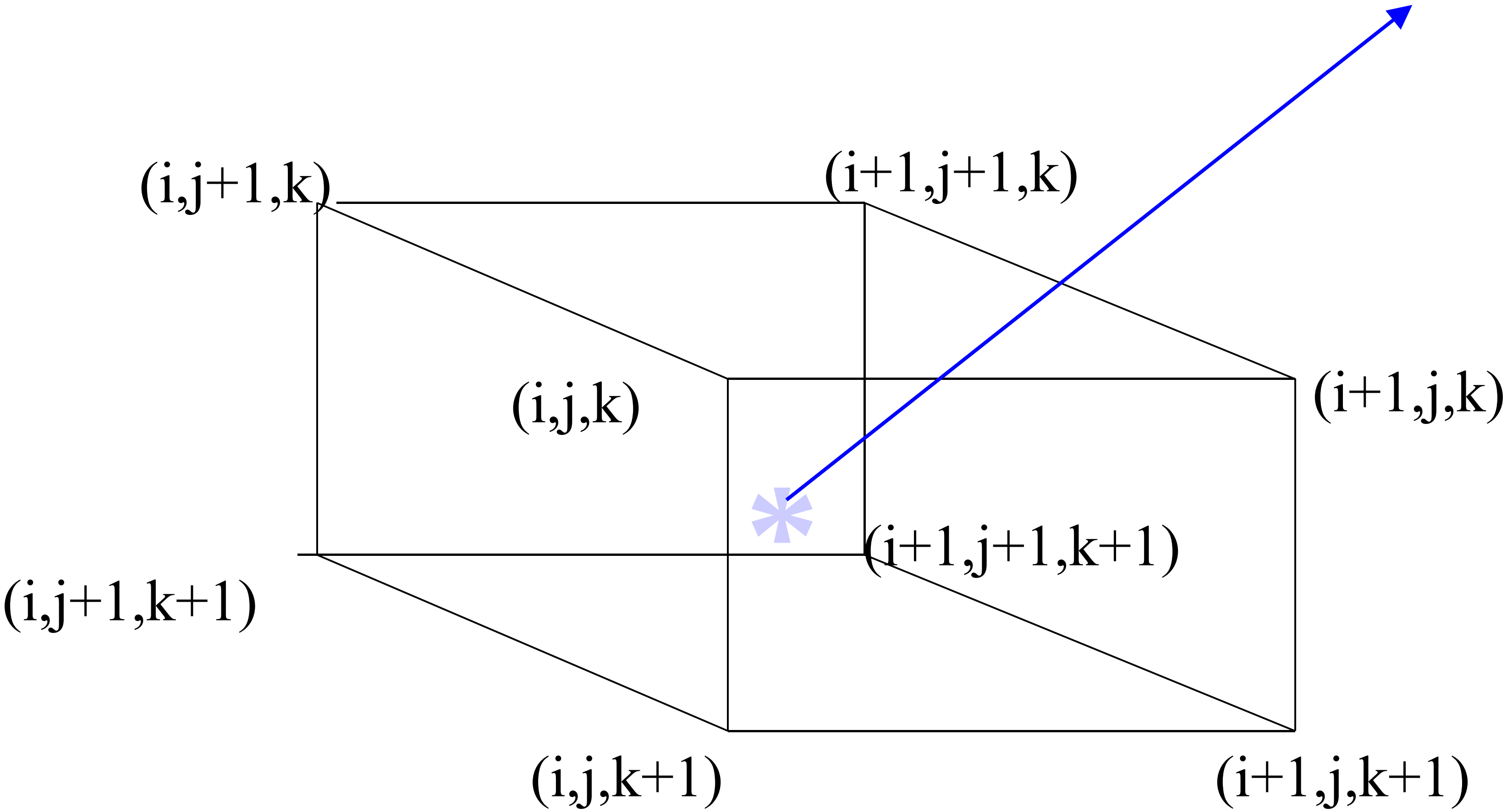

(i,j+1,k)
(i+1,j+1,k)
(i,j,k)
(i+1,j,k)
(i+1,j+1,k+1)
(i,j+1,k+1)
(i,j,k+1)
(i+1,j,k+1)

Relocated seismicity in the Taiwan region using the 3-D Vp and Vs models from this study – this is so far the best data to work with

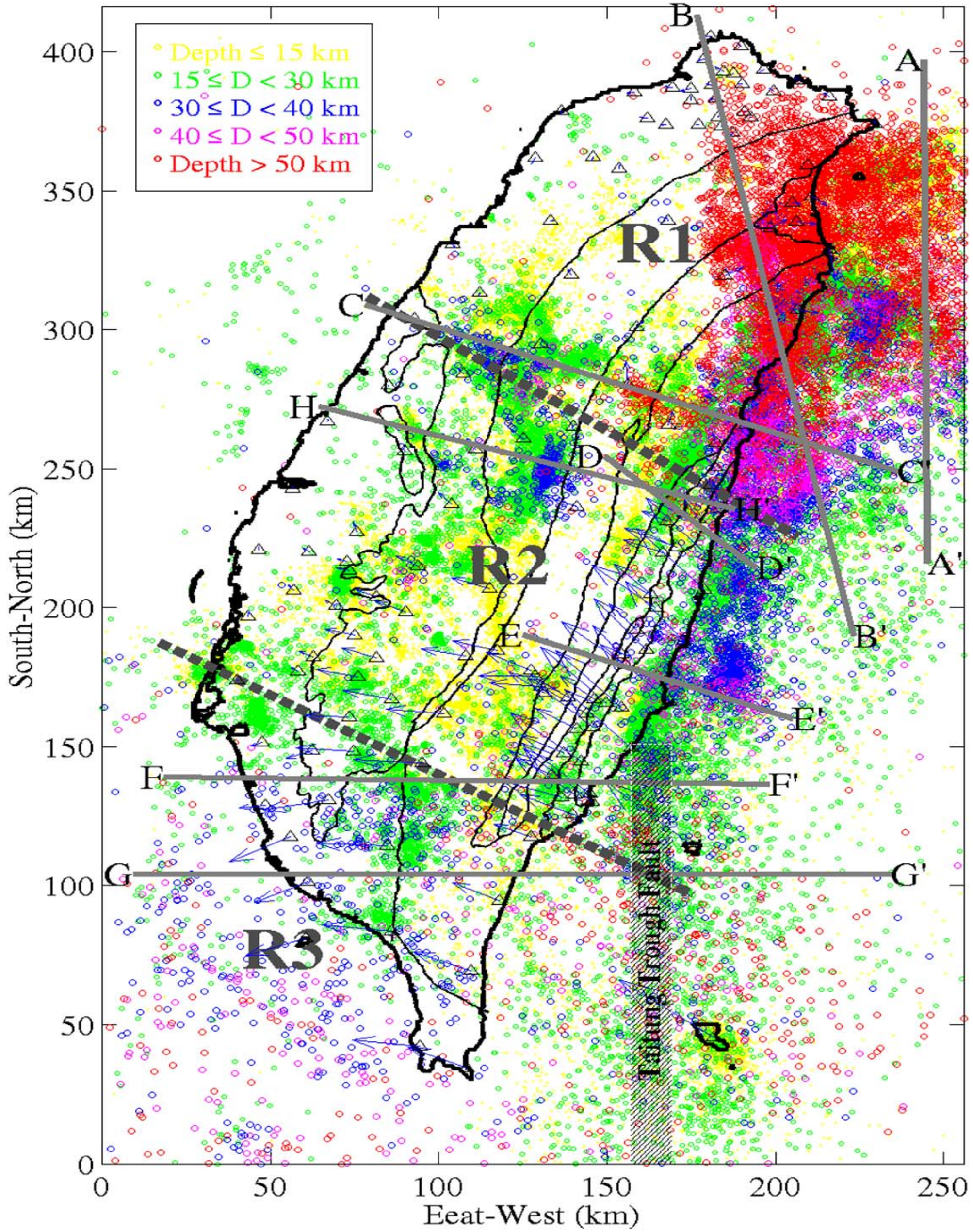

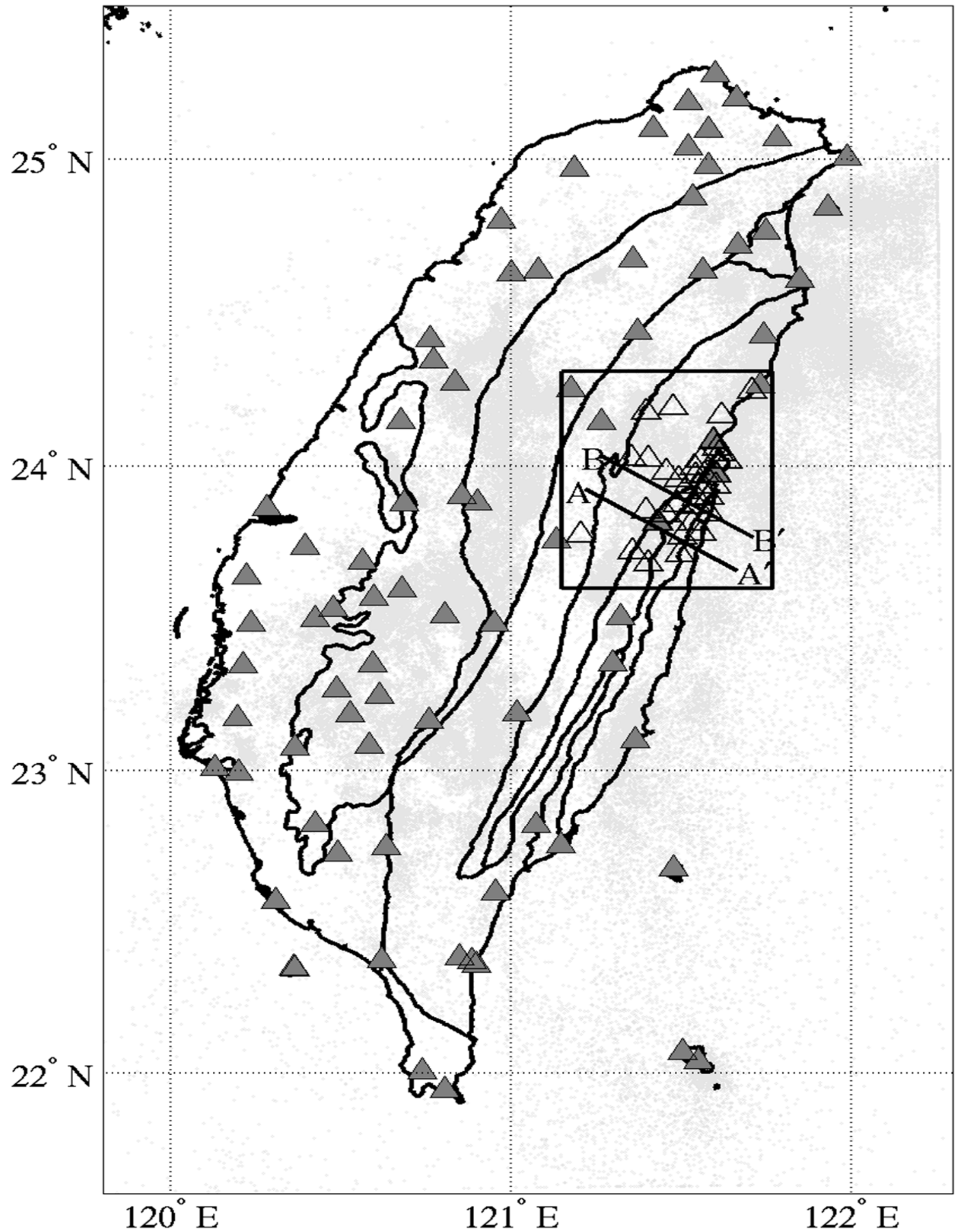

25° N
24° N
23° N
22° N
120° E
121° E
122° E
A
A′
B
B′

Comparison of hypocenters before (block open circles) and after (white open circles) in center eastern Taiwan.

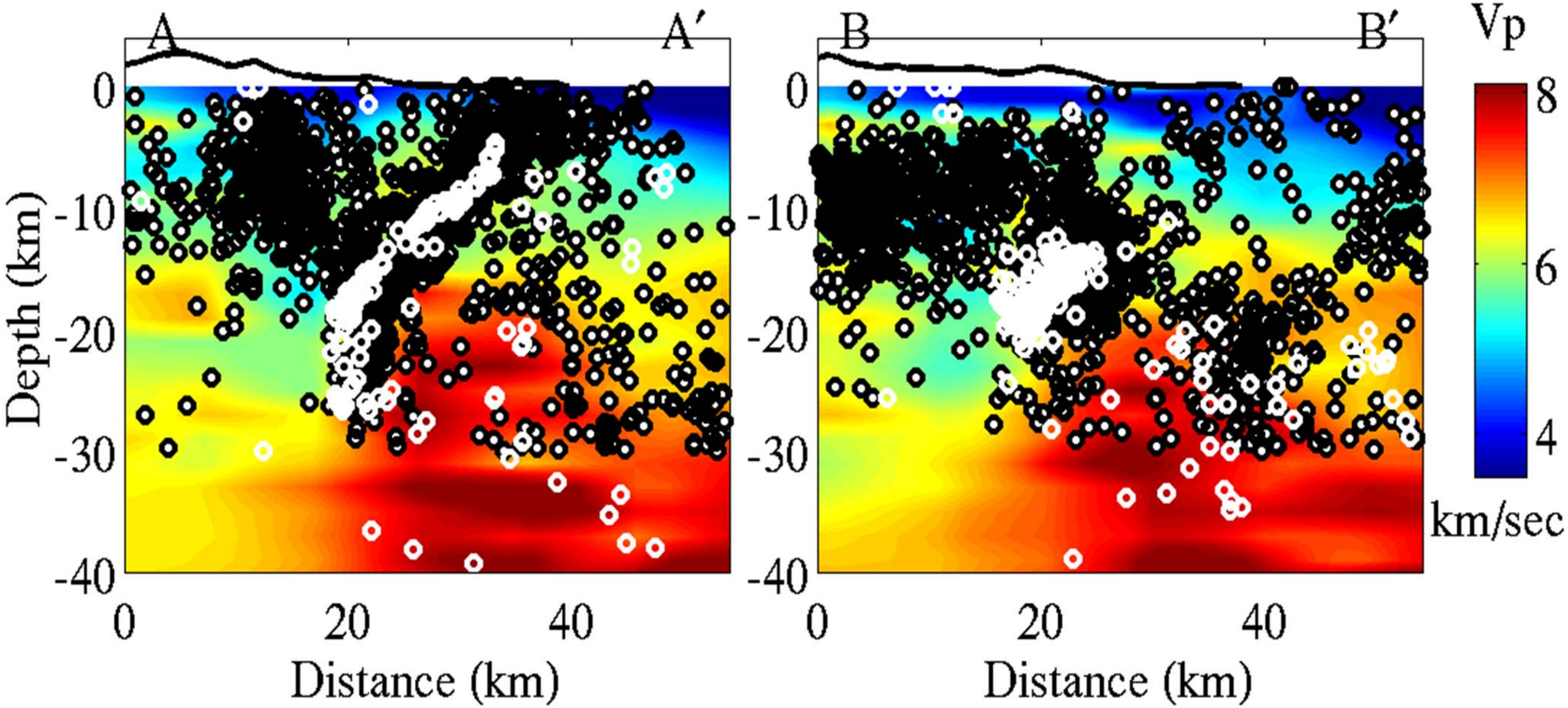

Example of impact of dense local seismic array on earthquake location to associate earthquake with active faults

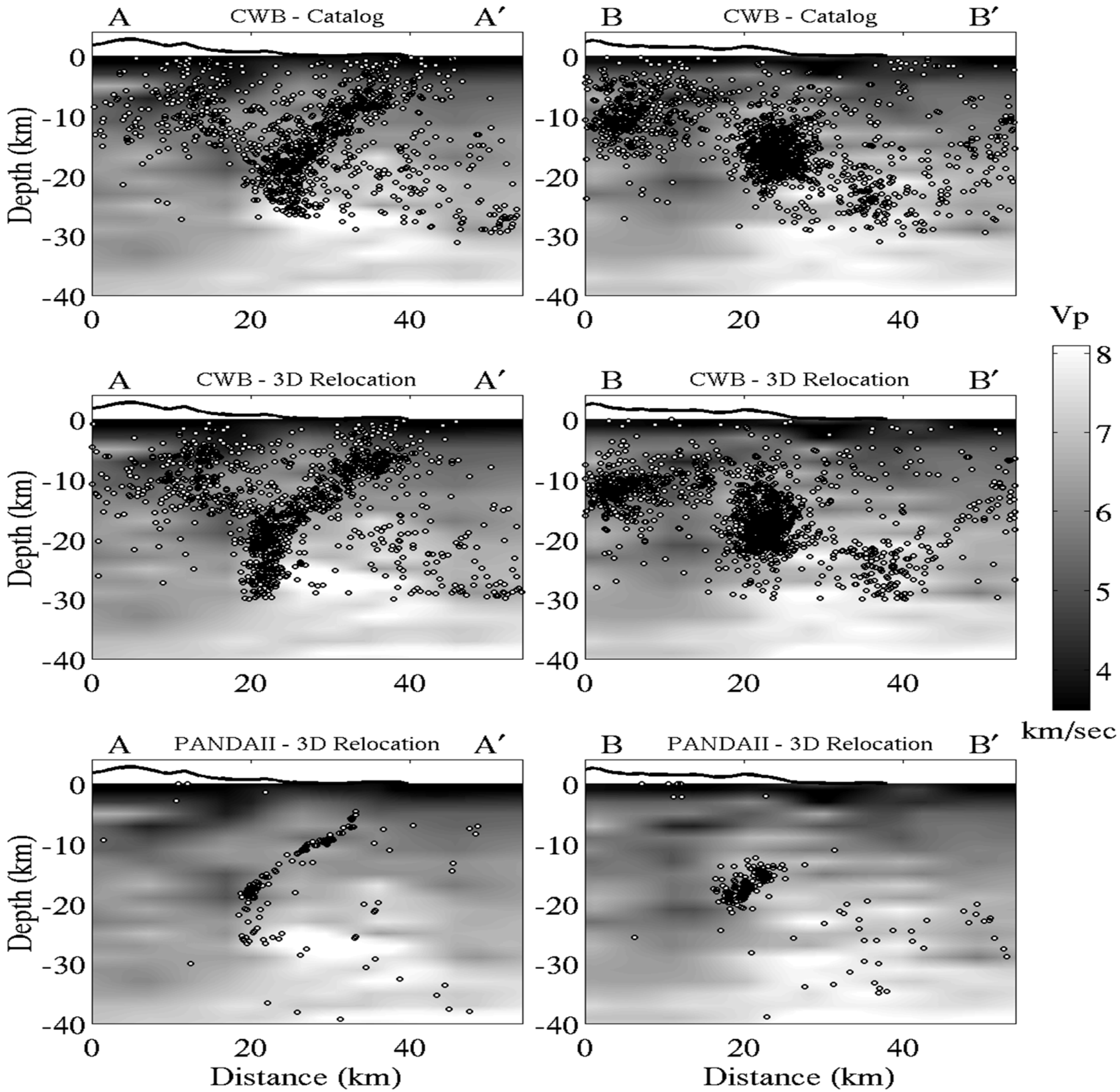

Relocated seismicity in the Taiwan region using the 3-D Vp and Vs models from this study – this is so far the best data to work with

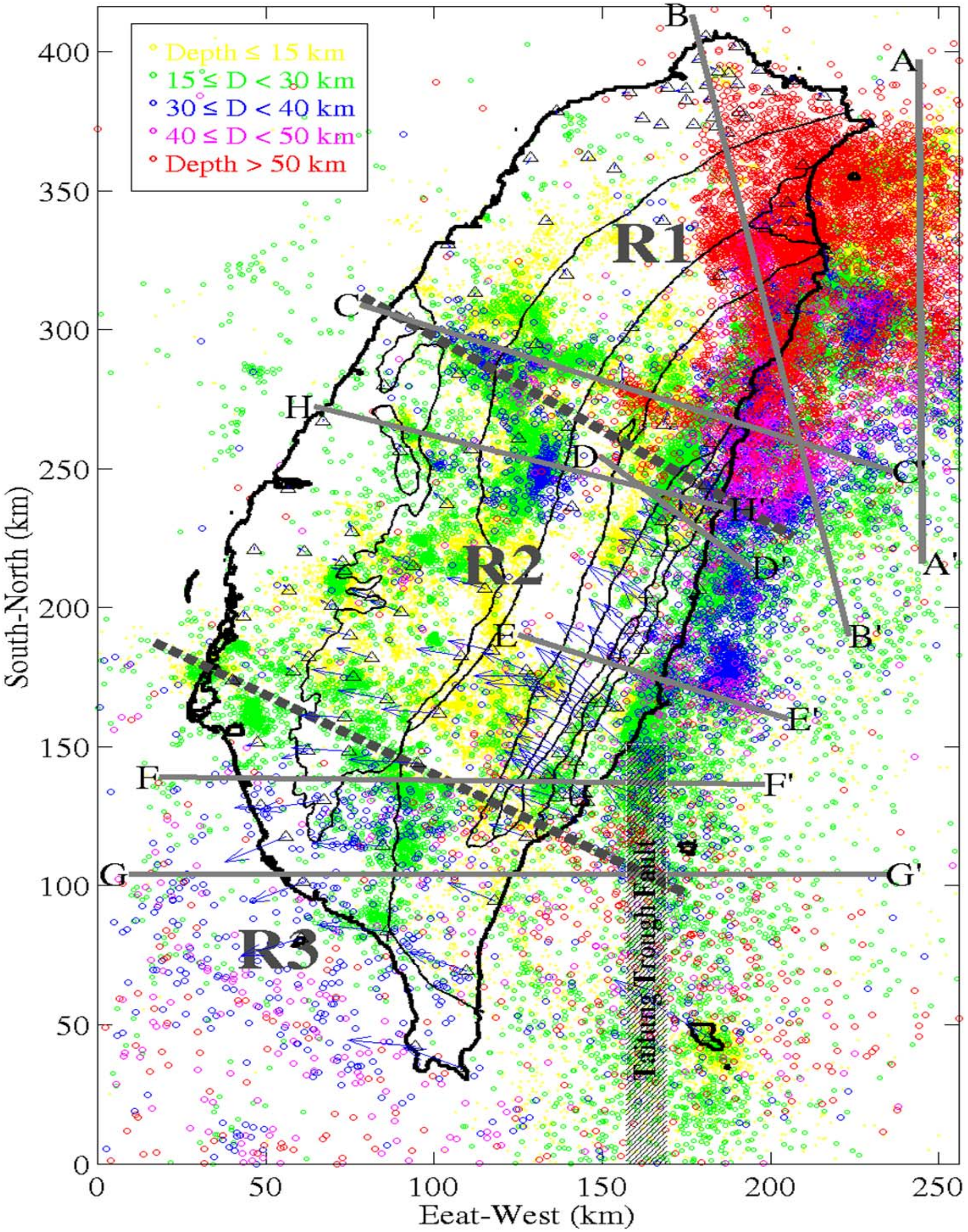

Sedimentary Basins

- Most sedimentary basins are located in western Taiwan
- Geometry and seismic response of most sedimentary basins in Taiwan are not well-known
- Lateral variations of velocity structures from beneath sedimentary basins to high mountains are very significant for both P and S-waves that hypocenters in Taiwan region are systematically mis-located

Major sedimentary basins in the Taiwan region are visible from a thin-sliced Vp image from the results of a 3-D tomographic inversion (Kim et al., 2005)

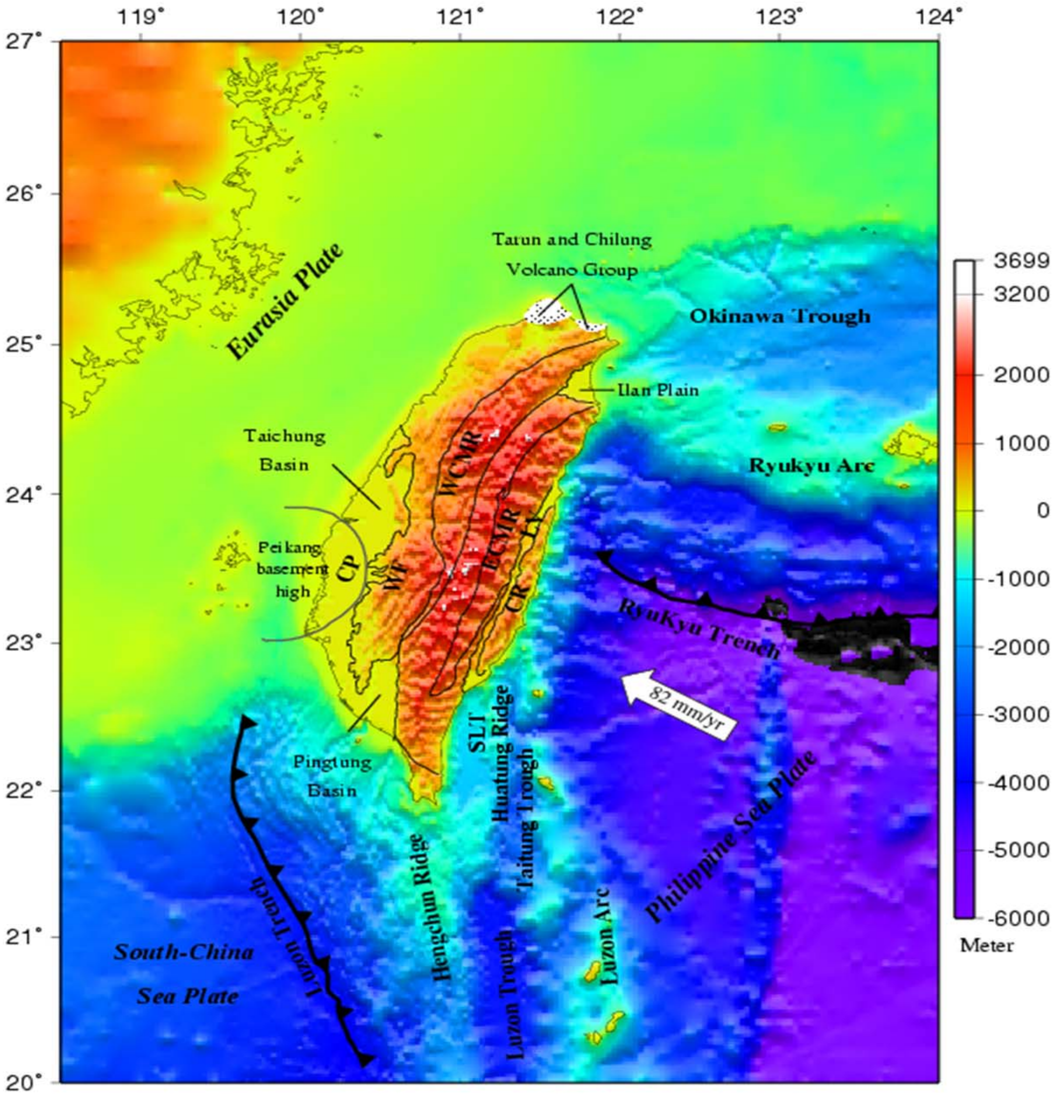

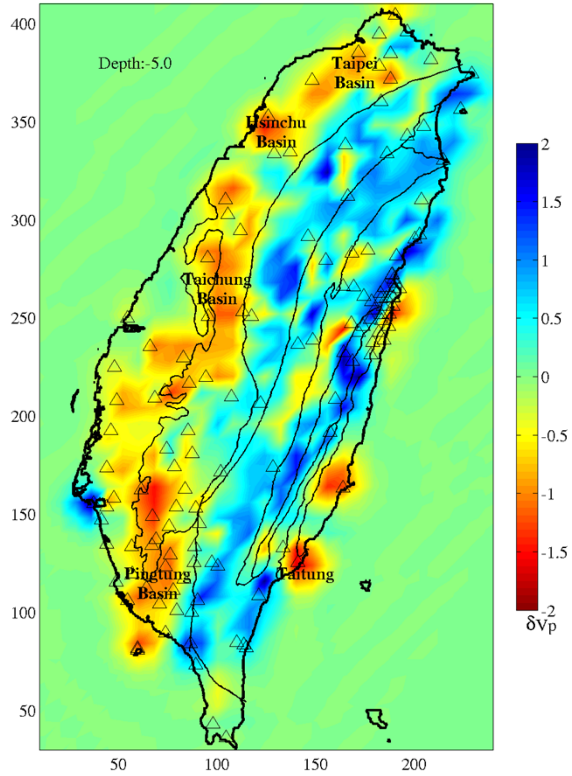

Significant impedance contrast across a layer boundary within sedimentary basin will have a significant impact on the amplification of seismic waves

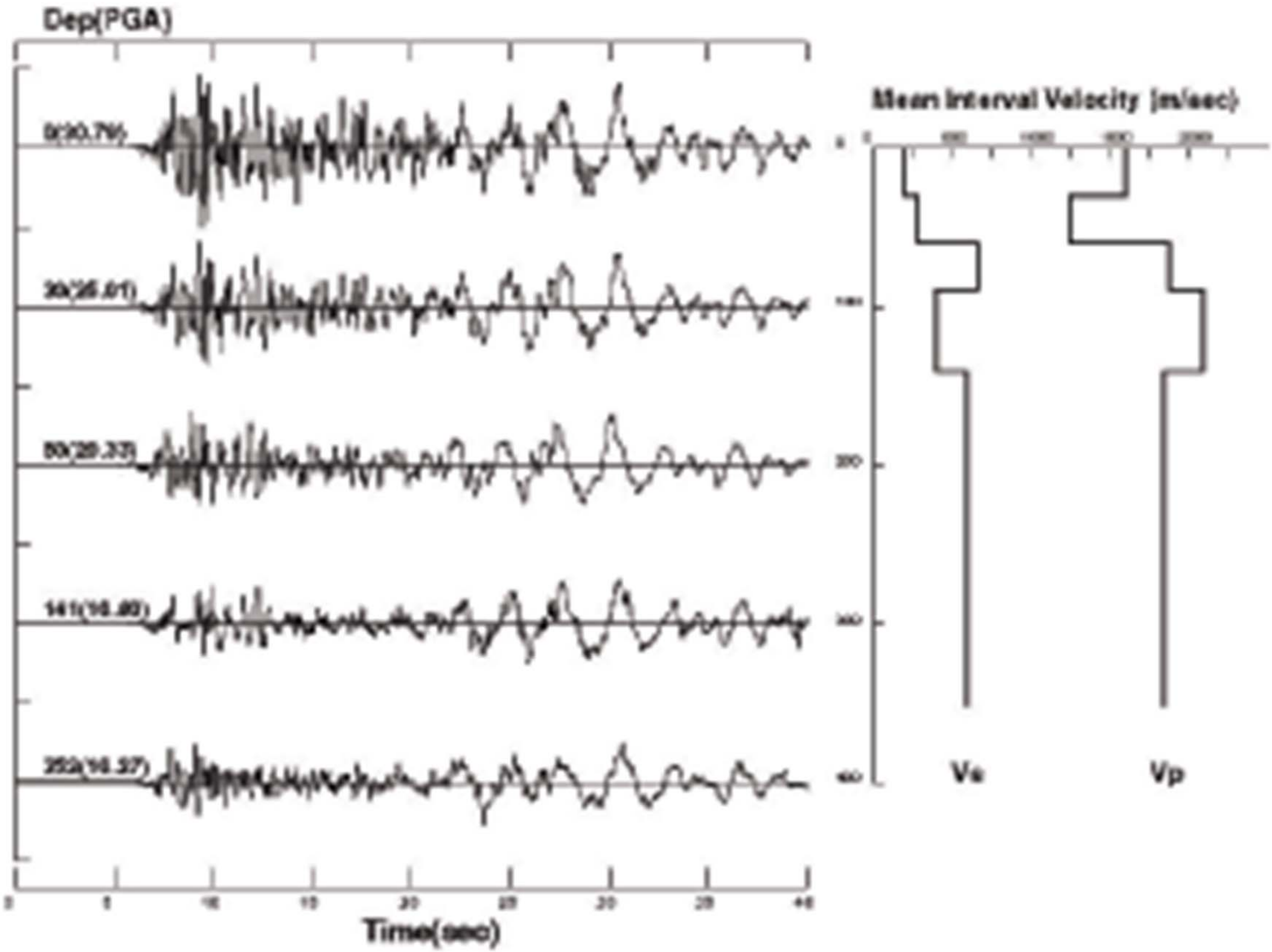

Index map of cross-secional views of velocity and seismicity across major sedimentary basins in the Taiwan region

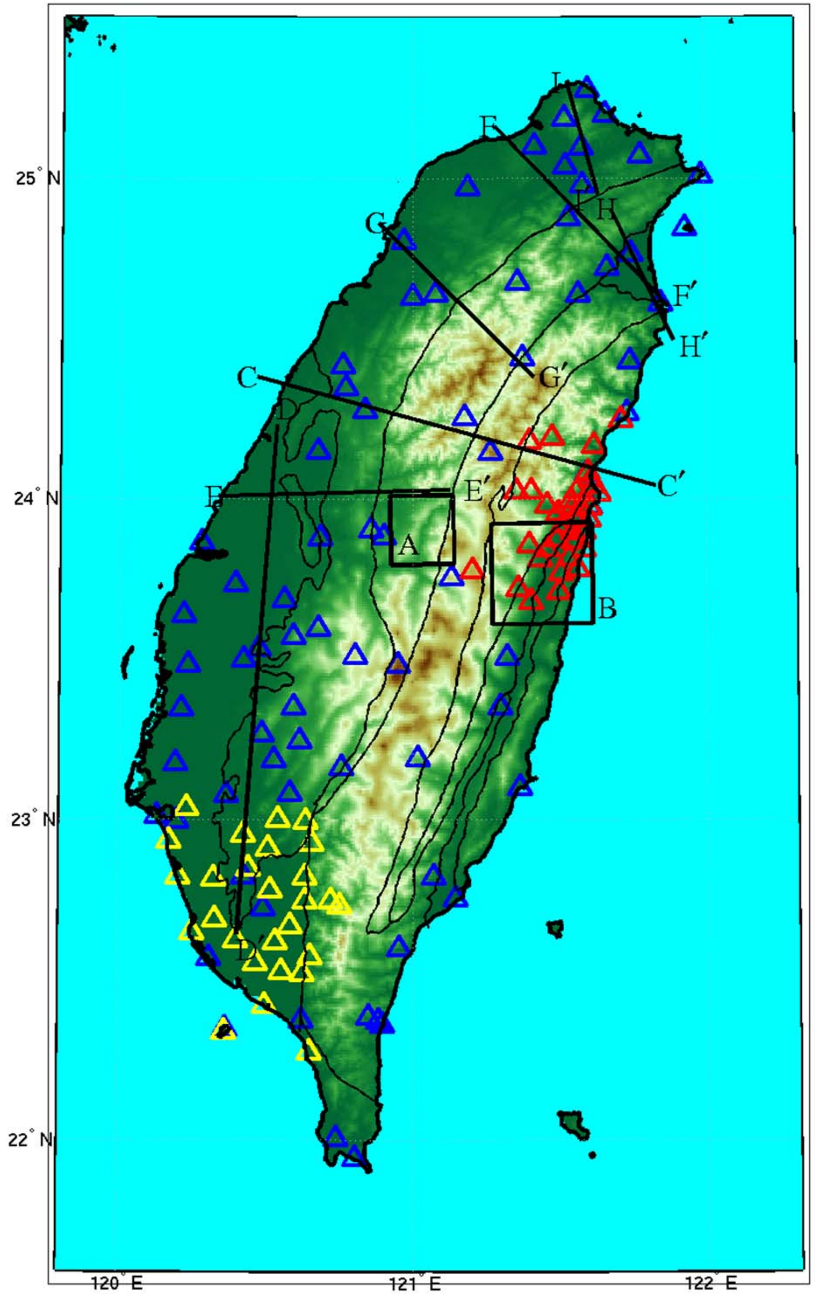

Low velocity basins

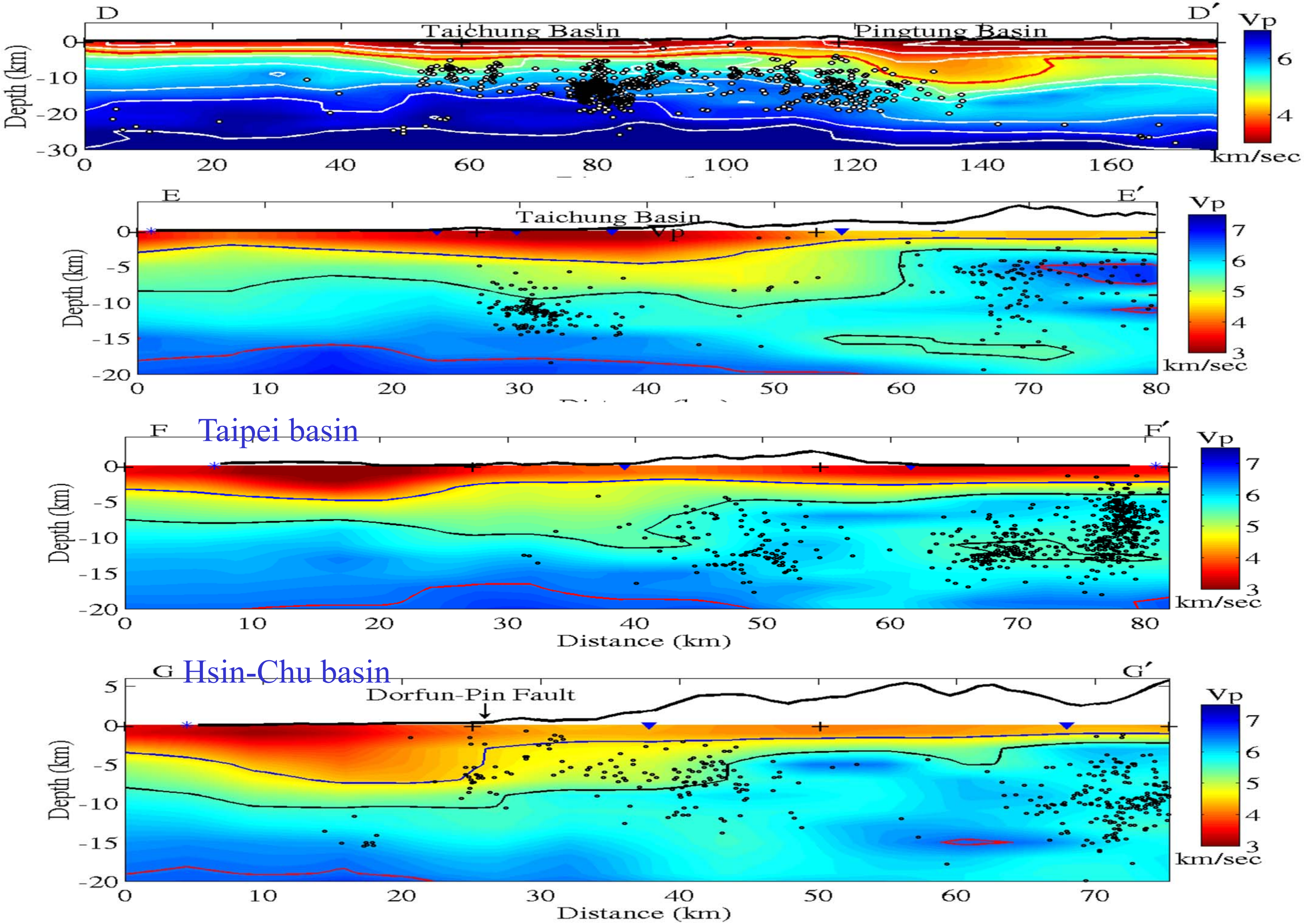

Index map of cross-secional views of velocity and seismicity across major sedimentary basins in the Taiwan region

HH’ from Taipei to Ilan

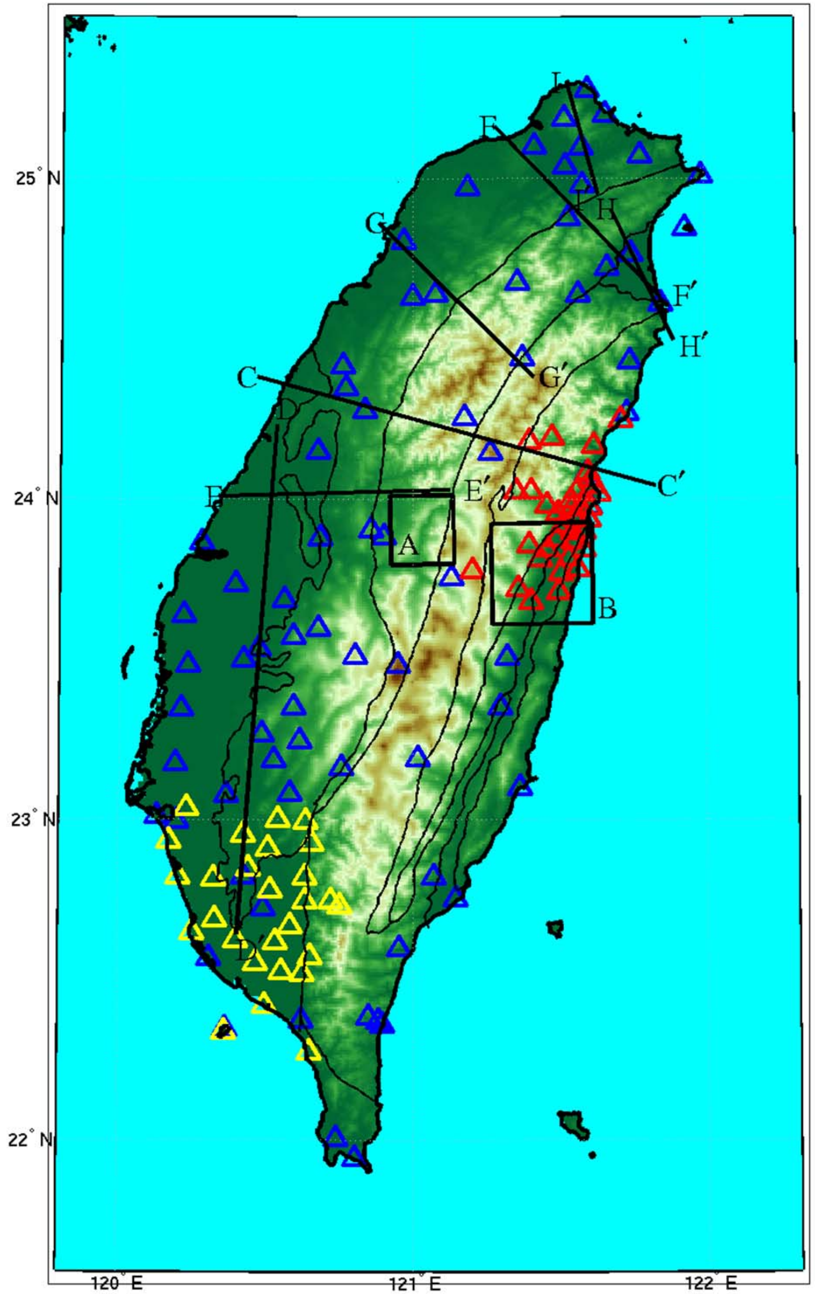

P-wave velocity profile across the Ilan Plain in northeastern Taiwan

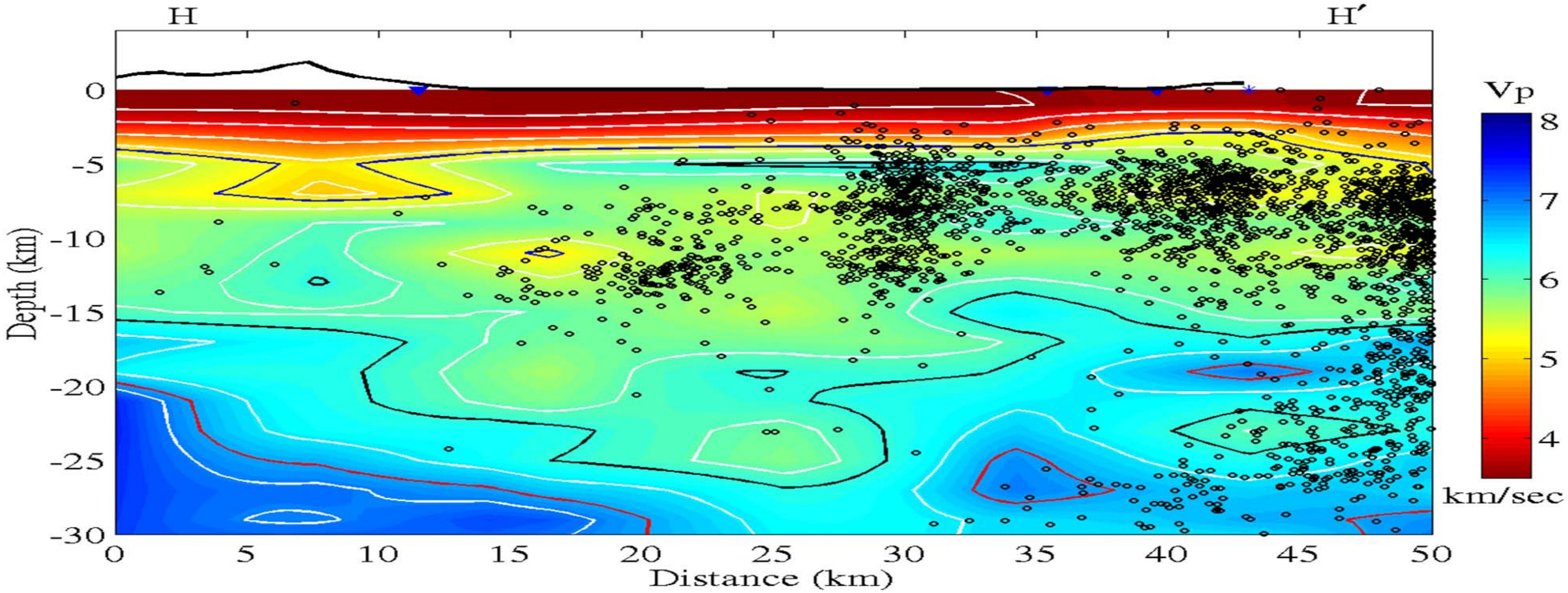

High geothermal and magmatic activity in shallow crust associated with backarc opening probably contribute to the low velocity and high seismic activities.

P-wave velocity profiles across the NS trending Chao-Chou fault in southern Taiwan

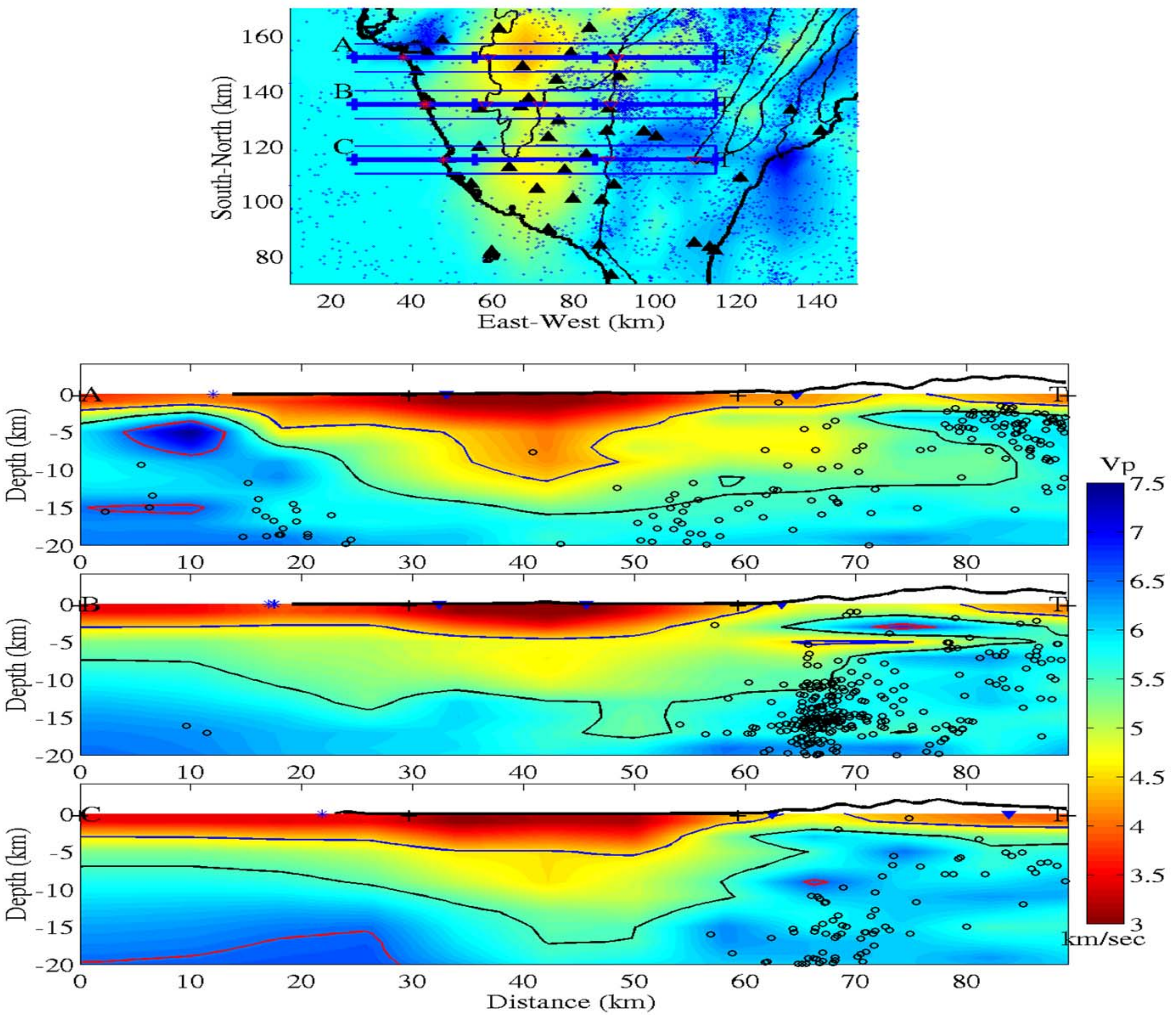

Cross-section of Vp (top) and Vp/Vs ratio (bottom) across the Tatung-Chilung volcanic group where volcanism ceased in Pliocene. The low Vp but high Vp/Vs ratio beneath the volcano may suggest the potential of the existence of partially melted magmatic reservoir at shallow depth.

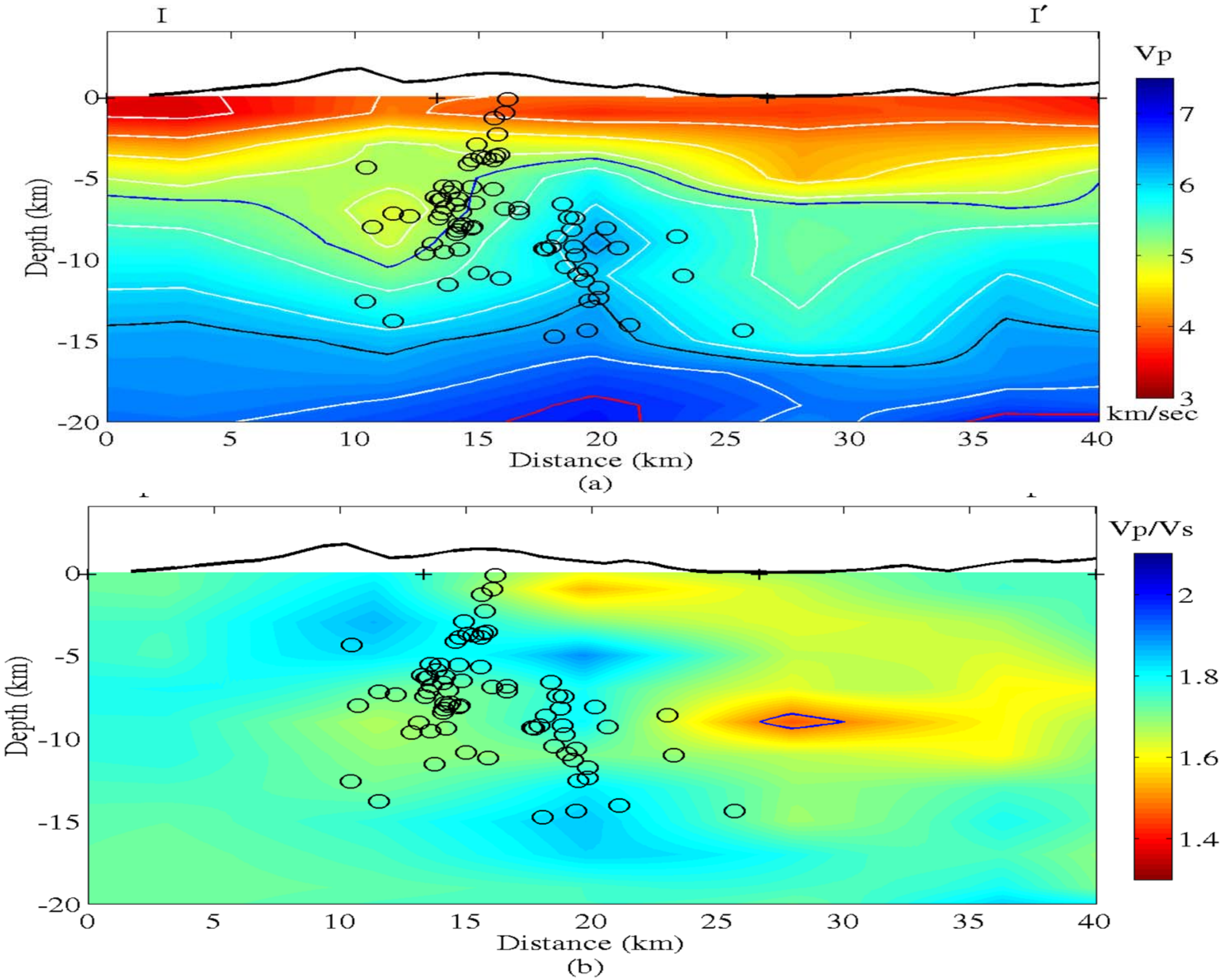

The Moho configuration from a few E-W cross-sectional views

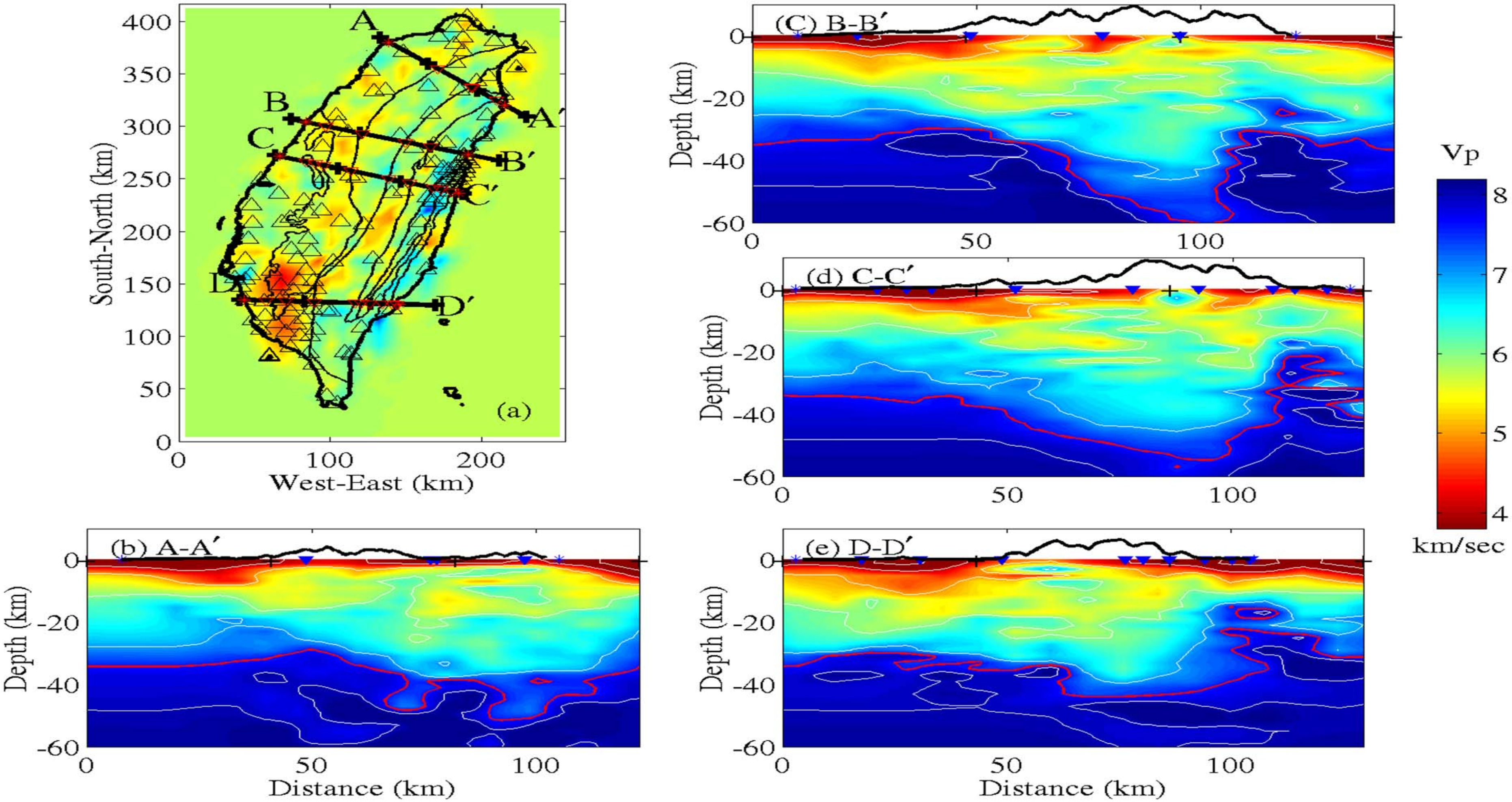

A New Tectonic Model of Central Taiwan from the New Data

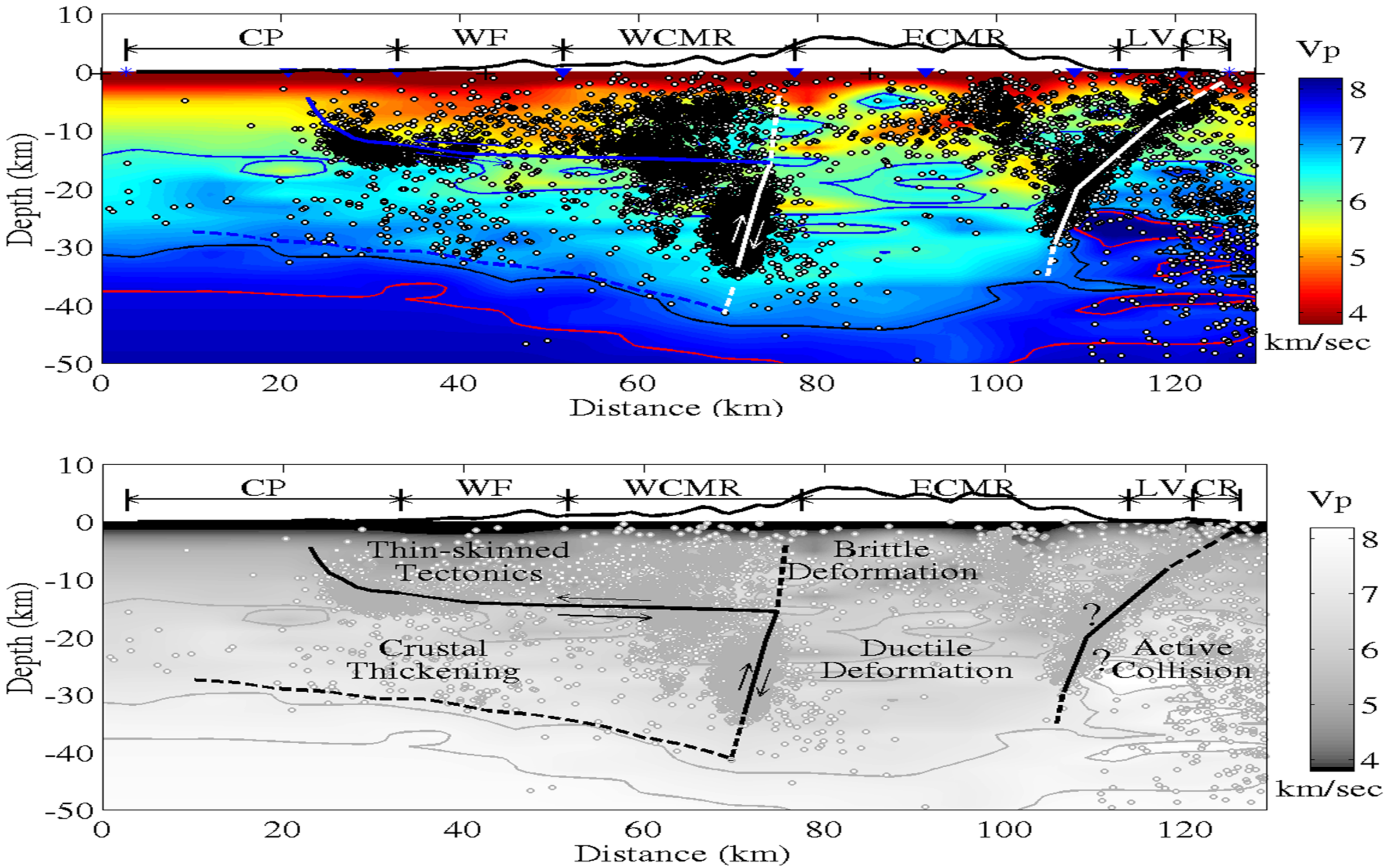

Examples from other areas

Near the interception between the Central and the SW segments

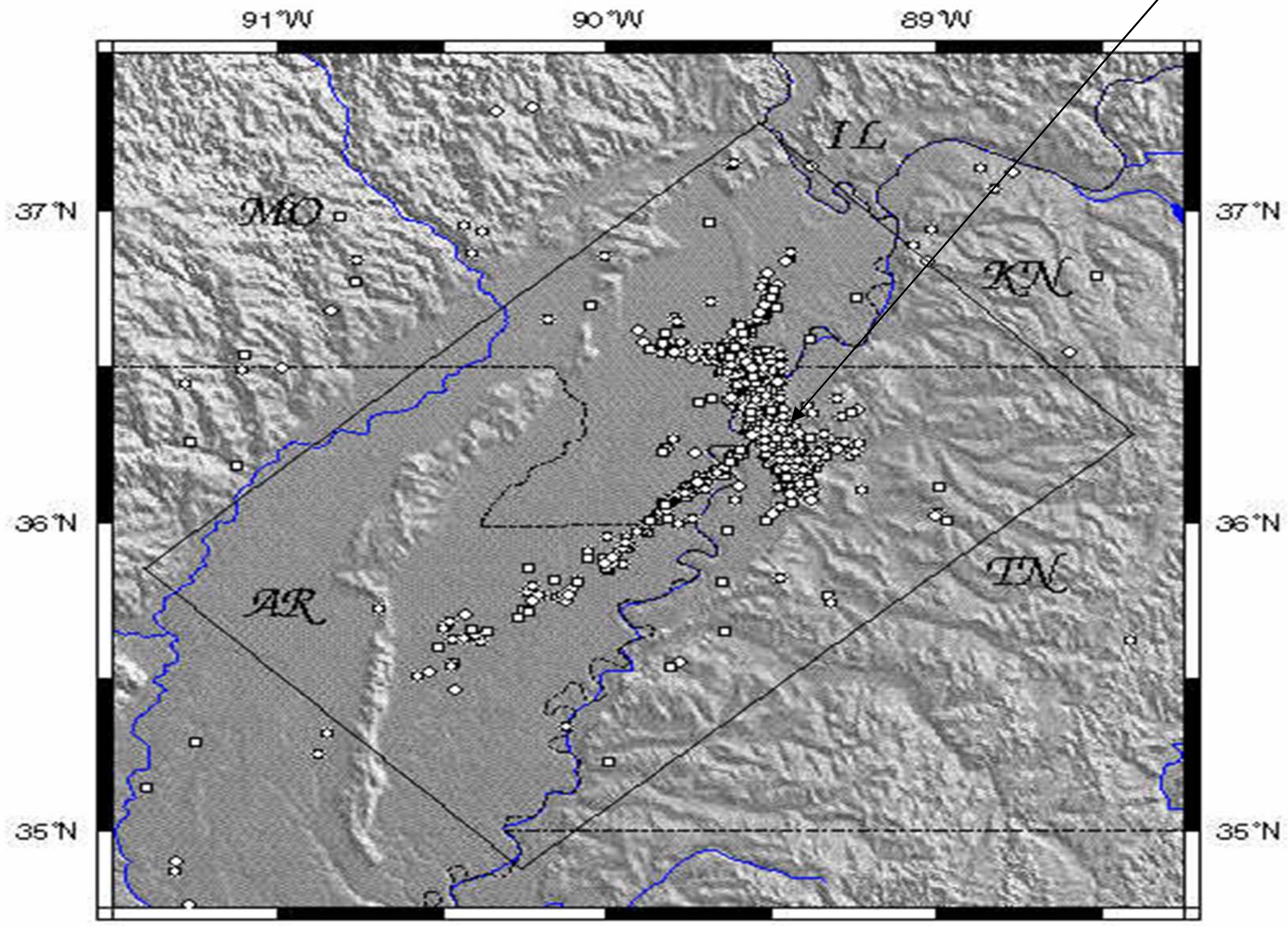

Figure 1. Map showing the original epicentral locatoins from PANDA and CERI regional seismic network. Study area is marked by the thick rectangle box.

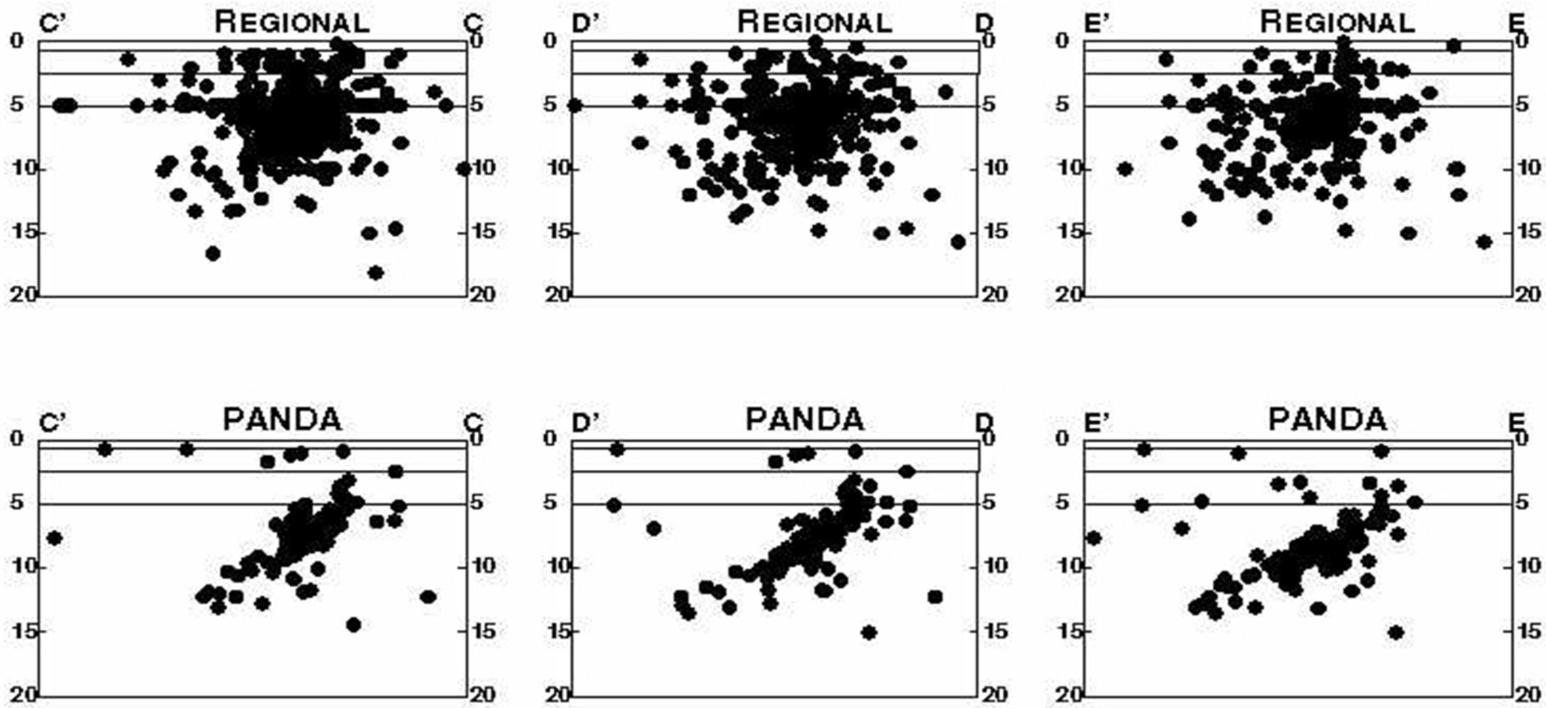

C'
REGIONAL
C
D'
REGIONAL
D
E'
REGIONAL
E
C'
PANDA
C
D'
PANDA
D
E'
PANDA
E
0
5
10
15
20

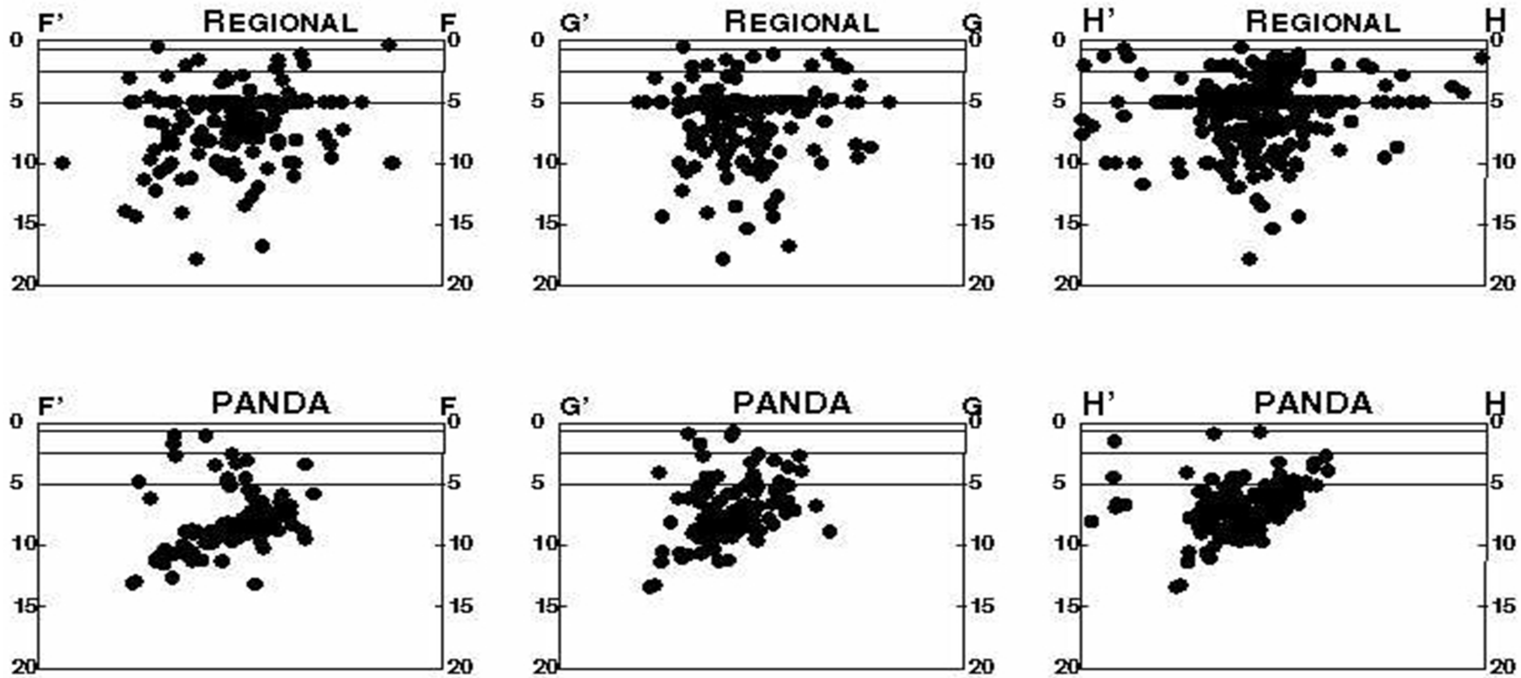

F'
REGIONAL
F
G'
REGIONAL
G
H'
REGIONAL
H
F'
PANDA
F
G'
PANDA
G
H'
PANDA
H
0
5
10
15
20

Southern Central segment

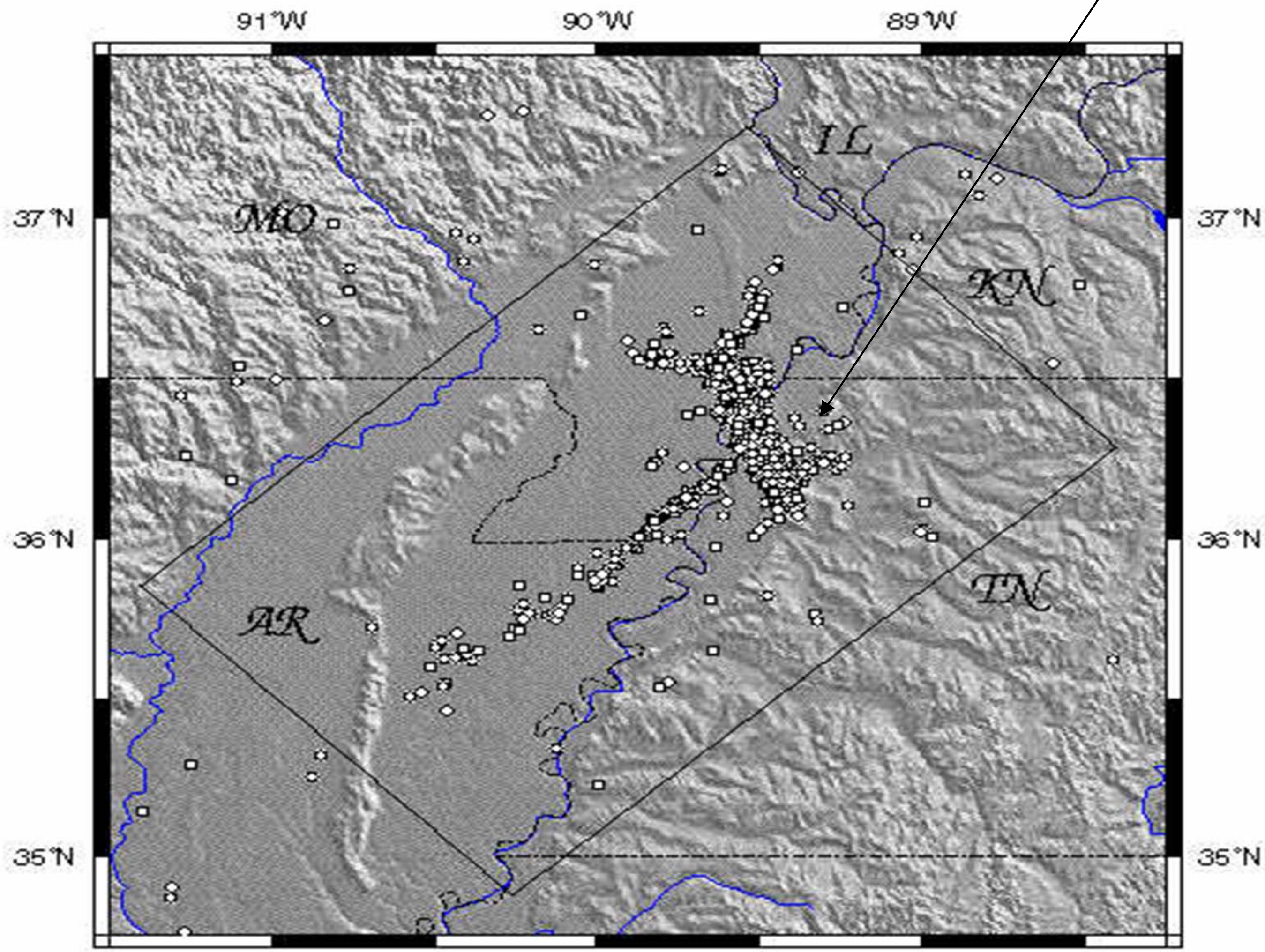

Figure 1. Map showing the original epicentral locatoins from PANDA and CERI regional seismic network. Study area is marked by the thick rectangle box.

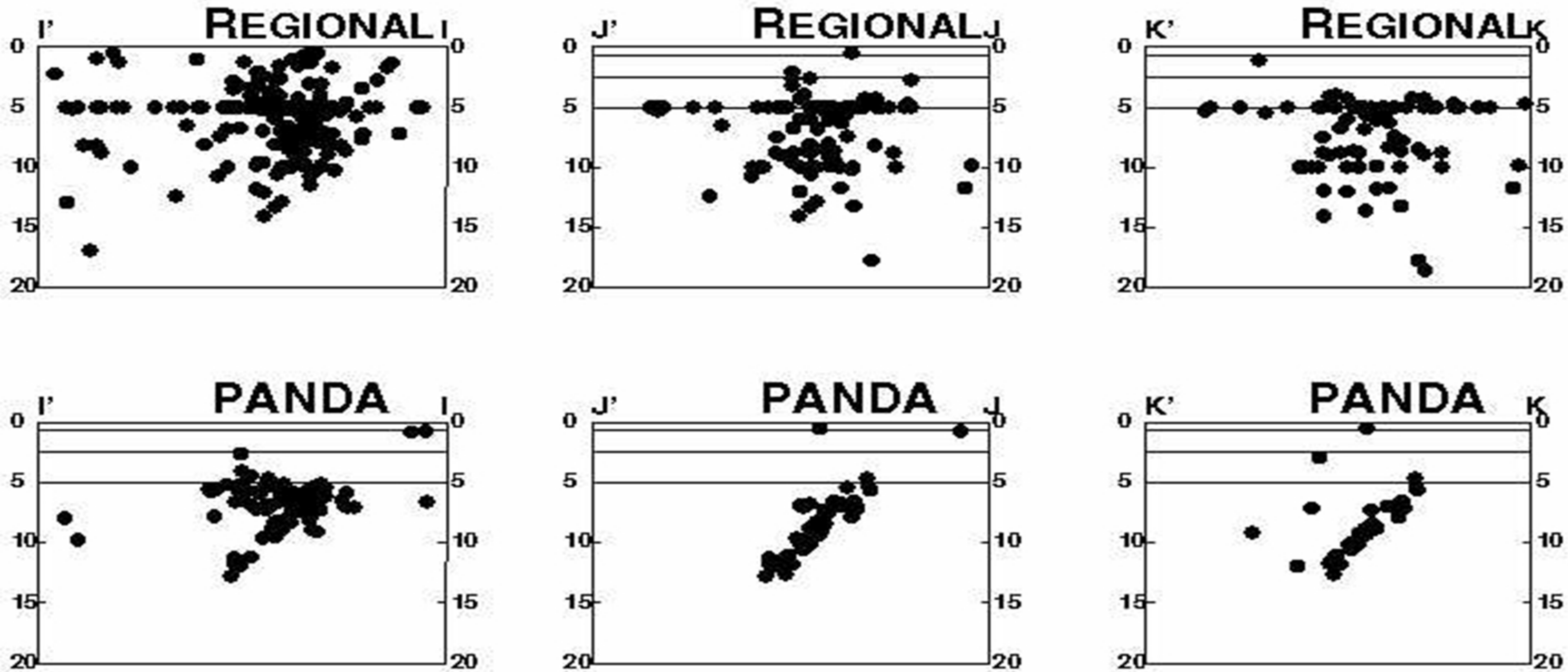

REGIONAL
I'
I
REGIONAL
J'
J
REGIONAL
K'
K
PANDA
I'
I
PANDA
J'
J
PANDA
K'
K
0
5
10
15
20

SW segment of the NMSZ

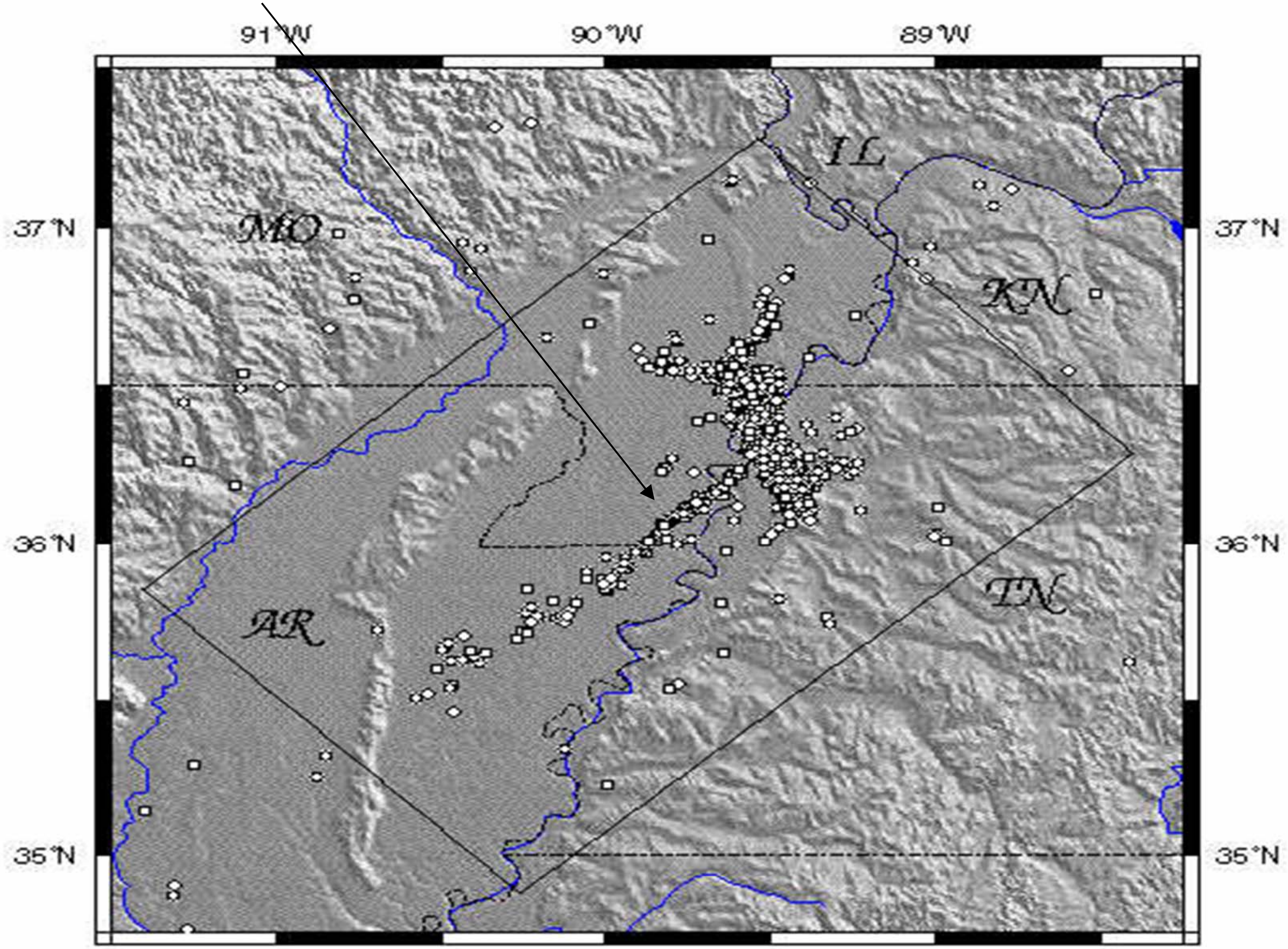

Figure 1. Map showing the original epicentral locatoins from PANDA and CERI regional seismic network. Study area is marked by the thick rectangle box.

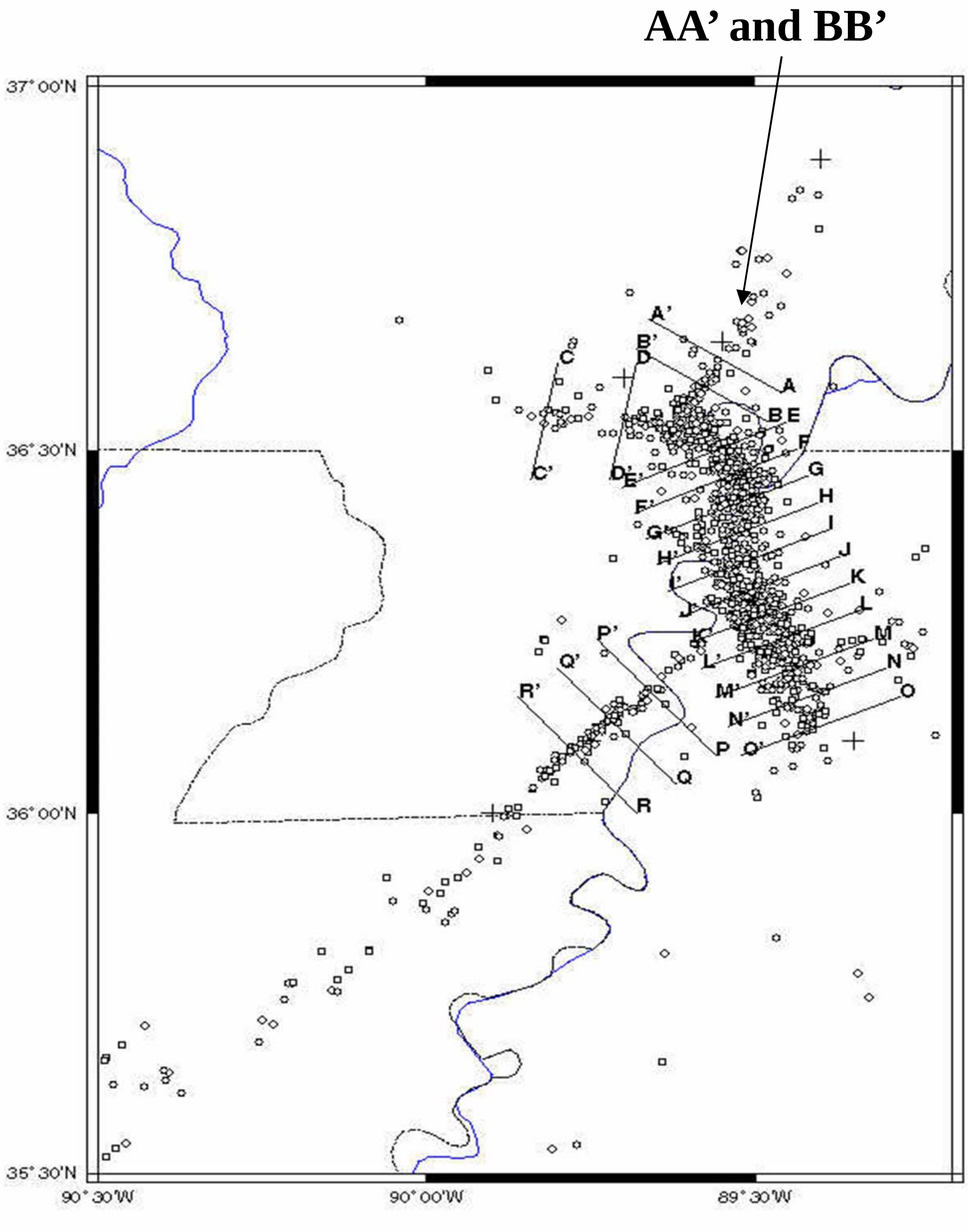
AA' and BB'
37° 00'N
36° 30'N
36° 00'N
35° 30'N
90° 30'W
90° 00'W
89° 30'W
A'
A
B'
B
C
C'
D
D'
E
E'
F
F'
G
G'
H
H'
I
J
J'
K
K'
L
L'
M
M'
N
N'
O
O'
P
P'
Q
Q'
R
R'

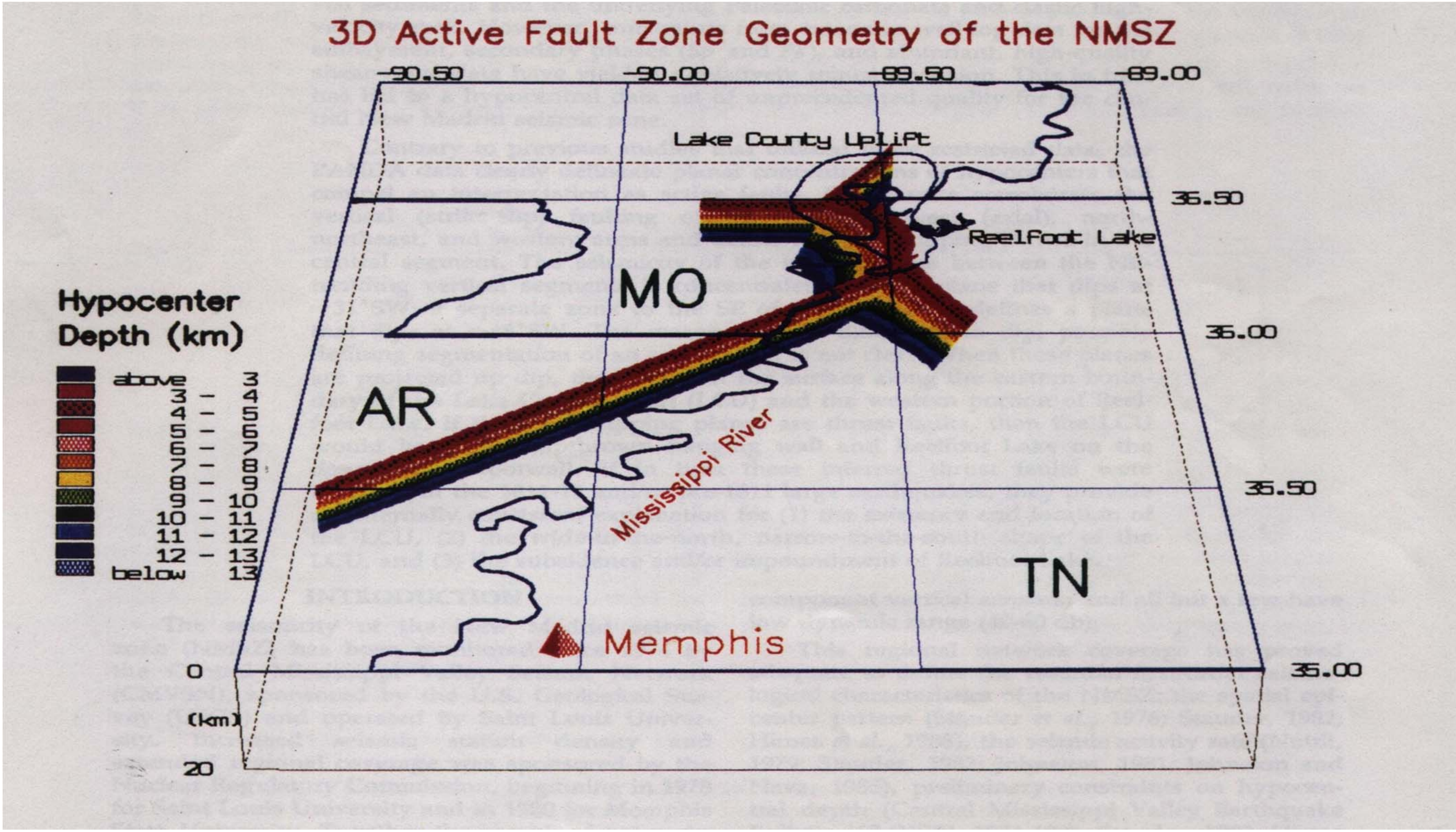
3D Active Fault Zone Geometry of the NMSZ
-90.50
-90.00
-89.50
-89.00
Lake County Uplift
Reelfoot Lake
36.50
36.00
35.50
35.00
MO
AR
TN
Mississippi River
Memphis
Hypocenter Depth (km)
above 3
3 - 4
4 - 5
5 - 6
6 - 7
7 - 8
8 - 9
9 - 10
10 - 11
11 - 12
12 - 13
below 13
0
(km)
20

Examples of a few cross-sectional views of seismicity showing that thickness of seismogenic zone is generally 20~40 km.

Earthquake locations are very poor due to lack of reliable velocity structure.

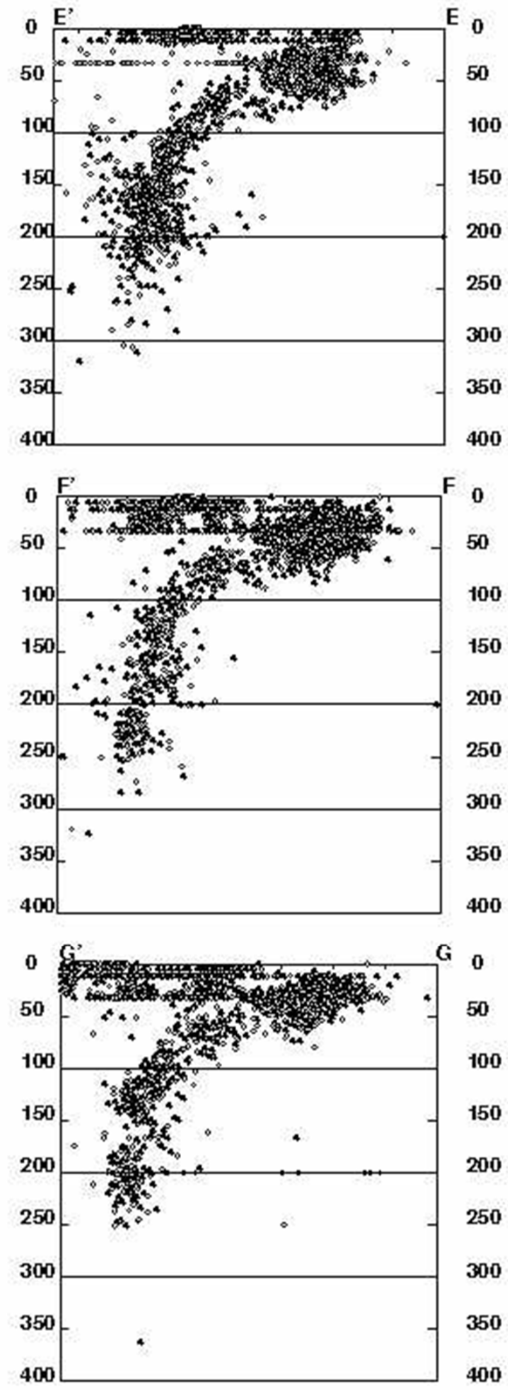

In order to reliably locate earthquakes in subduction zone region, internal velocity structure inside a subduction zone has to be resolved first.

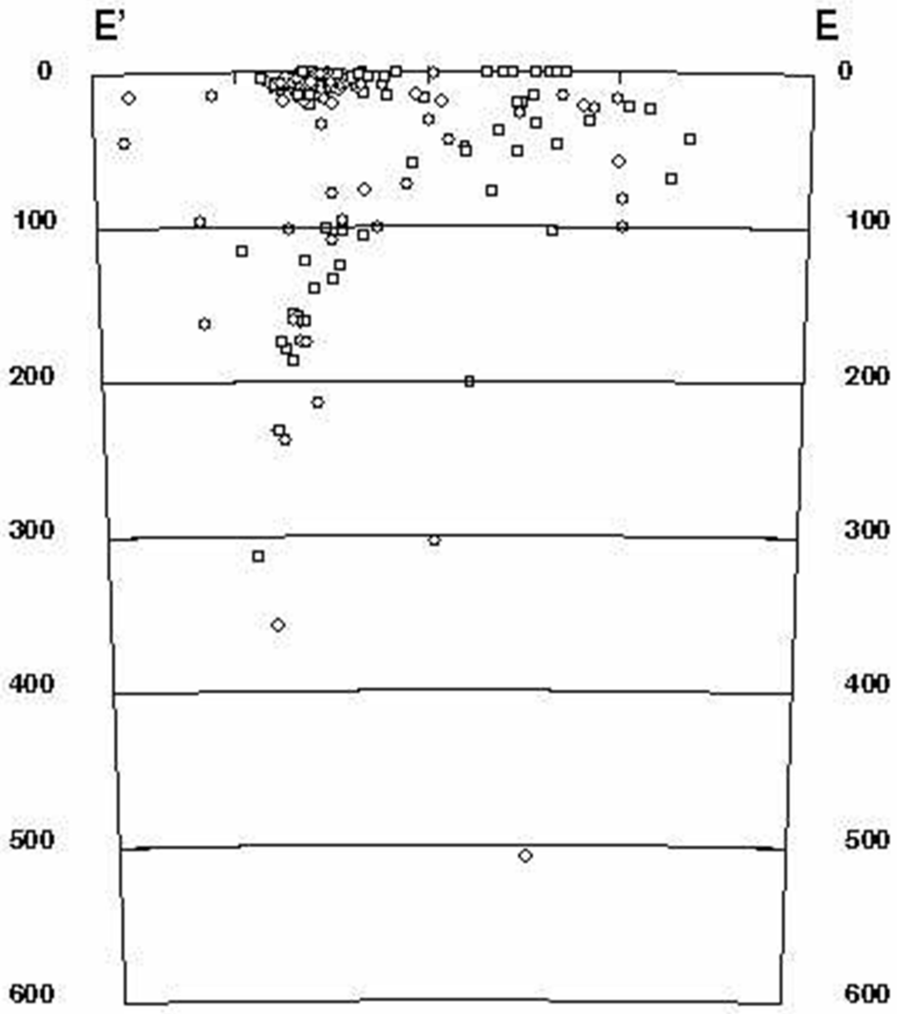

Earthquake locations above a flat subduction zone in South American are not affected by the complicated internal structure of a subduction zone.

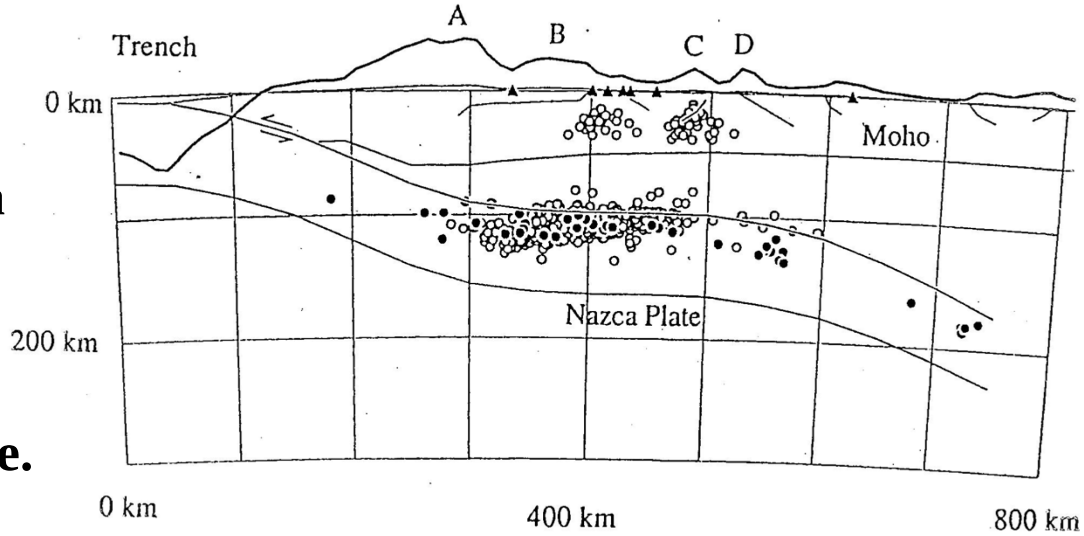

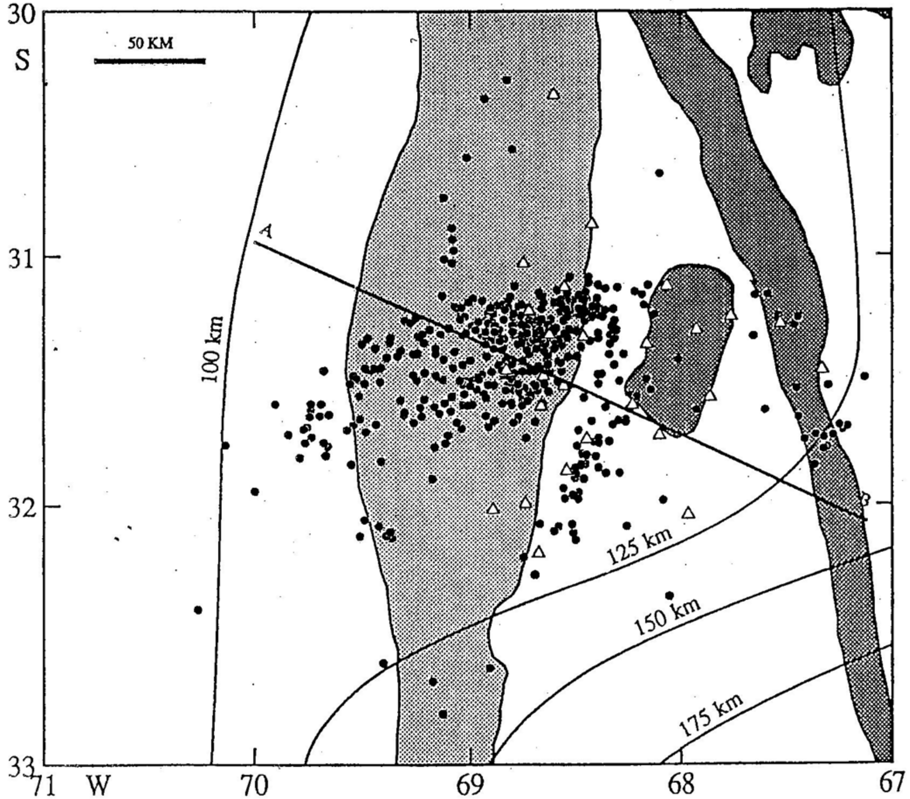

Traditionally, it is well accepted that thickness of seismogenic zone is 20~20 km in most subduction zones.

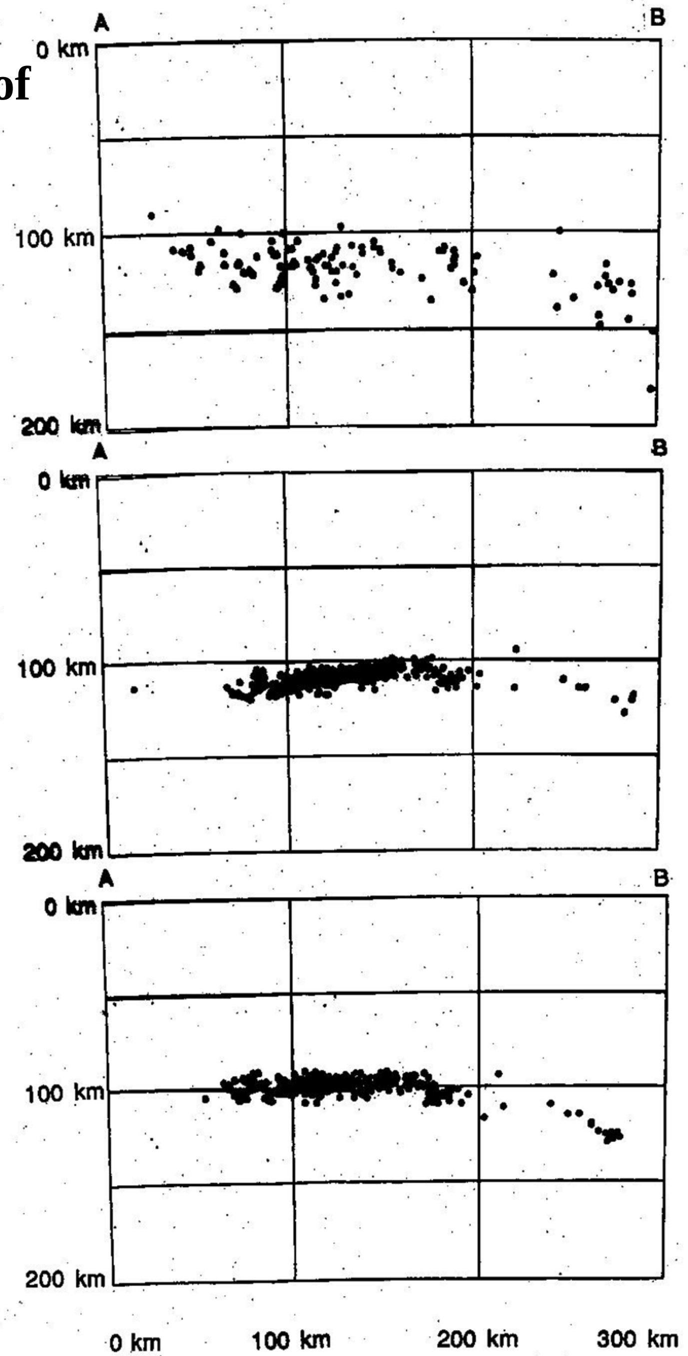

ISC data

PANDA data – original location

PANDA data – JHD relocation

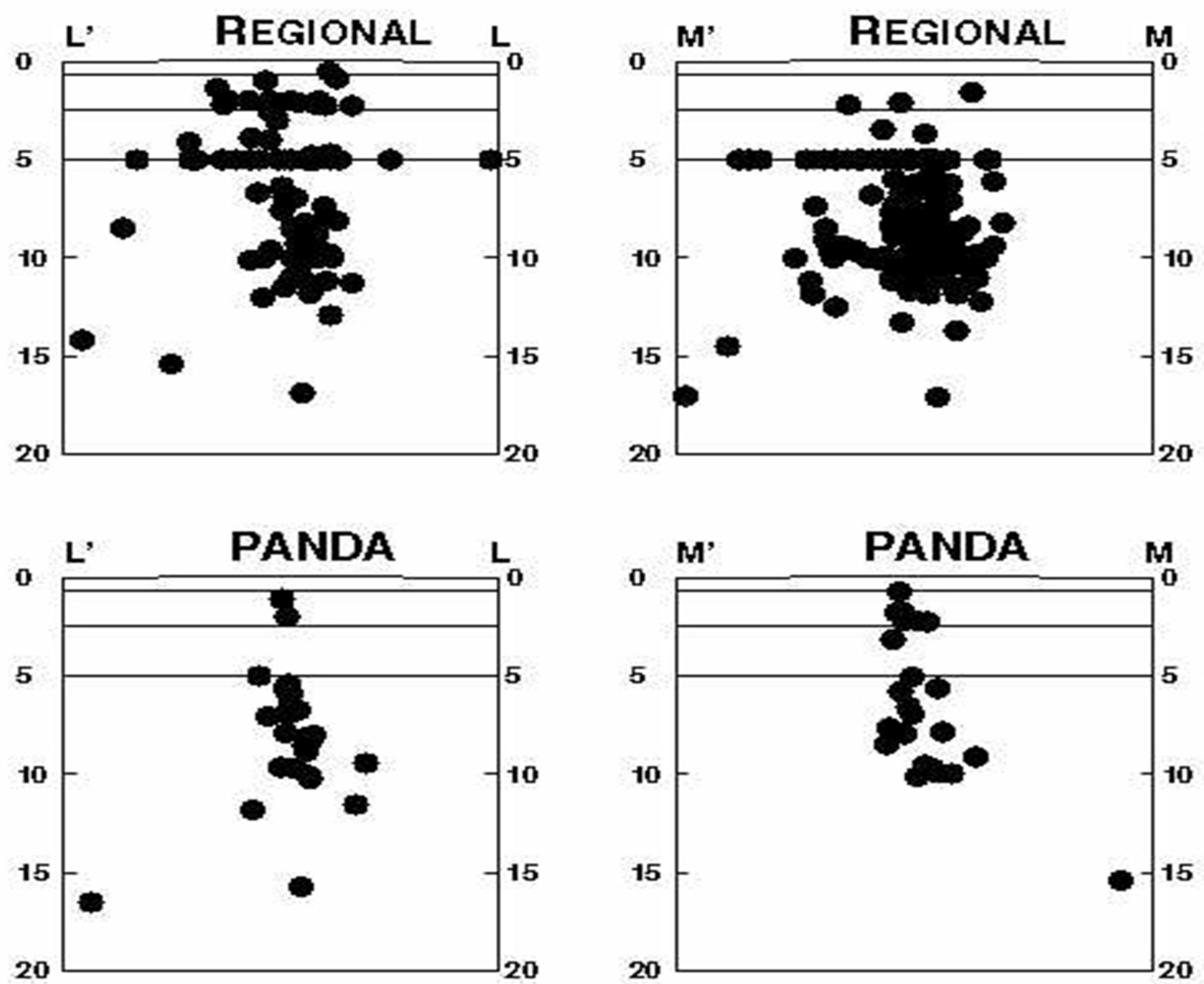
L'
REGIONAL
L
M'
REGIONAL
M
L'
PANDA
L
M'
PANDA
M
0
5
10
15
20

Solution for a reliable earthquake location

(a) Determination of a reliable 3-D Vp and Vs velocity model – a big challenge for seismologists

(b) Development of a single-earthquake location algorithm using the resultant 3-D Vp and Vs velocity model -- a dream

(c) A reliable arrival time picks for both P- and S-waves – additional analysis tools are needed to verify the arrival time picks, especially for the S-wave. Tools such as cross-correlation, stacking (summing), bandpass filter, and polarization filter can be applied.

3. Comparison of the observed gravity data with that converted from the resultant velocity models

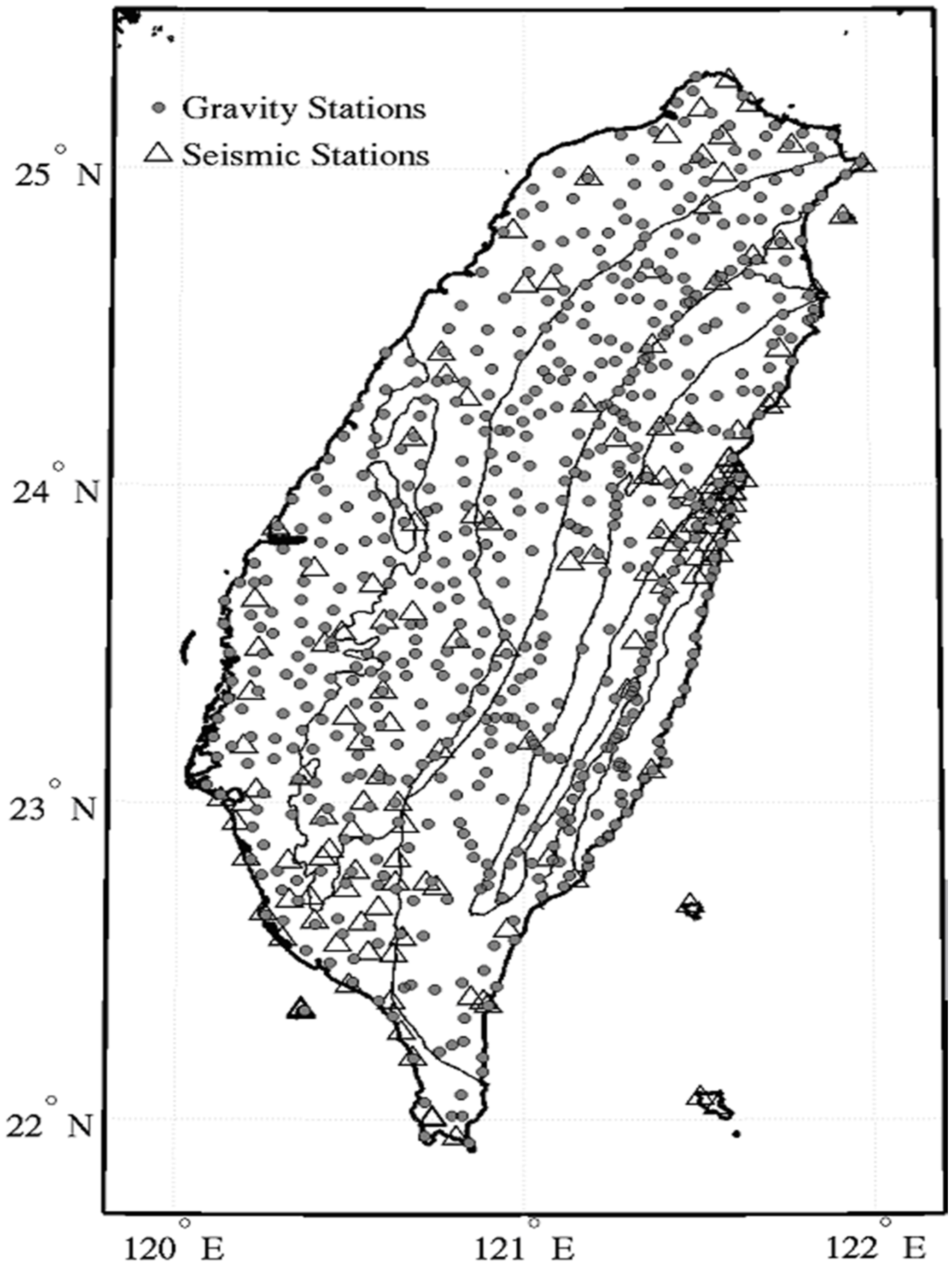
Gravity Stations
Seismic Stations
25° N
24° N
23° N
22° N
120° E
121° E
122° E

The first island-wide gravity map generated for the entire Taiwan region.

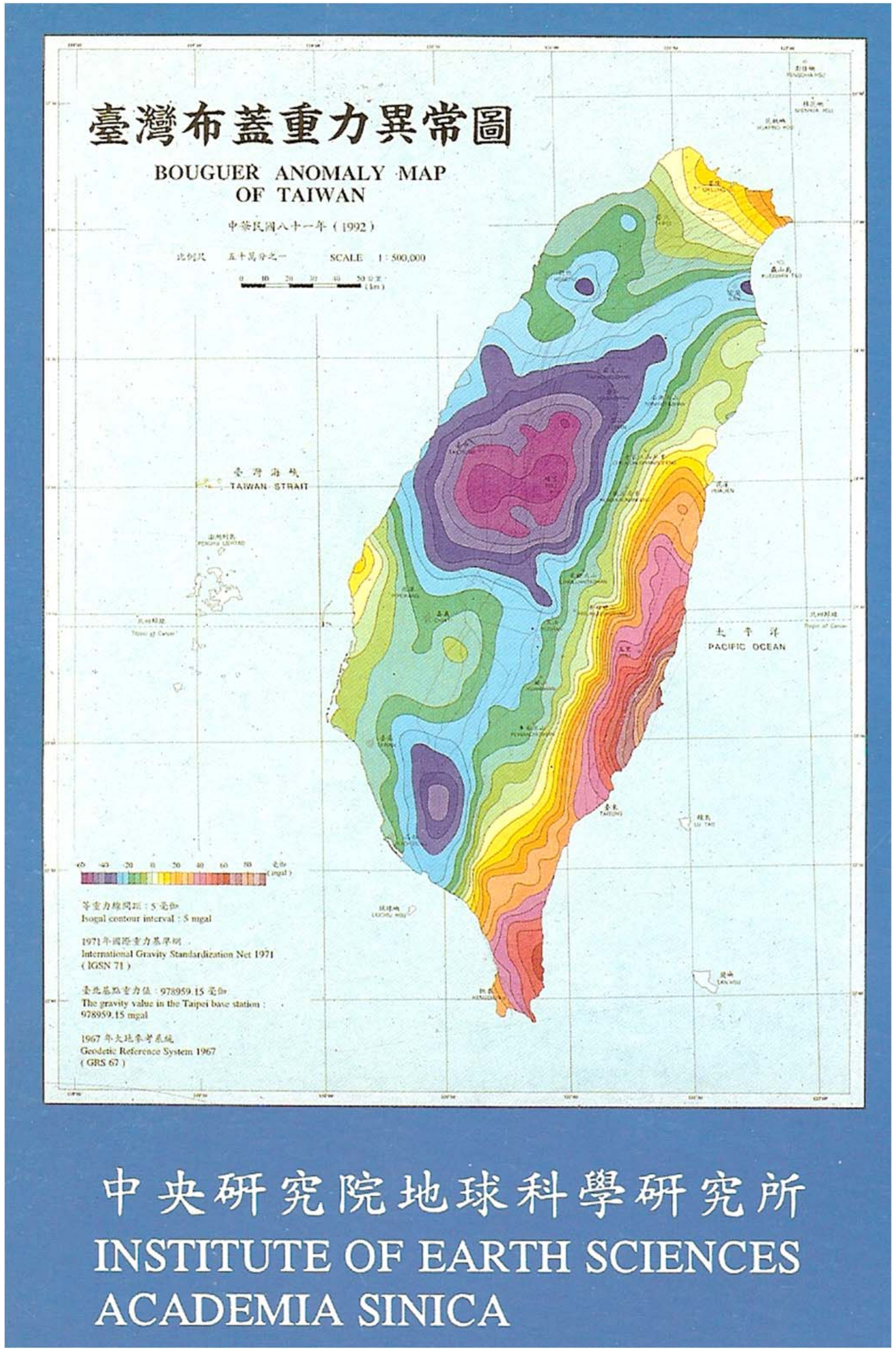

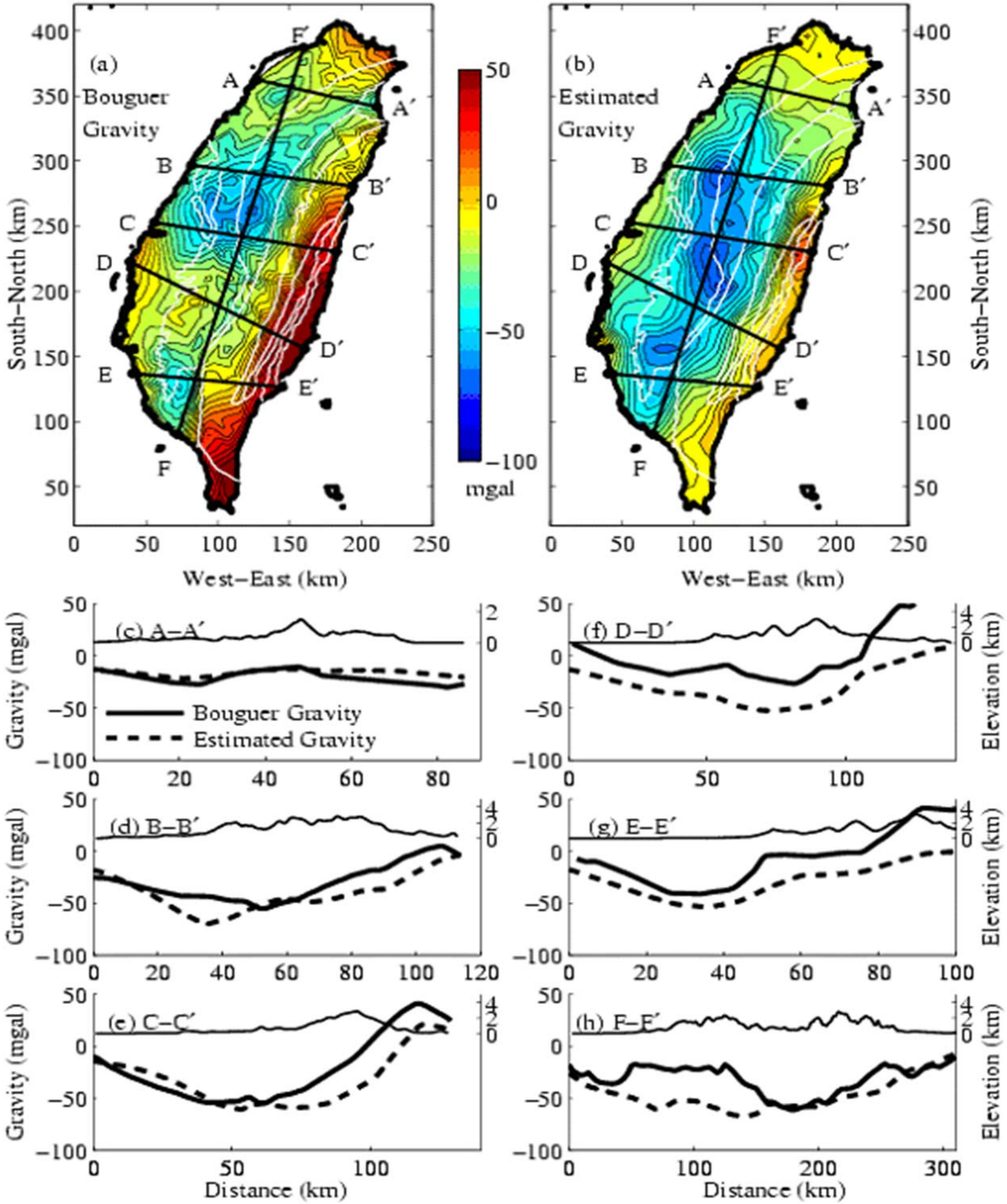

(a) Bouguer Gravity
(b) Estimated Gravity
South-North (km)
West-East (km)
mgal
(c) A–A′
(d) B–B′
(e) C–C′
(f) D–D′
(g) E–E′
(h) F–F′
Bouguer Gravity
Estimated Gravity
Gravity (mgal)
Elevation (km)
Distance (km)

No other 3-D models for the Taiwan region can produce such a match or small mismatch with the observed gravity information

– per Y.H.Yen